

MURTHY C.R. (1977)



**Environment
Canada**

**Canada
Centre
For Inland
Waters**

**Environnement
Canada**

**Centre
Canadien
Des Eaux
Intérieures**

CCIW

SEP 26 1997

LIBRARY

COASTAL BOUNDARY LAYER CHARACTERISTICS

AT DOUGLAS POINT, LAKE HURON

C. R. MURTHY and D. S. DUNBAR

**Canada Centre for Inland Waters
Burlington, Ontario
Canada**

**UNPUBLISHED REPORT
RAPPORT NON PUBLIE**

TD

7

**M87
1977**

**COASTAL BOUNDARY LAYER CHARACTERISTICS
AT DOUGLAS POINT, LAKE HURON
C. R. MURTHY and D. S. DUNBAR
Canada Centre for Inland Waters
Burlington, Ontario
Canada**

June 1977

INTRODUCTION

During 1974, the Canada Centre for Inland Waters and Ontario Hydro carried out an extensive experimental program to study in some detail the coastal zone environment off the Bruce Nuclear Power Development, in the vicinity of Douglas Point, Lake Huron. Based on this data, a comprehensive report giving statistical and climatological summaries of coastal currents, temperature and meteorological data was prepared in compliance with the International Joint Commission Task 2 Program on Waste Heat (CCIW Report No. 17).

One of the scientific objectives of this program was to resolve the large scale horizontal transport and exchange processes in the coastal boundary layer. Towards this objective, detailed calculations were performed to determine the mean flow properties, horizontal turbulence, current shear and dispersion characteristics of coastal currents.

The data is comprised of long time series current meter data and it is often difficult to analyze such data in a meaningful manner. Keeping in mind the basic objective

of this report, we have selected "episodes" where persistent strong shore parallel currents occurred. These currents are of practical interest owing to their capability to transport and disperse effluents discharged at the coastline.

Three "episodes" where strong NE shore parallel currents persisted for periods ranging from 10 - 30 days were selected based on statistical summaries shown in Figures 1 - 3. Additional general details of the data base pertaining to these calculations are summarized in Table 1. In the report we will present the rationale and details of the calculations with some general interpretation of the results from the three episodes.

DATA ANALYSIS

The time series current meter data are recorded at 20 min. intervals and are available in the form (S_i, θ_i) where S_i

is the integrated speed in cm sec^{-1} and θ_i is the instantaneous direction in degrees measured from north. The 20 min. data was then resolved into shore-parallel (U) and shore-perpendicular (V) components, using the following relations:

$$\begin{aligned} U_i &= S_i \cos (\phi - \theta_i) \\ V_i &= S_i \sin (\phi - \theta_i) \end{aligned} \quad (1)$$

where ϕ is the angle from north of the local shoreline. For the Douglas Point region $\phi = 30^\circ$. This preliminary analysis results in two time series $U(t)$ and $V(t)$, which are then used as basic data for further calculations.

In order to calculate parameters characteristic of transport and exchange processes, it is necessary to "isolate" the "mean flow" from time series data. Numerical filtering techniques developed by Graham (1963) were used to define the "mean" and the "fluctuations". Filters were selected based on the characteristics of a typical kinetic energy spectra, $E_u(f)$ constructed from 61 days of continuous data from a current meter located approximately 5 km from the shore (Fig. 4). The energy spectra points out two characteristic features: a dominant peak around 16 hrs. corresponding to the theoretical inertial period at the latitude of Lake Huron. Behind the inertial peak, there is a minimum at a period of about 24 hrs. This minimum is probably a characteristic property of energy transfer from large-scale lakewide circulation. The periods corresponding

to this minimum can be used as a transition between the "mean flow" and the "fluctuations". Alternatively, the dominance of motion with periods in the inertial band (approximately from 12-24 hrs.) suggests a natural partitioning of the "mean flow" and the "fluctuations". The precise partitioning of the "mean flow" and the "fluctuations" from long time series data is rather difficult and in whatever way one defines these quantities, they are bound to be arbitrary to the other. However, following the above arguments, we have constructed two low-pass filters, one with a 10-14 hr. cutoff range which retains the inertial motion as a part of the "mean flow", the other with an 18-24 hr. cutoff in which the inertial motion is included as a part of the "fluctuations". The response characteristics of the two filters are discussed in some detail in Appendix A .

Having selected the two filters, let us now apply them to a set of data to derive "running means" $\bar{U}(t)$ and $\bar{V}(t)$. Figures 5 and 6 show plots of a set of data from episode 1 with $\bar{U}(t)$ and $\bar{V}(t)$ derived by applying the two filters to the original unfiltered data. Figure 5 plots refer to a nearshore current meter (about 300 m. from shore) whereas Fig. 6 plots refer to current meters further off shore (about 6 km from shore). Shown in these plots are the unfiltered data with 20 min. sampling interval and the running means $\bar{U}(t)$ and $\bar{V}(t)$ derived from applying the two filters.

The performance of the two filters is best illustrated in Fig. 6. A comparison of the running means $\bar{U}(t)$ and $\bar{V}(t)$ reveals that the 10 - 14 hr filter essentially retains the dominant inertial oscillations as expected, whereas the 18 - 24 hr. filter effectively filters out all inertial motion.

The next step in the analysis is to calculate the "fluctuations" $U^1(t)$ and $V^1(t)$. The "running mean" values $\bar{U}(t)$ and $\bar{V}(t)$ are merely subtracted from the instantaneous values $U(t)$ and $V(t)$ to define the fluctuations $U^1(t)$ and $V^1(t)$. A statistical quantity which is used as a measure of the magnitude of velocity fluctuations is the variance i.e., the mean square fluctuations. For the U-component, the variance was calculated using

$$\overline{U^{12}}(t) = \overline{|U(t) - \bar{U}(t)|^2}$$

where the overbar indicates averaging. One-half of this quantity $\frac{1}{2} \overline{U^{12}}(t)$ (per unit mass) is the kinetic energy in the fluctuations. The mean-flow kinetic energy was then calculated simply as the difference between the total kinetic energy and the fluctuational kinetic energy. Mean velocities, variance, turbulence coefficient, eddy diffusivities and kinetic energy (in the mean flow and fluctuations) were calculated for the three episodes and are summarized in Tables 2 - 4. Several diagrams were then constructed to show the variability of these parameters as a function of the distance from shore (Appendices B, C, D). These illustrations form the basis for discussion

to interpret the characteristics of the coastal boundary layer.

COASTAL BOUNDARY LAYER CHARACTERISTICS

(a) Mean Flow

Figures 7 - 9 show plots of $\bar{U}(y)$ and $\bar{V}(y)$ for the three episodes; (y is the distance from the shore). Some interesting observations can be made from these figures:

- i) The strong northeasterly shore parallel current (U -component) dominates the flow field in the coastal boundary layer. This is accompanied by a reasonably strong offshore flow (V -component). Why a strong northeasterly shore parallel flow generates offshore flow may be an interesting hydrodynamical problem to investigate.
- ii) The mean velocities increase with distance from the shore and reach a maximum at 2 - 3 km from the shore. This is followed by a decrease in mean velocities with distance from the shore. The distance at which maximum mean velocities occur vary from episode to episode. This suggests the possibility of two distinct zones in the flow field within the coastal boundary layer.

(b) Kinetic Energy Transfer

Several plots were prepared to look at the distribution of KE in the mean flow and fluctuations, with distance from the shore. Fig. 10 shows the partition of kinetic energy in the mean flow and the fluctuations (calculated using a low-pass 18 - 24 hr filter) for episode 1. The mean flow KE dominates everywhere

except for the very nearshore meter where the fluctuational KE is very much greater than the mean flow KE. A plausible explanation for this is that the shore and bottom friction generates large-scale mechanical turbulence resulting in higher fluctuational KE. In Fig. 11 the distribution of KE in the U and V components is shown. Clearly, the KE in the shore-parallel component accounts for almost 95 per cent of the total KE everywhere except for the very nearshore meter, where the KE in the U and V components are comparable.

The total KE increases fairly rapidly, attaining its maximum value at about 2 - 3 km from the shore and then decreases with distance from the shore. The distribution of KE also suggests the possibility of two distinct flow characteristics within the coastal boundary layer.

Figures 12 and 13 show the distribution of fluctuational KE in the U and V components calculated using the two low-pass filters with 18 - 24 hr cutoff and 10-14 hr cutoff, respectively. The fluctuational KE is rather small everywhere except for the meter closest to the shore, where there is a marked increase in fluctuational KE in both the U and V components. As mentioned earlier, this is attributed to the generation of large scale mechanical turbulence due to shore and bottom friction. Further, it is of interest to note that there is a gradual increase of fluctuational KE with the 18-24 hr cutoff filter (Fig. 12), reflecting the contribution of inertial oscillations further offshore.

(c) Horizontal Turbulence

As remarked earlier, the variance or "mean square fluctuations" is generally used as a quantitative measure of the velocity fluctuations. A convenient non-dimensional parameter in characterizing velocity fluctuations is the "relative intensity" or "turbulence coefficient" defined as the ratio of root mean square value of the velocity fluctuations to a characteristic mean velocity. For the U component, the relative intensity $i_u = \sqrt{U^{12}} / \bar{s}$, where \bar{s} , the scalar mean speed is used as a characteristic mean velocity. The turbulence coefficients i_u and i_v were calculated using the two low-pass filters. Figs. 14 and 15 show plots of i_u and i_v VS distance from the shore for episode 1. The turbulence coefficients are remarkably large very near shore, reflecting the turbulence level in the flow field. Further, it is interesting to note that there is a gradual increase of i_u and i_v with 18 - 24 hr cutoff filter (Fig. 14), again reflecting the contribution of inertial oscillations further off shore. It is also of interest to point out that i_u is generally greater than i_v indicating the "anisotropy" in the turbulence structure.

Following Gezenstsvei (1968), pseudo eddy diffusivities A_x and A_y were calculated using the calculated values of i_u and i_v . Figures 16 and 17 show plots of A_x and A_y as a function of the distance from the shore for episode 1. Conclusions similar to the above can be drawn from these plots.

(d) Current Shear

Lateral shear in the horizontal mean current is an important parameter in the dispersion of pollutants discharged into the coastal zone. "Running mean" currents with oscillations having periods less than 18 hr removed (i.e., using the low-pass 18-24 hr cutoff filter) were used to calculate the lateral shear $\frac{d\bar{U}}{dy}$ and $\frac{d\bar{V}}{dy}$, where dy is the separation of current meters. Lateral shear calculations were performed using only the data from current meters closest to the shore (meter nos. 16 and 15, and 15 and 14). Fig. 18 shows time series plot of $\frac{d\bar{U}}{dy}$ and $\frac{d\bar{V}}{dy}$ for episode 1. The lateral shear $\frac{d\bar{U}}{dy}$ is remarkably high, often reaching as high as five times the local Coriolis parameter. Episodes of large lateral shear in the nearshore zone are particularly important in the dispersion of pollutants.

(e) Width of the Coastal Boundary Layer

In Fig. 19 we have shown the kinetic energy spectra of coastal currents measured at distances ranging from 1 km to 6 km from the shore for a typical summer period. It is of interest to note that while the inertial currents dominate offshore, these currents are drastically modified nearshore. As a consequence, there is a transition zone where rotary inertial currents are gradually modified and are forced to flow more or less parallel to the local shoreline. The distance from the shore of this transition zone

could be defined as the width of the coastal boundary layer, where shore-parallel currents prevail. Towards establishing a criteria to determine the transition zone, we have calculated the fraction of the kinetic energy in the inertial band from the spectra using numerical integration:

$$E_i = \frac{\int_{f_1}^{f_2} E_u(f) df + \int_{f_1}^{f_2} E_v(f) df}{\int_0^{\infty} E_u(f) df + \int_0^{\infty} E_v(f) df}$$

where $f_1 = \frac{1}{24}$ and $f_2 = \frac{1}{12}$ are frequencies defining the inertial band in the spectra.

Figs. 20, 21 and 22 show plots of $E_i(y)$, where y is the distance from the shore for the three episodes. During stratified conditions E_i gradually increases (except for the anomaly close to the shore) with distance from the shore, reflecting the contribution of kinetic energy due to inertial oscillations. If we define the width of the coastal boundary layer as the distance from the shore to the transition zone beyond which inertial oscillations dominate, then it is approximately 2 km for episode 1 and 3 km for episode 2. This definition breaks down during unstratified conditions since E_i remains more or less constant with distance from the shore.

This points out that the "width" of the coastal boundary layer at Douglas Point, Lake Huron is about 2 - 3 km, considerably less than 8 - 10 km proposed by Csanady (1972), Blanton (1975) and recently Boyce (1977) for the Oshawa coastal region of Lake Ontario.

REFERENCES:

1. Blanton, J. O. 1975. Nearshore lake currents measured during upwelling and downwelling of the thermocline in Lake Ontario. *J. Phys. Oceanog.* 5, pp 11-24
2. Boyce, F. M. 1977. Response of the coastal boundary layer on the north shore of Lake Ontario to a fall storm. *J. Phys. Oceanog.* (in press)
3. CCIW Report No. 17. 1976. Coastal zone Limnological Observations in Lake Huron at Bruce Nuclear Power Development. May - Nov. 1974.
4. Csanady, G. T. 1972. The Coastal Boundary Layer in Lake Ontario. Part II. The Summer-Fall regime. *J. Phys. Oceanog.* 2, pp 168-176
5. Gezenstsvei, A. N. 1968. Horizontal Large-scale Turbulent Transfer in the Black Sea. pp. 114-132. In *Problems in Dynamical Oceanography*. Edited by A. I. Fel'zenbaum.
6. Graham, R. J. 1963. Determination and Analysis of Numerical Smoothing Weight. NASA Technical Report R-179

EPISODE 1

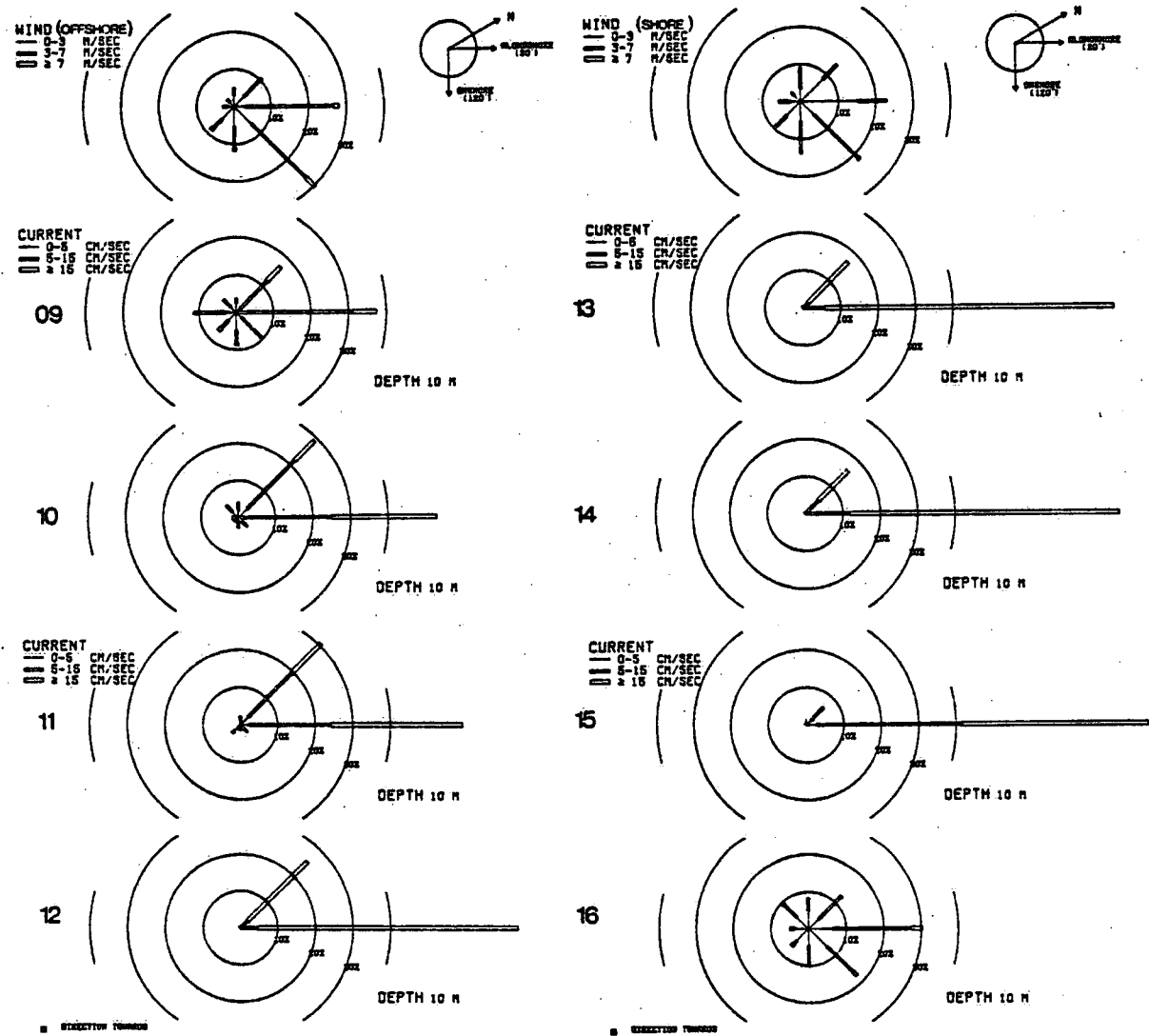


Figure 1.

EPISODE 2

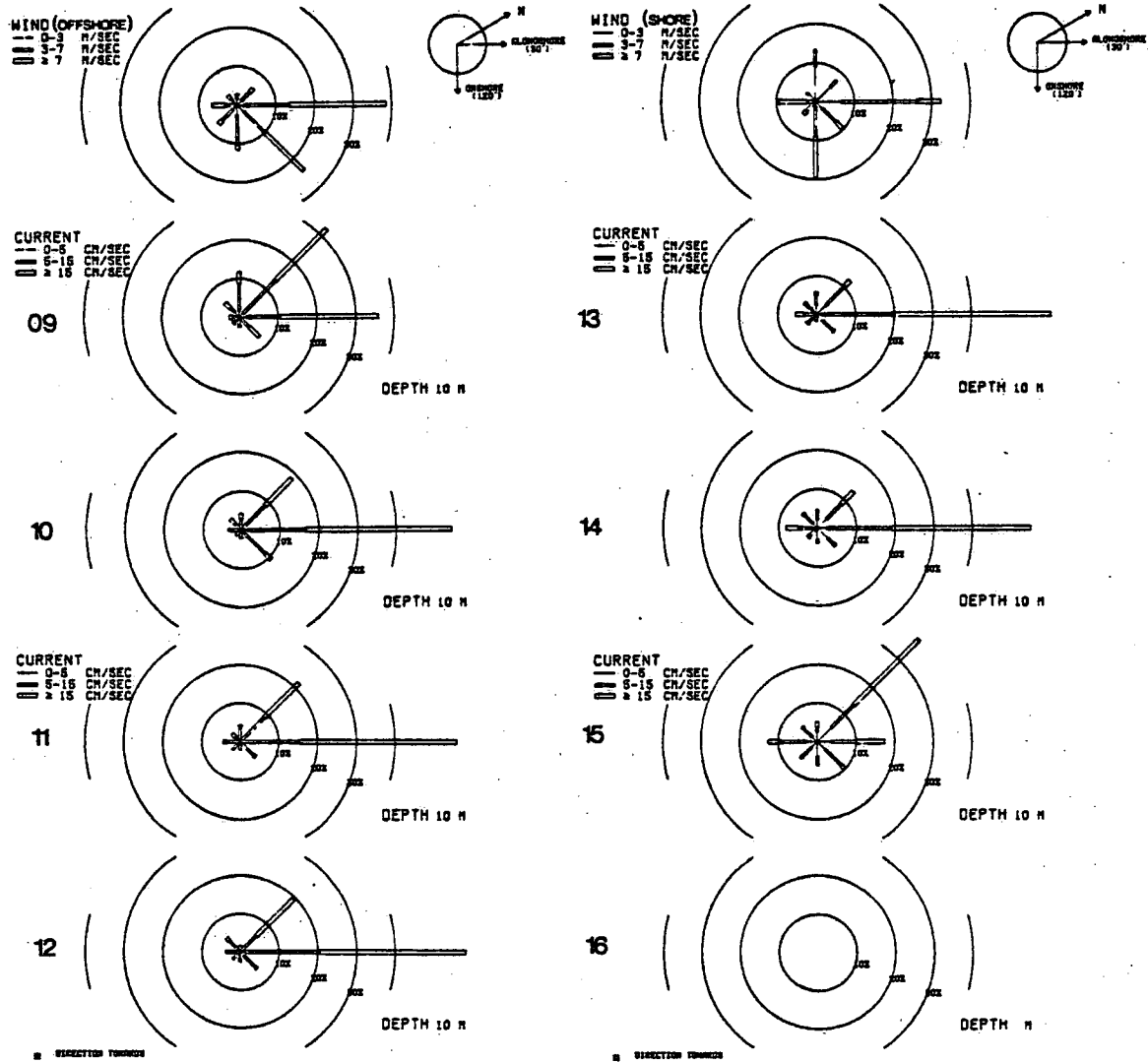


Figure 2.

EPISODE 3

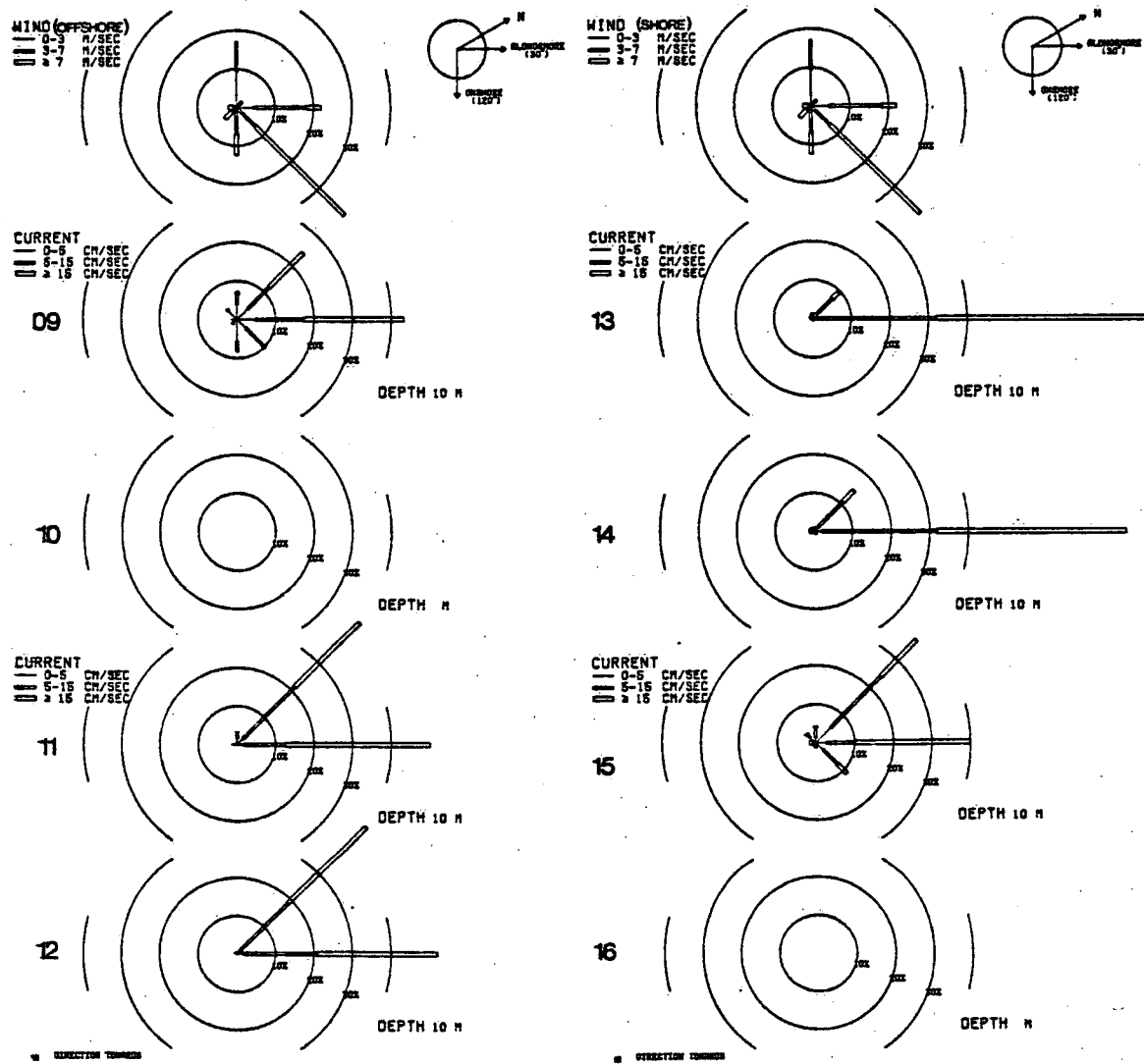


Figure 3.

*** U-COMPONENT ***

***** SPECTRAL ANALYSIS FOR METER 09, SERIES B *****

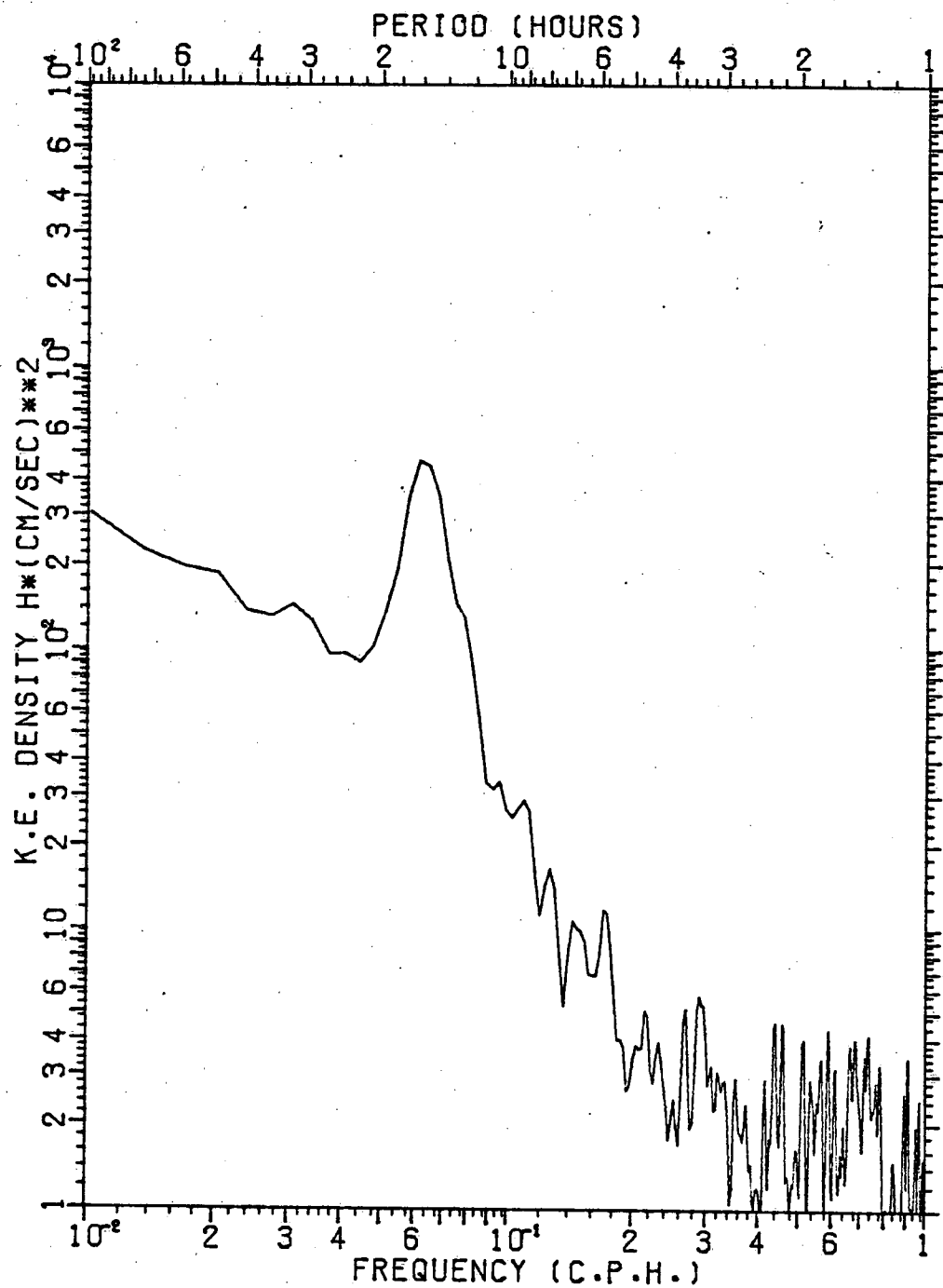


Figure 4.

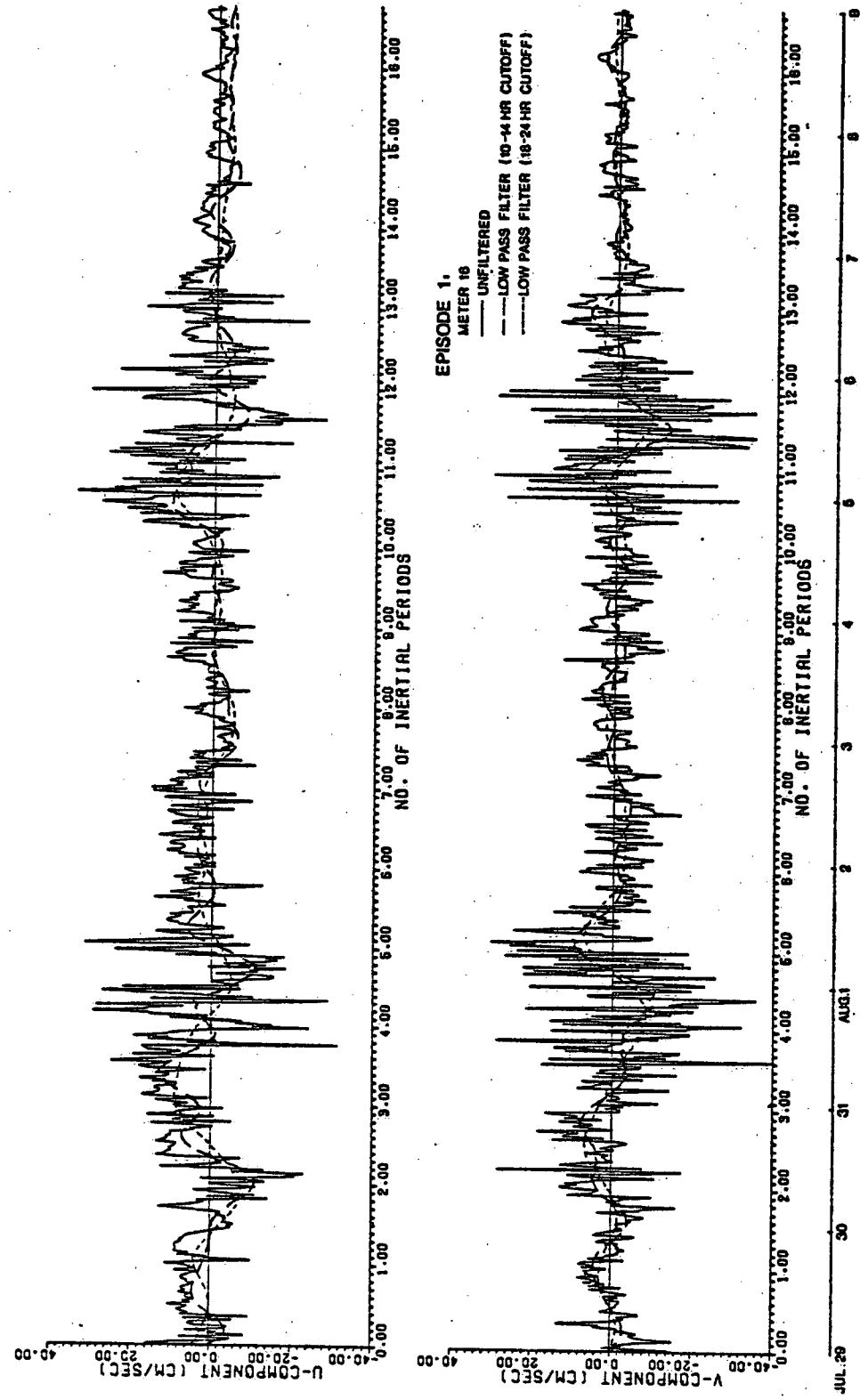


Figure 5.

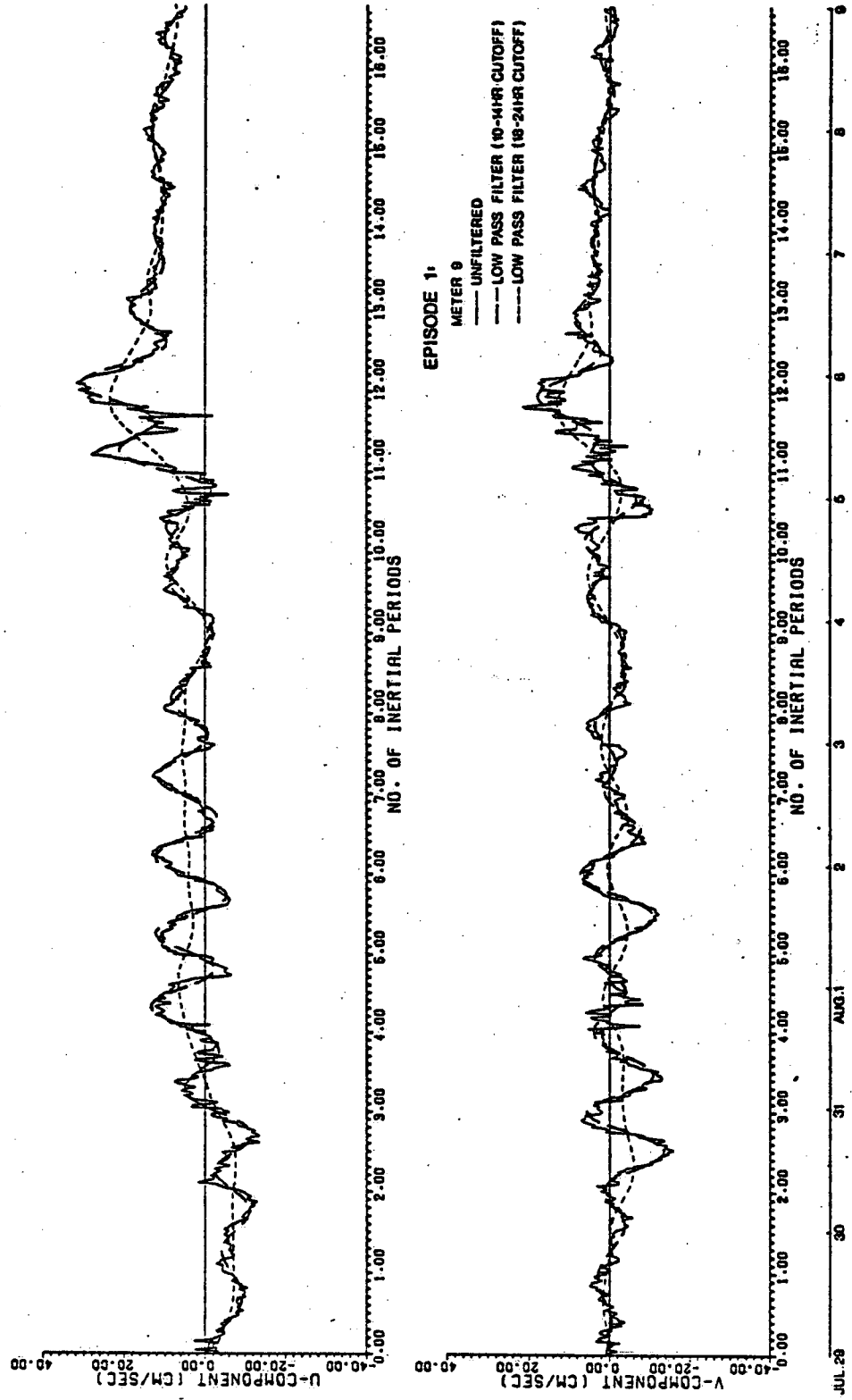


Figure 6.

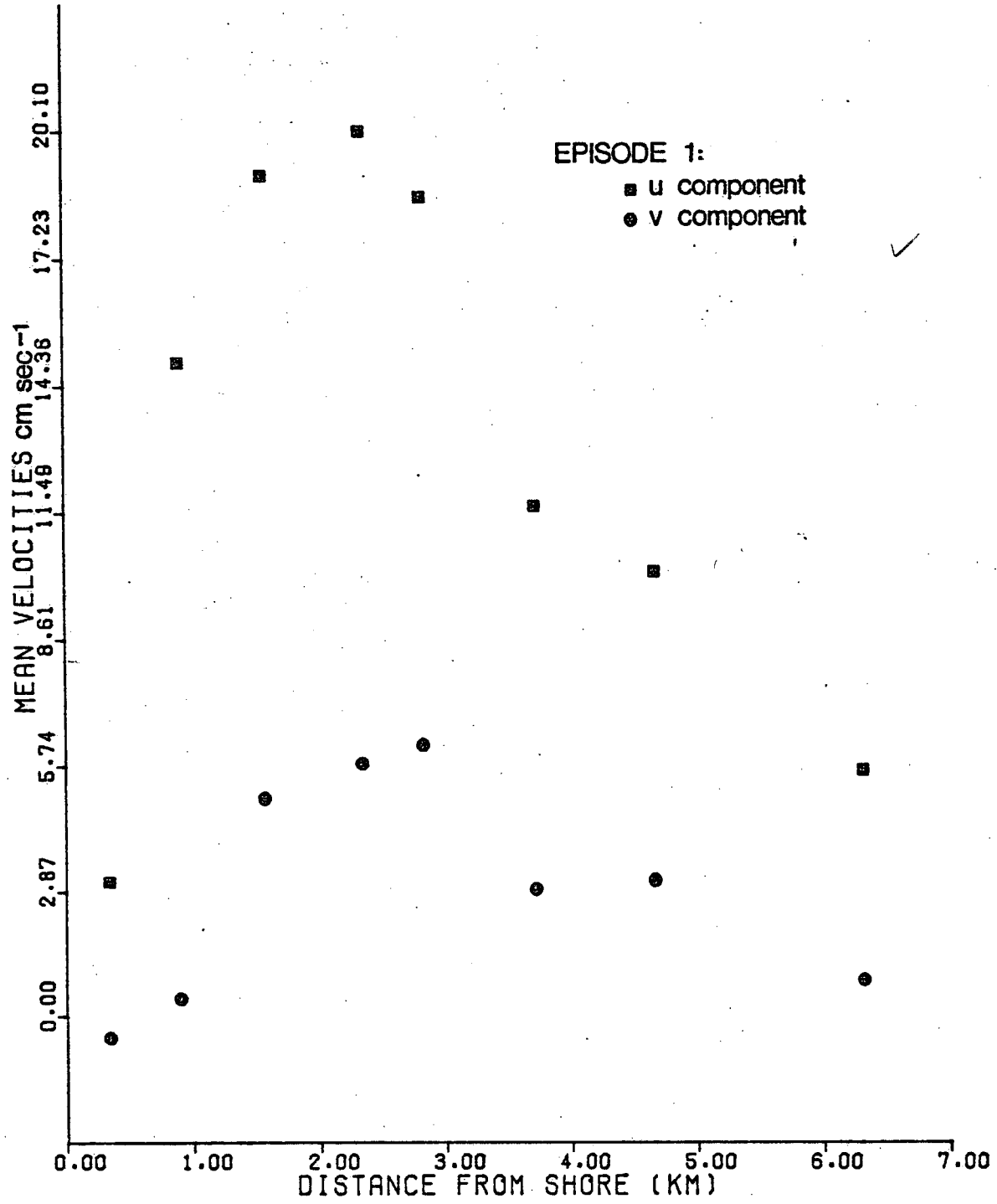


Figure 7.

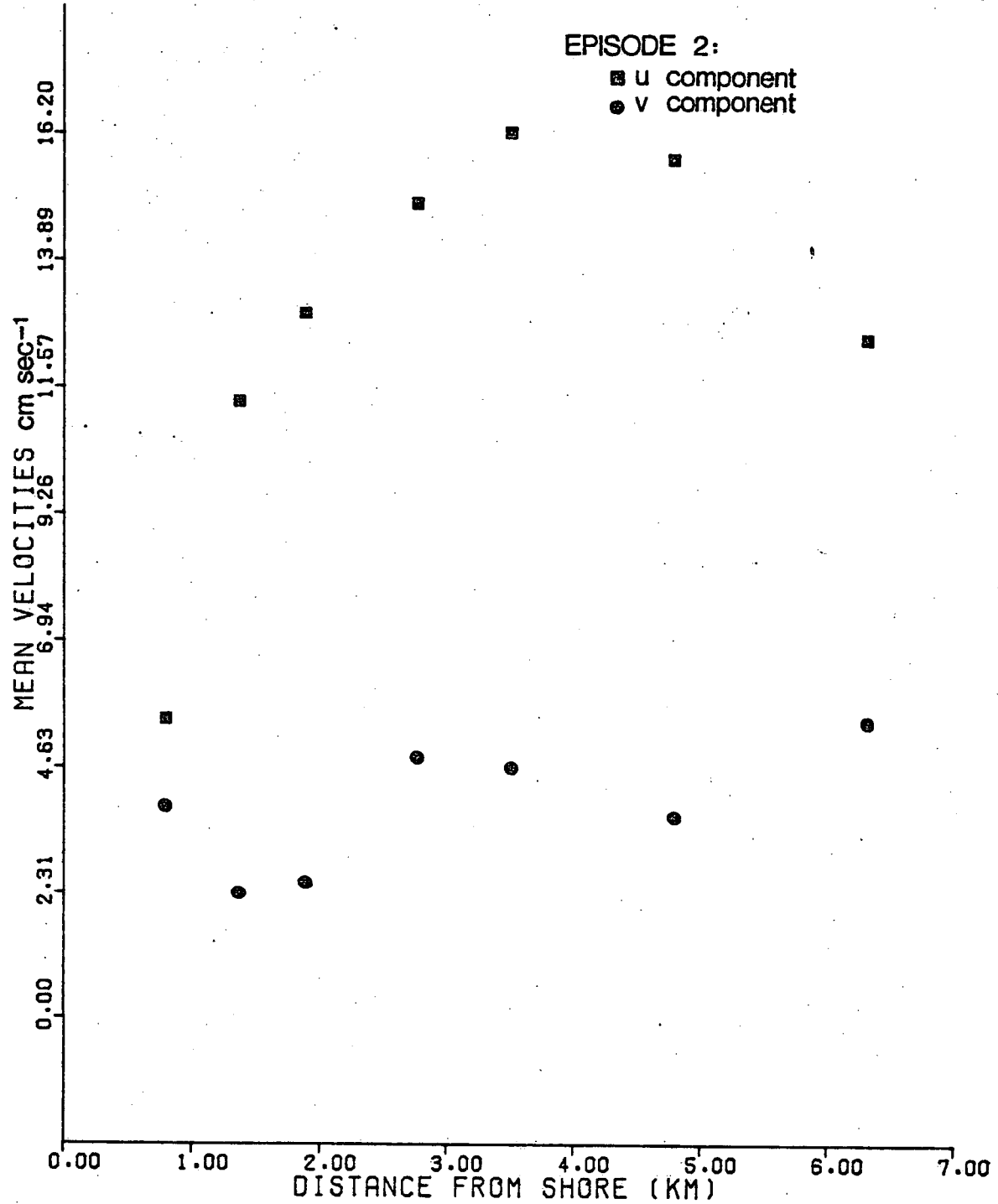


Figure 8.

EPISODE 3:

- u component
- v component

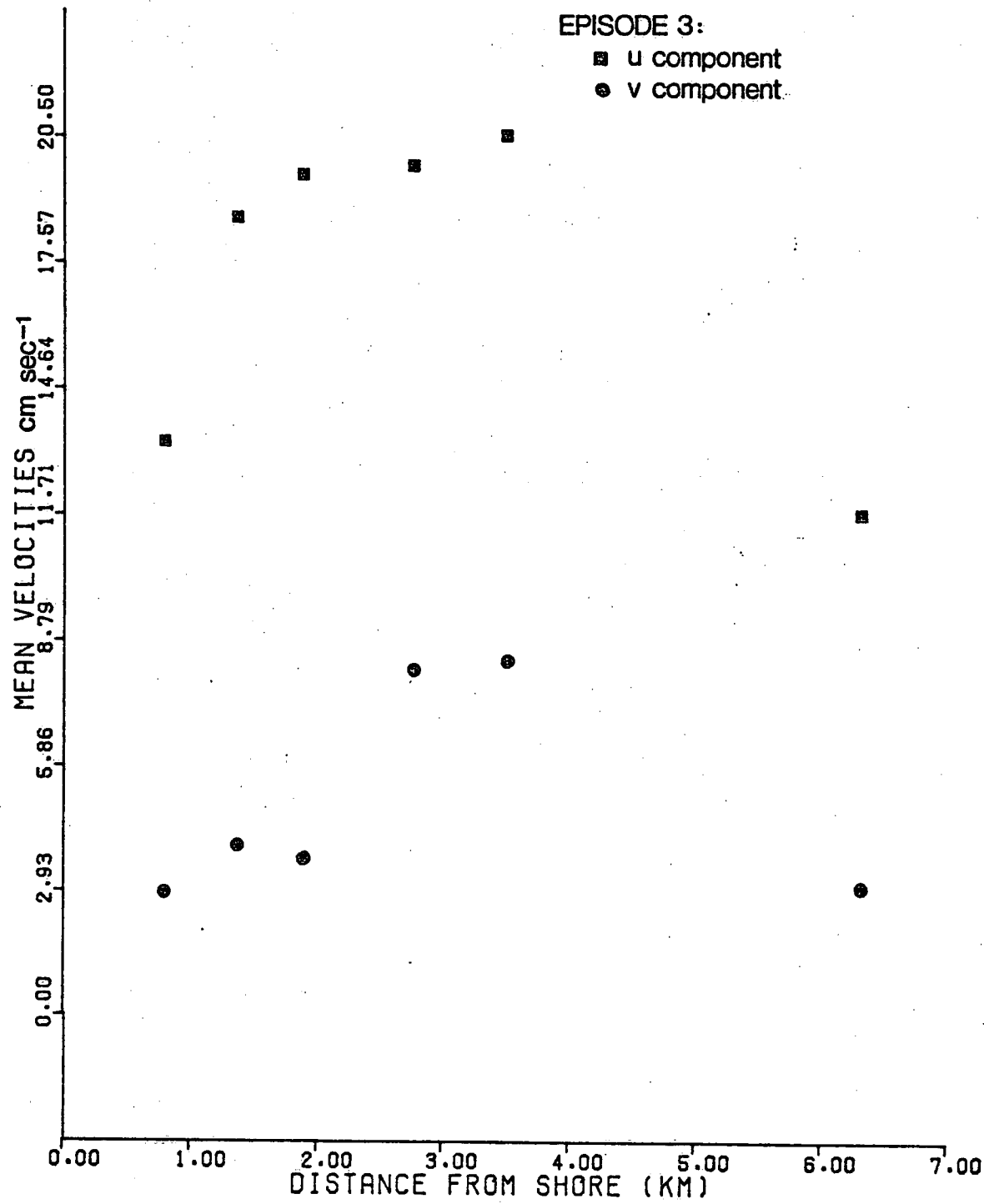


Figure 9.

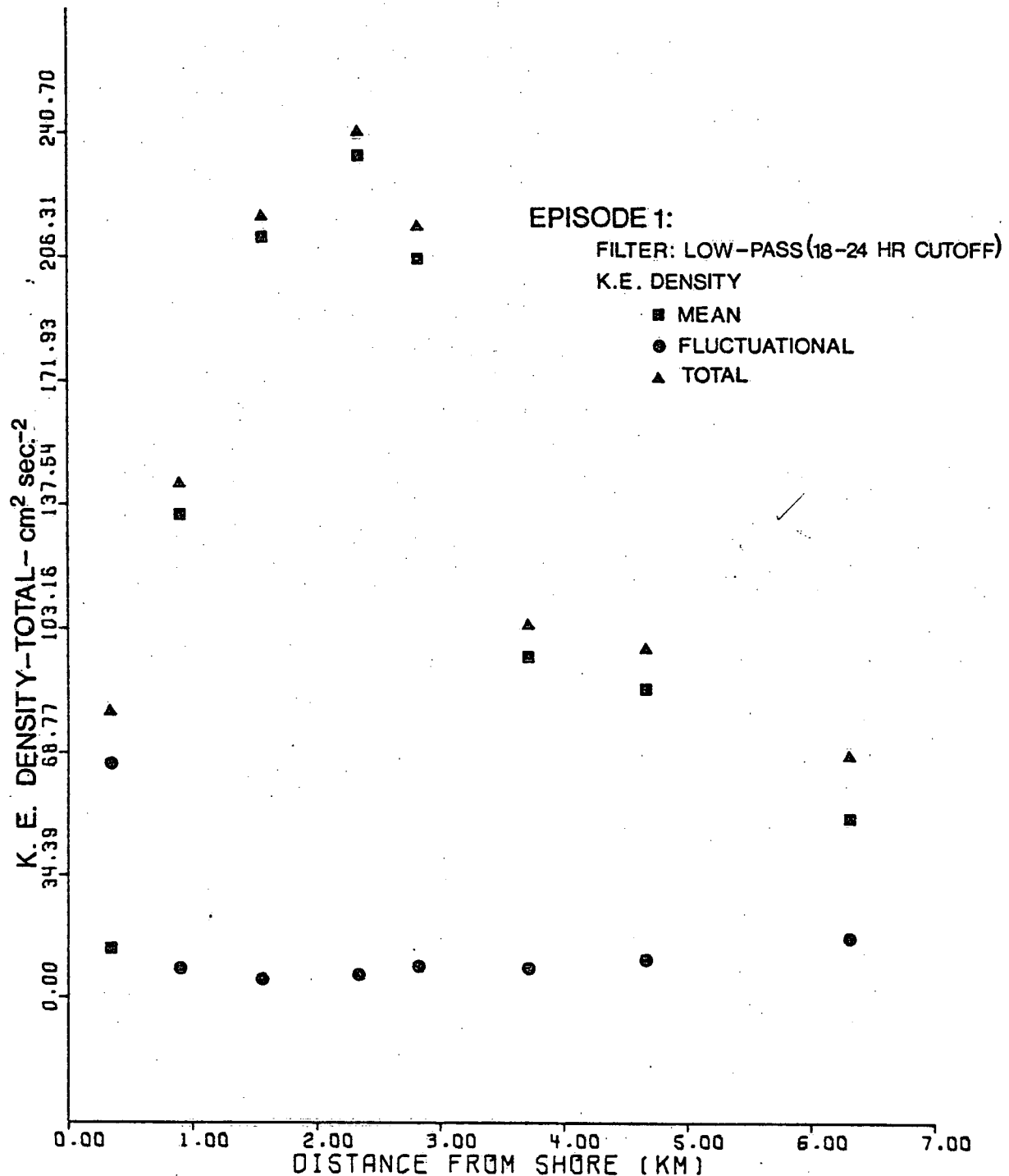


Figure 10.

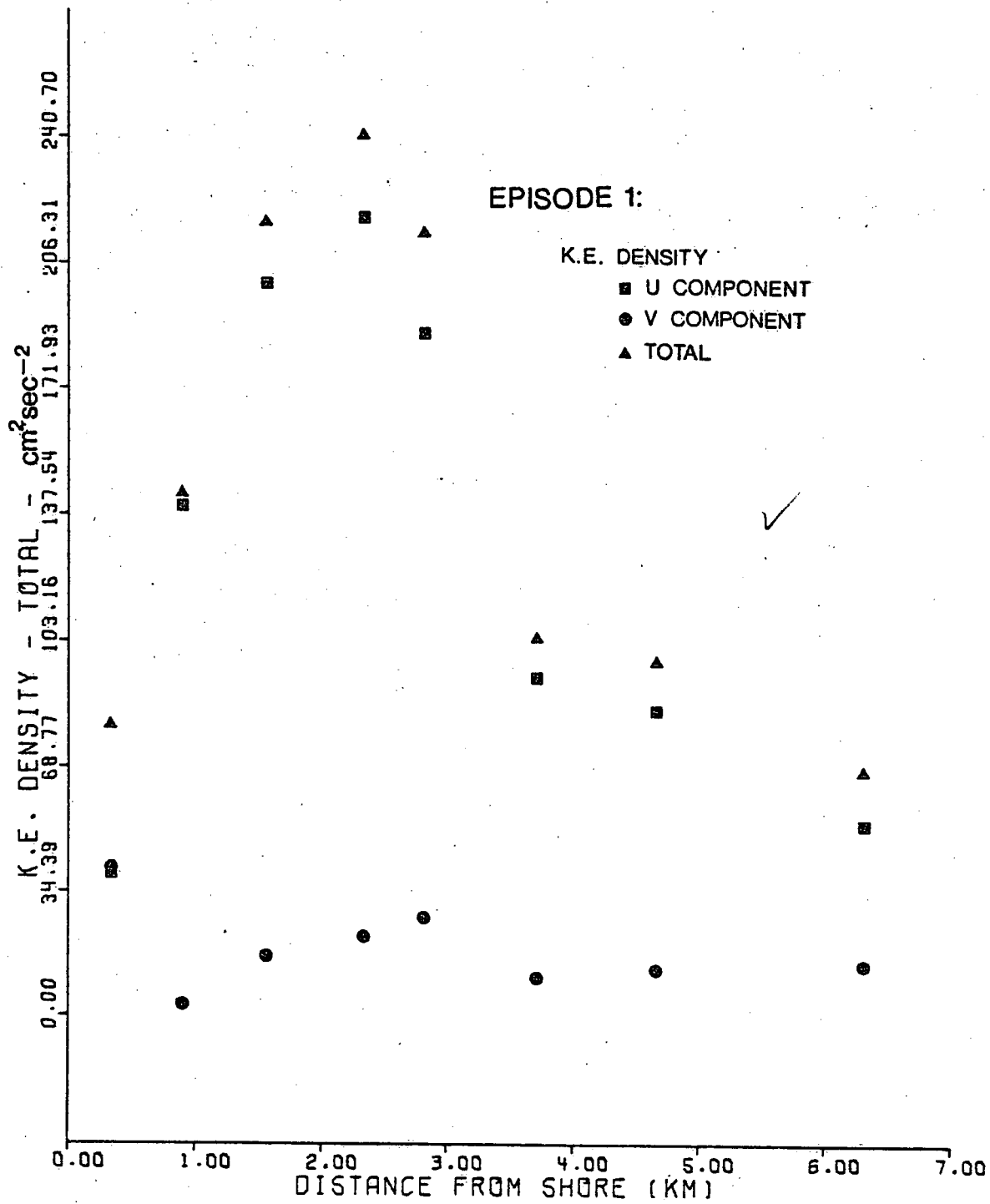


Figure 11.

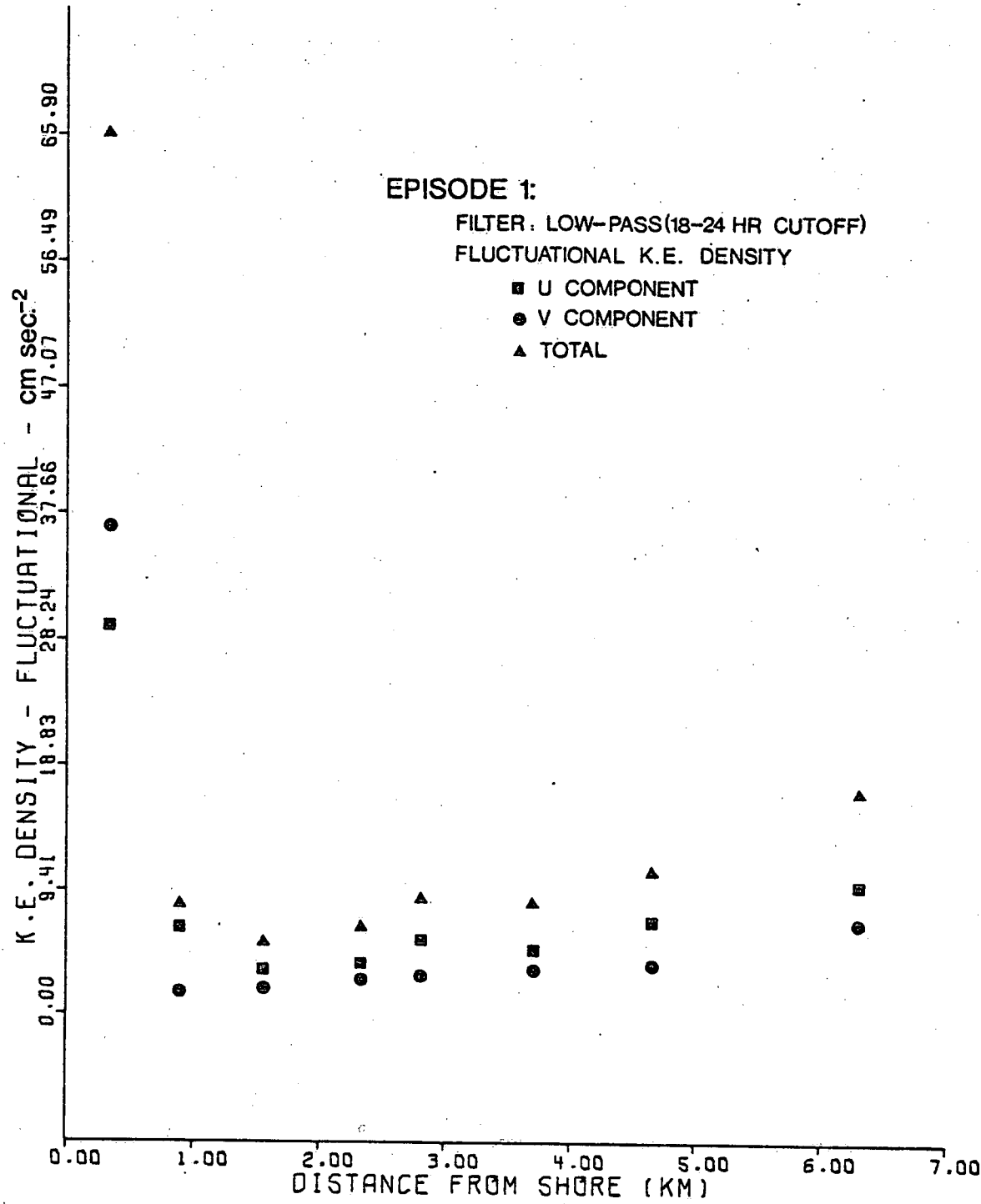


Figure 12.

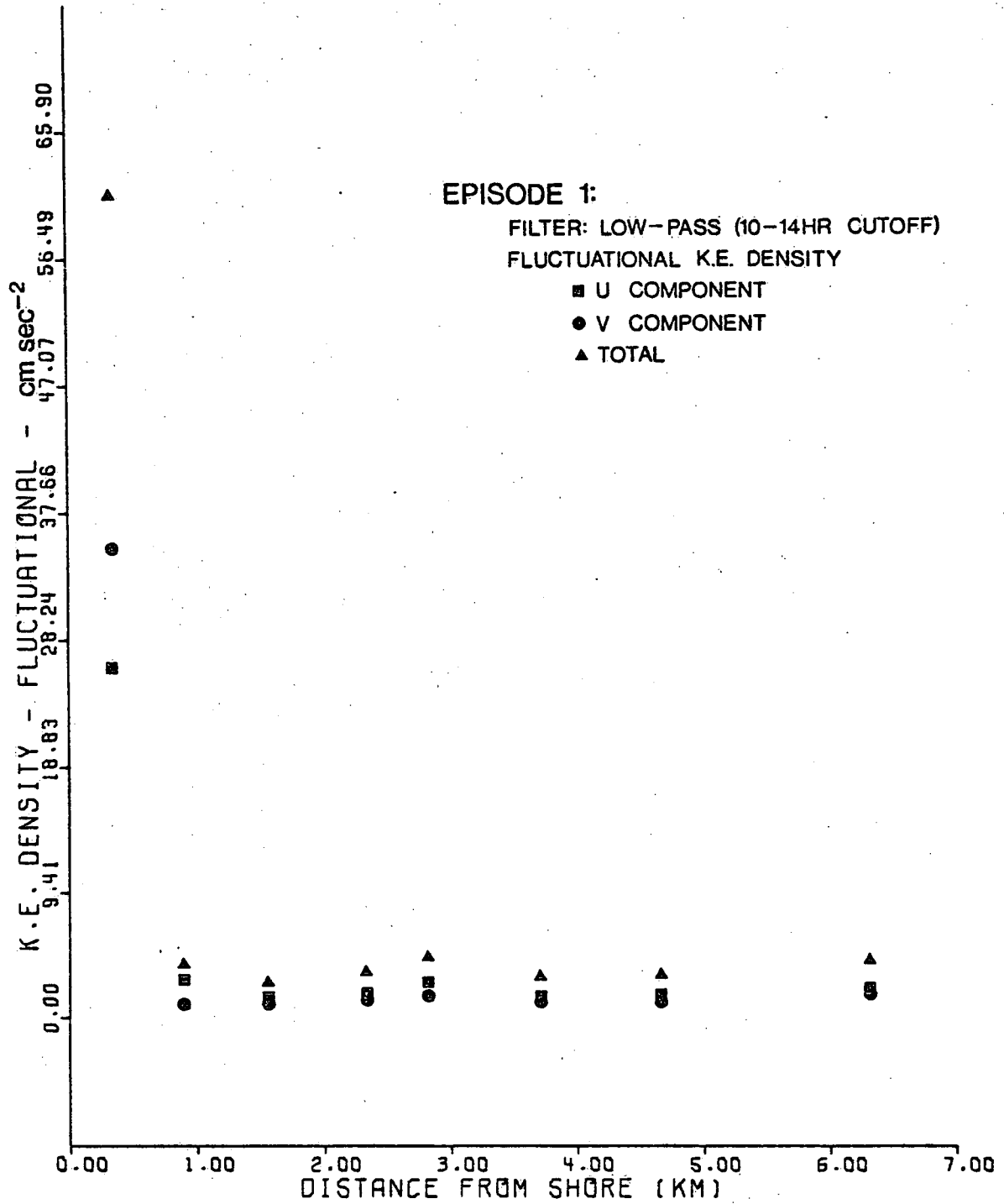


Figure 13.

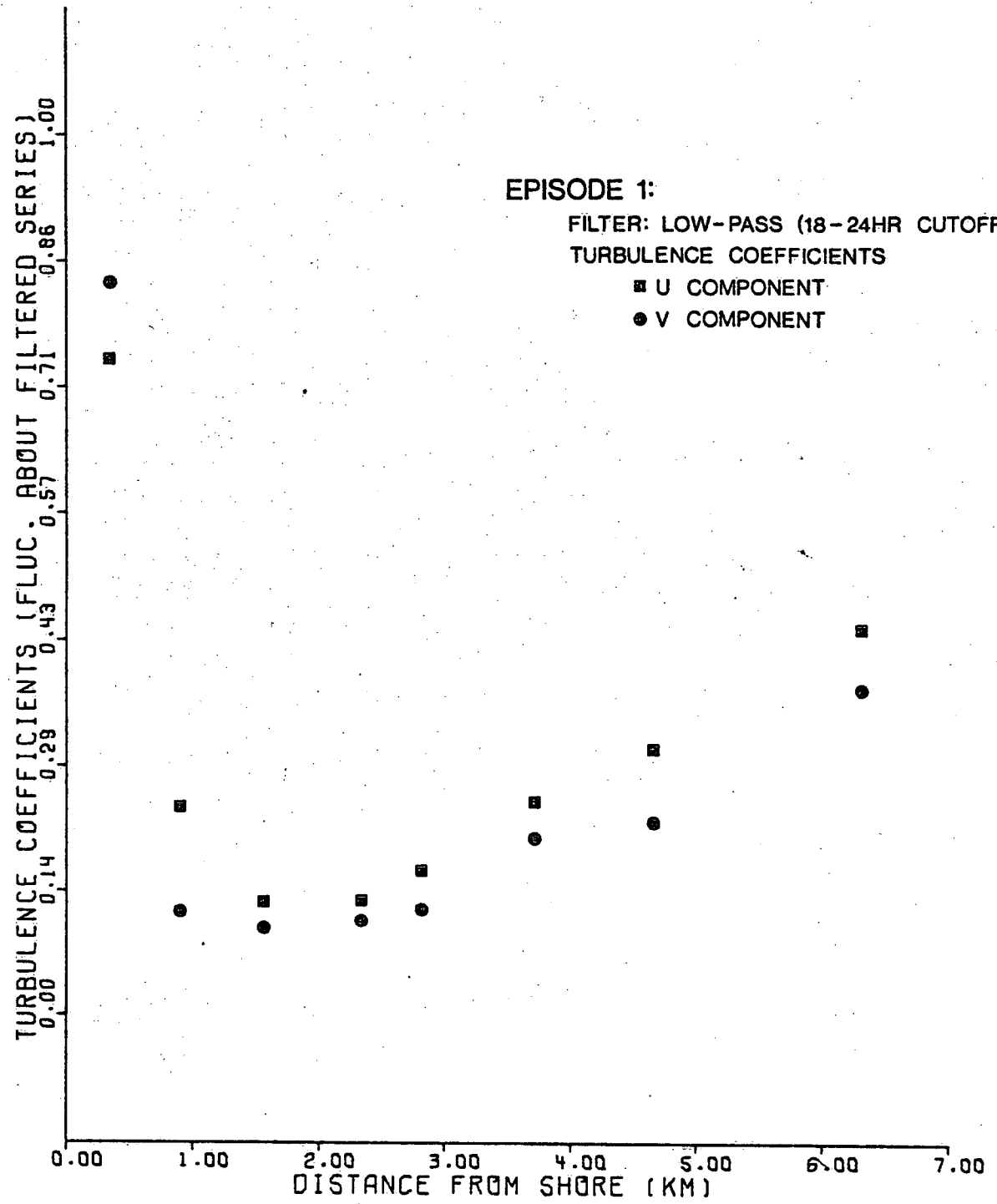


Figure 14.

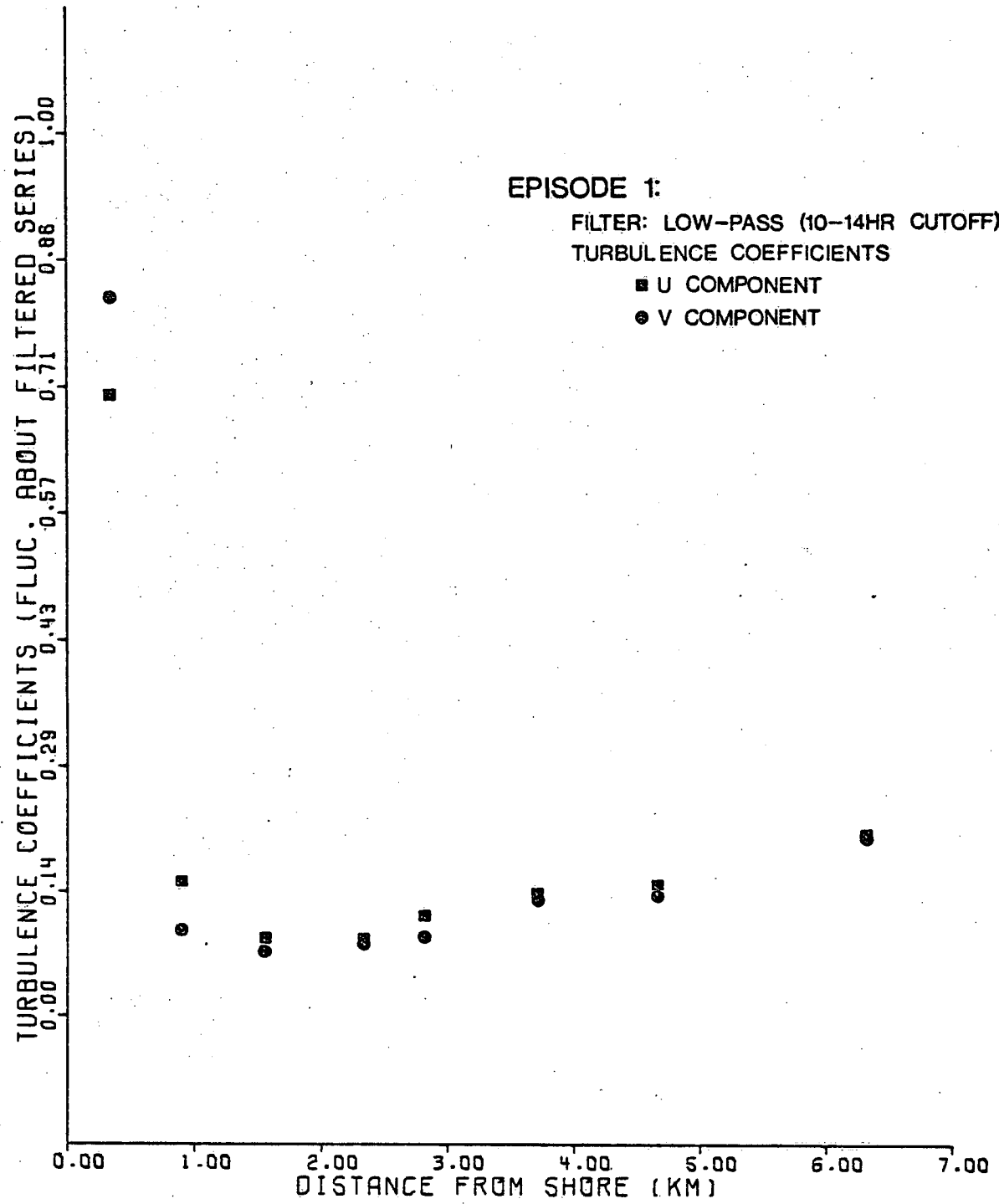


Figure 15.

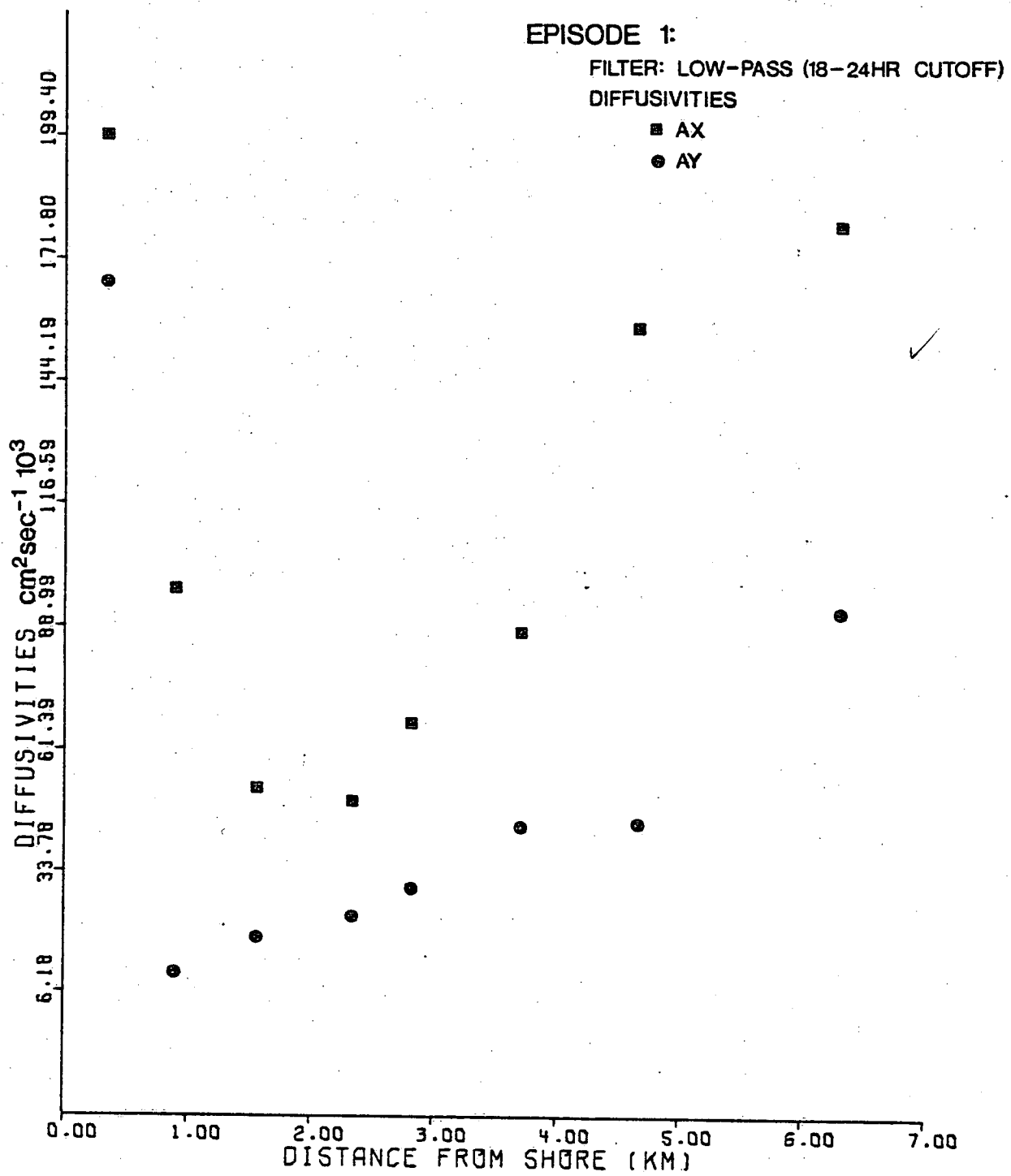


Figure 16.

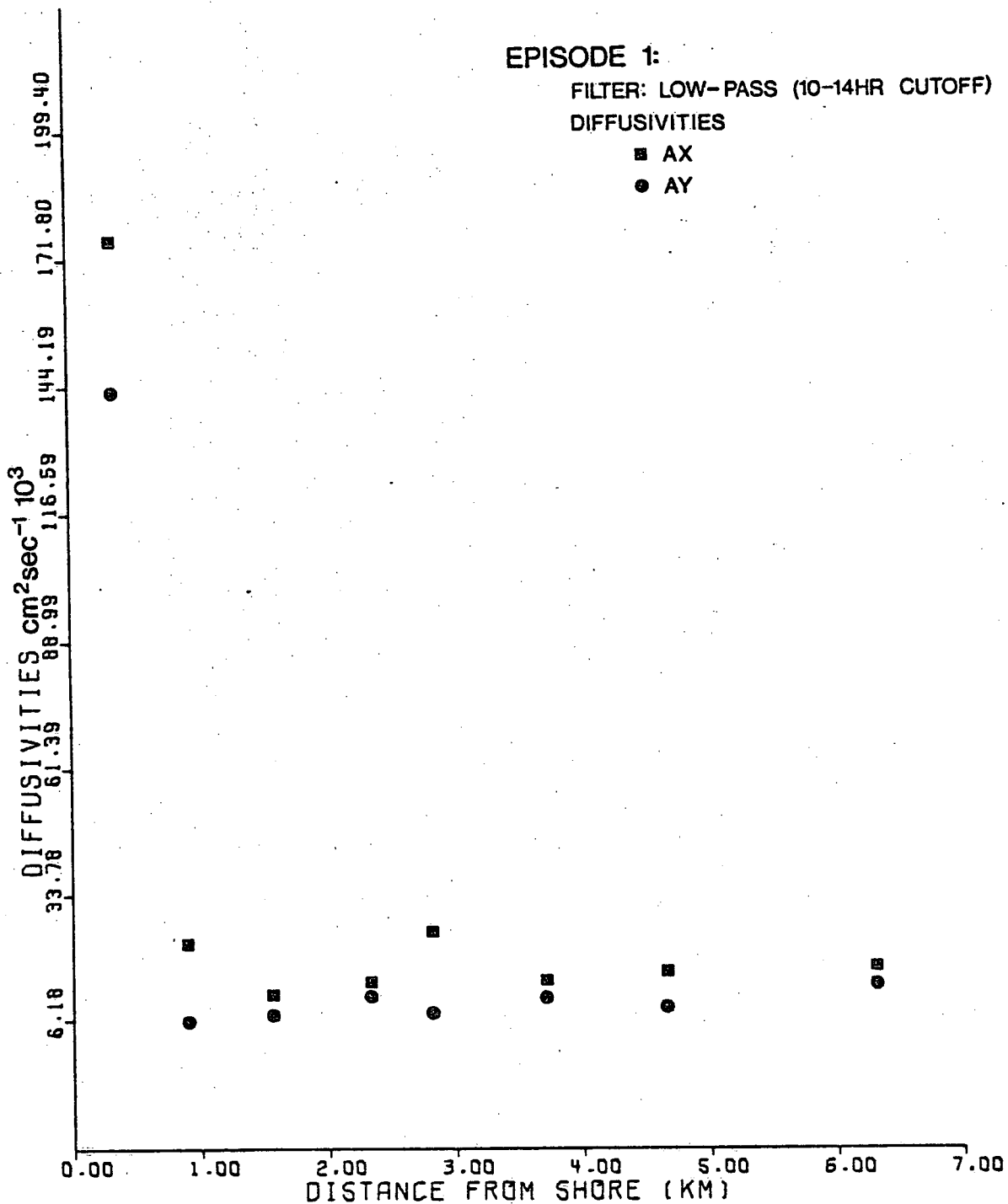


Figure 17.

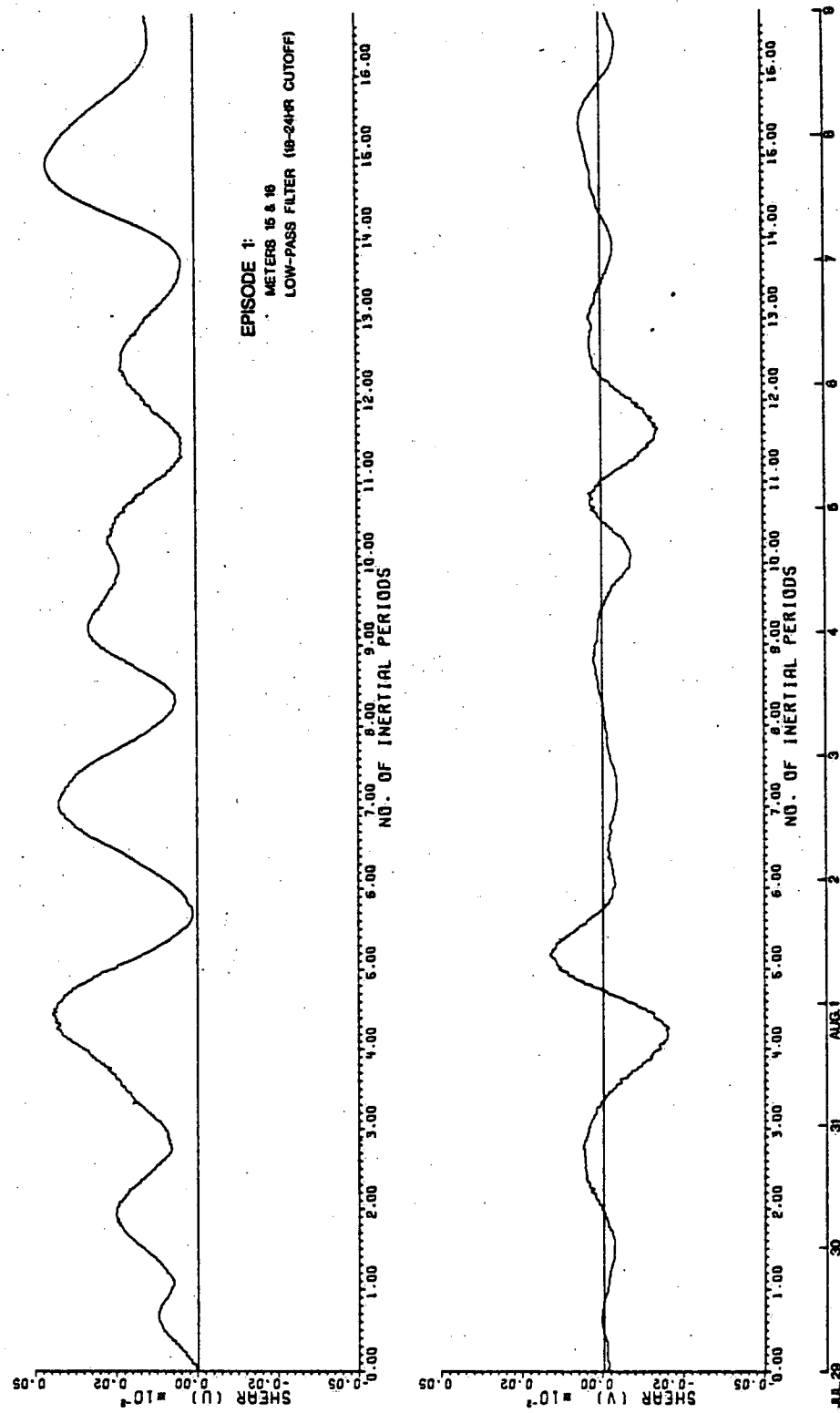


Figure 18.

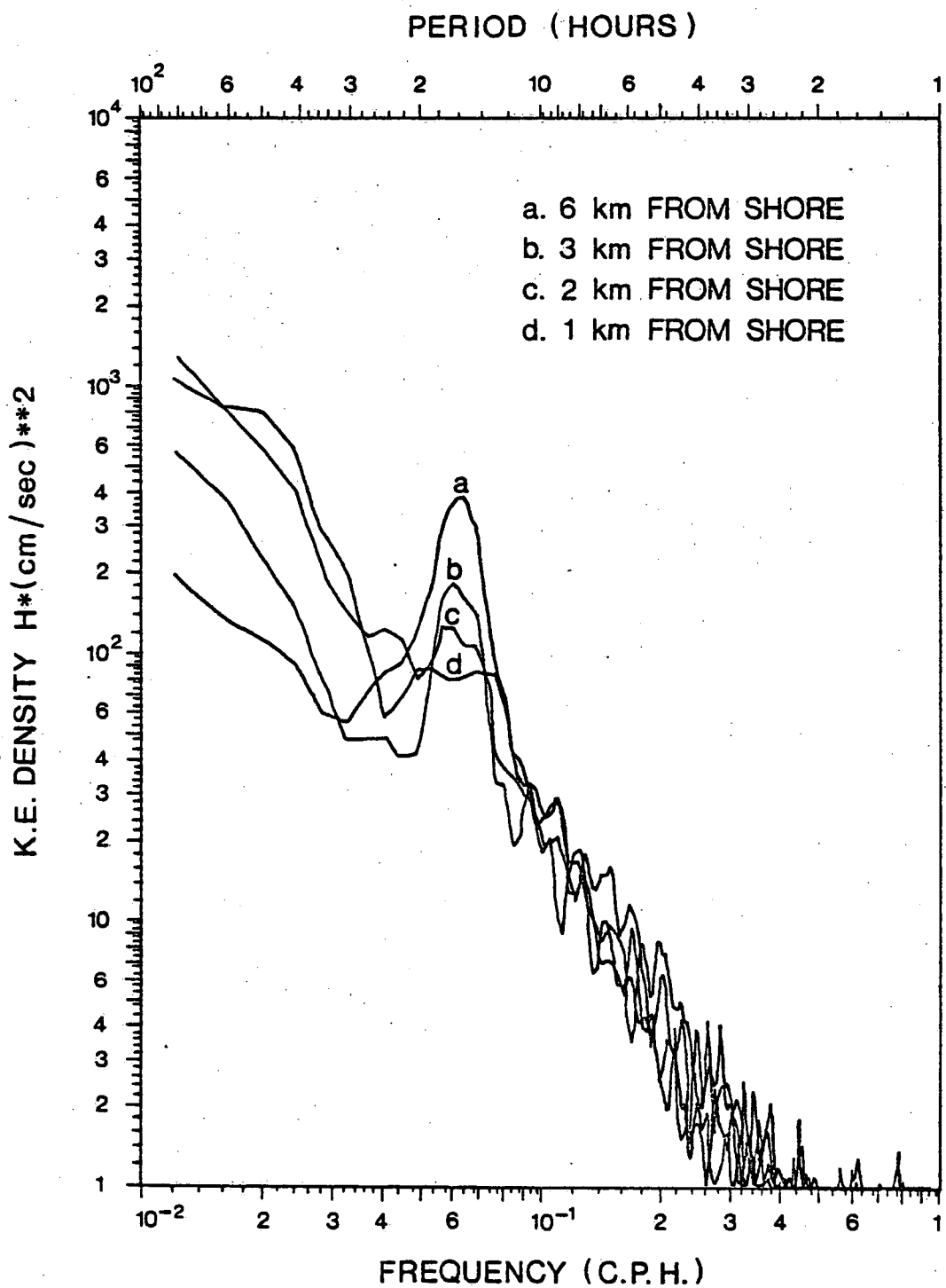


Figure 19.

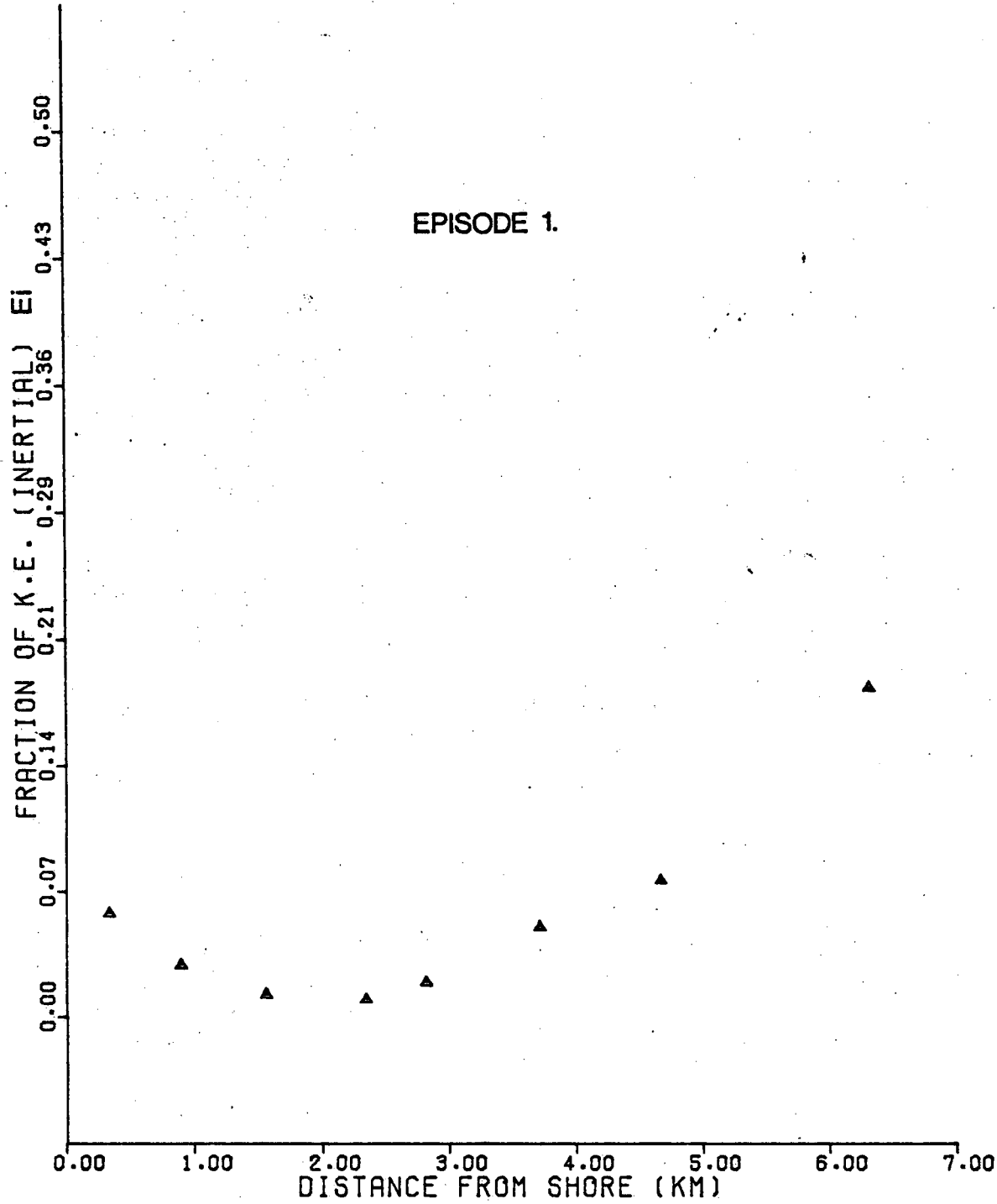


Figure 20.

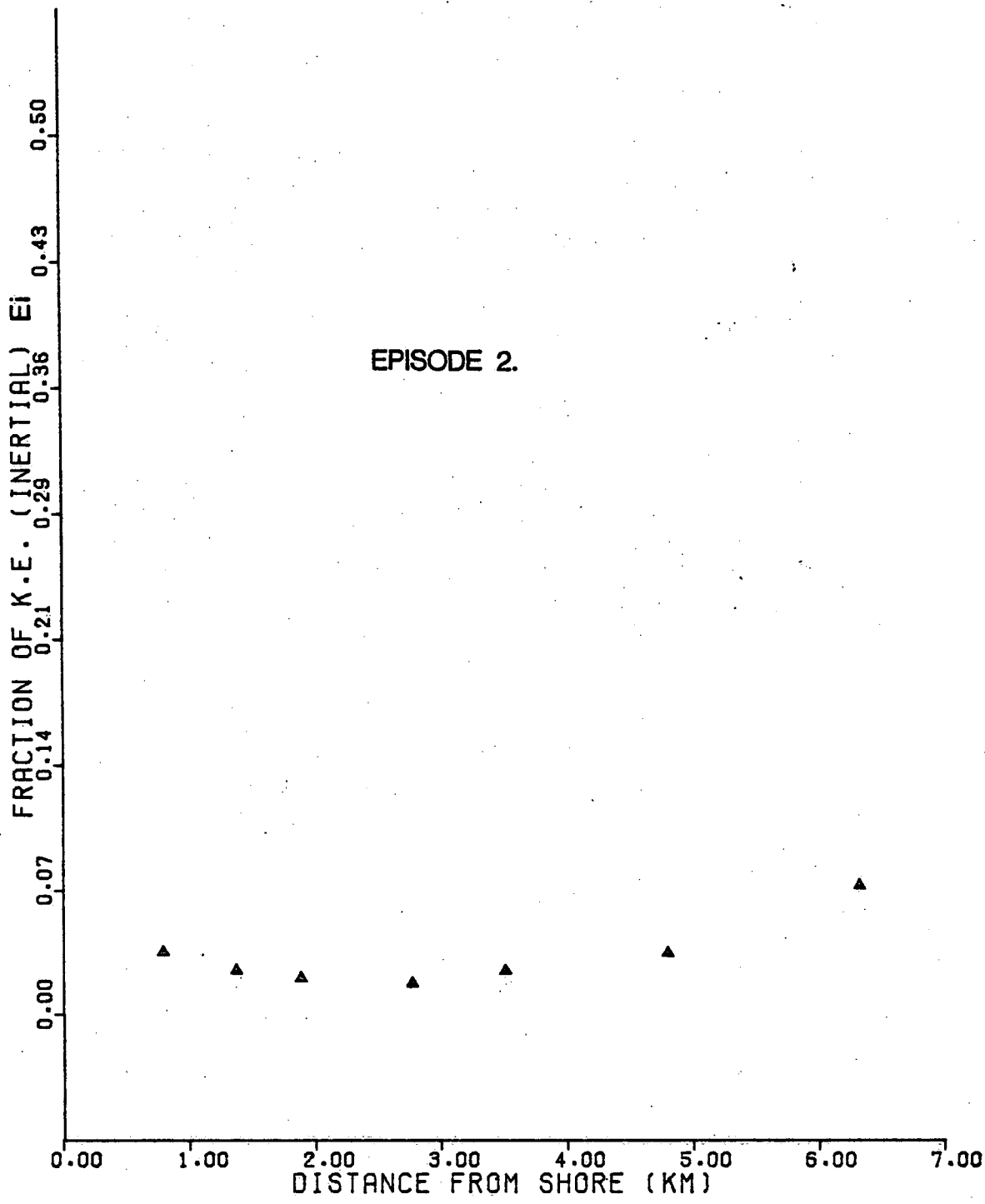


Figure 21.

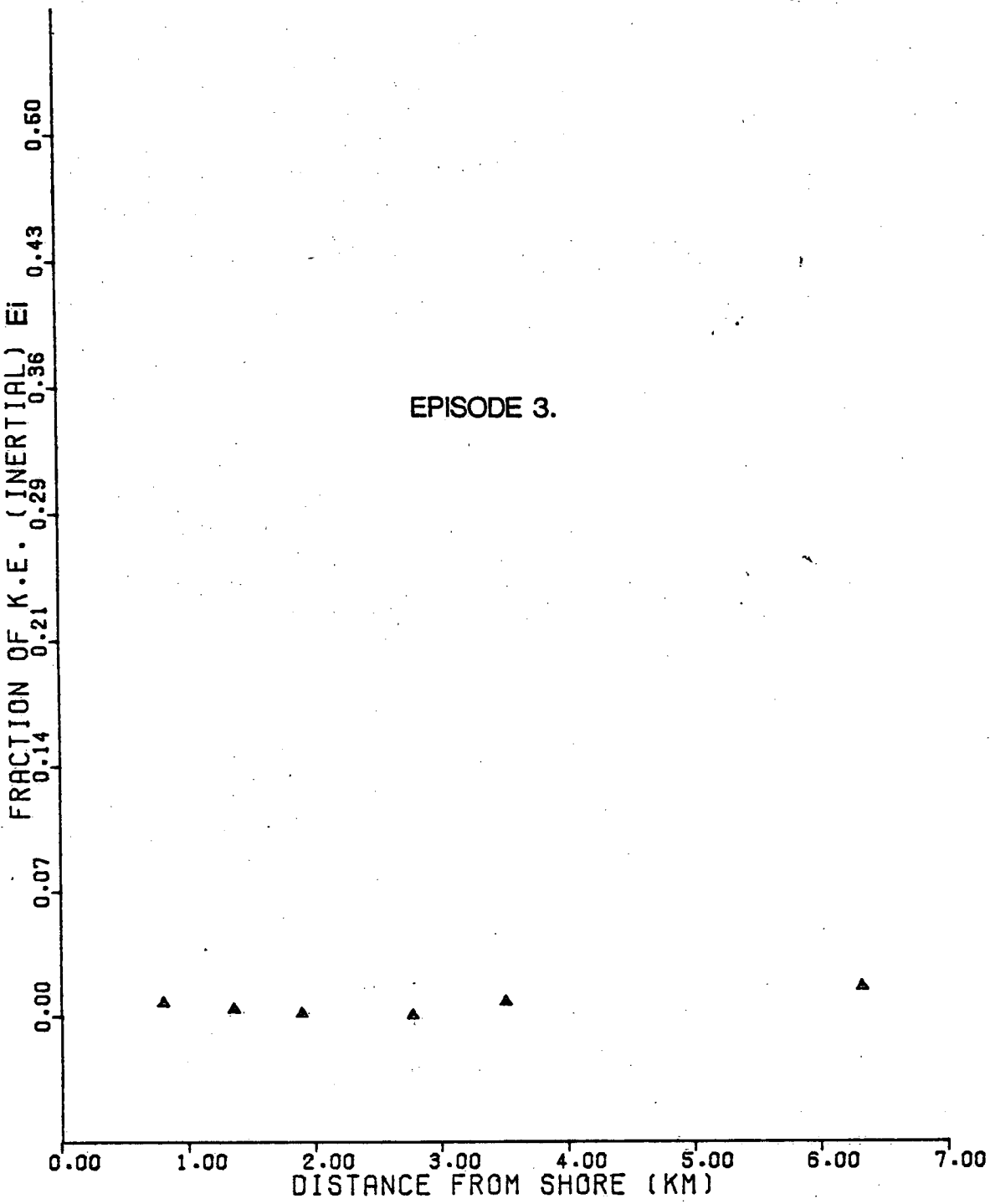


Figure 22.

TABLE 1a: GENERAL DETAILS OF THE DATA BASE

Current Meter No.	Type	Depth (M)	Sample Rate (Min)	Dist. from Shore (KM)				Duration (HHMM-DD-MM)				
				Series			Series A			Series B		
				A	B	C	Start	Finish	Start	Finish	Start	Finish
16	Geodyne	10	.33	.33	—	—	2230-22-07	1450-25-08	—	—	—	—
15	Plessey	10	20	90	90	79	2227-09-06	2228-22-07	1441-18-09	1617-18-09	1503-22-11	1503-22-11
14	Plessey	10	20	1.58	1.56	1.36	1248-18-05	1250-19-07	1348-19-07	0023-19-09	0121-19-09	1321-26-11
13	Plessey	10	20	1.95	2.34	1.88	1305-18-05	1345-19-07	1458-19-07	2356-18-09	0029-19-09	1357-26-11
12	Plessey	10	20	2.82	2.82	2.77	1348-18-05	0308-18-06	0404-27-07	2305-18-09	0037-19-09	1417-26-11
11	Plessey	10	20	3.71	3.71	3.51	1441-18-05	2341-08-06	1144-19-07	2220-18-09	2313-18-09	1434-26-11
10	Plessey	10	20	4.67	4.67	4.80	1520-18-05	2300-18-07	0047-19-07	2120-18-09	2211-18-09	1051-15-10
09	Plessey	10	20	6.31	6.31	6.31	—	—	1629-19-07	1832-18-09	2105-18-09	1830-26-11

TABLE 1b: DETAILS OF THE EPISODES

Episode	Current Meters (No.)	Series	Duration (HHMM-DD-MM)		No. of Hours	Remarks
			Start	Finish		
1	9-16 (8)	B	0000-29-07	0000-09-08	264	Persistent alongshore (NE) current; stratified conditions
2	9-15 (7)	C	0000-21-09	0000-14-10	672	Persistent alongshore (NE) current; stratified conditions
3	9, 11-15 (6)	C	0000-09-11	1500-21-11	303	Persistent alongshore (NE) current; unstratified conditions

TABLE 2. Episode 1

Meter	Dist. (km)	Mean (Cm . Sec ⁻¹)		Variance (Cm ² . Sec ⁻²)				Turbulence Coefficient				Diffusivity (x 10 ⁴ Cm ² .Sec ⁻¹)			
		U	V	10-14	18-24	10-14	18-24	10-14	18-24	10-14	18-24	Ax	Ay		
16	0.3	3.1	0.5	52.4	58.6	70.1	73.1	.71	.75	.82	.83	17.6	19.9	14.3	18-24
15	0.9	14.9	-0.4	5.7	13.3	2.3	3.3	.16	.24	.10	.12	2.3	9.7	0.6	1.1
14	1.6	19.1	-5.0	3.2	6.8	2.3	4.0	.09	.13	.08	.10	1.2	5.3	0.8	1.9
13	2.3	20.1	-5.8	3.6	7.8	3.4	5.4	.09	.13	.09	.11	1.5	5.0	1.2	2.4
12	2.8	18.6	-6.2	5.5	11.4	3.4	6.0	.12	.17	.09	.12	2.6	6.7	0.8	3.0
11	3.7	11.6	-2.9	3.3	9.9	3.0	6.9	.14	.25	.14	.21	1.5	8.8	1.1	4.4
10	4.7	10.1	-3.1	3.5	14.1	2.9	7.5	.15	.31	.14	.22	1.7	15.6	0.9	4.5
09	6.3	5.6	-0.8	4.3	19.6	4.3	14.0	.21	.44	.21	.37	1.8	17.9	1.4	9.2

Meter	Dist. (km)	K.E. (Cm ² .Sec ⁻²)			K.E. (Cm ² . Sec ⁻²)			Total			K.E. Ratio (Fluc./ Total)			
		Mean		Fluc.	Mean		Fluc.	K.E.		U	V	Total		
		U	V	10-14	18-24	10-14	18-24	10-14	18-24	10-14	18-24	10-14	18-24	
16	0.3	40	40	19	14	61	66	80	.66	.74	.87	.91	.77	.82
15	0.9	140	3	139	135	4	8	143	.02	.05	.33	.52	.03	.06
14	1.6	200	17	214	212	3	5	217	.01	.02	.07	.12	.01	.02
13	2.3	219	22	237	234	4	7	241	.01	.02	.08	.12	.01	.03
12	2.8	187	27	210	205	4	9	214	.01	.03	.06	.11	.02	.04
11	3.7	93	11	101	96	3	8	104	.02	.05	.14	.32	.03	.08
10	4.7	84	13	94	86	3	11	97	.02	.08	.11	.29	.03	.11
09	6.3	53	14	63	50	4	17	67	.04	.18	.15	.49	.06	.25

TABLE 3. Episode 2.

Meter	Dist. (km)	Mean (Cm . Sec ⁻¹)	Variance (Cm ² . Sec ⁻²)				Turbulence Coefficient				Diffusivity (x 10 ⁴ Cm ² . Sec ⁻¹)				
			U	V	10-14	18-24	U	V	10-14	18-24	U	V	10-14	18-24	
15	0.8	5.5	-3.9	46.0	50.7	51.4	56.8	.49	.52	.52	.55	15.6	20.0	13.0	16.0
14	1.4	11.3	-2.3	8.7	14.6	16.4	19.7	.19	.24	.26	.28	4.6	7.4	3.0	5.5
13	1.9	12.9	-2.5	9.4	14.1	17.3	21.6	.18	.22	.25	.28	4.8	7.6	2.6	4.6
12	2.8	14.9	-4.8	8.5	13.5	8.3	11.8	.16	.20	.16	.19	3.8	6.6	1.8	3.9
11	3.5	16.2	-4.6	6.7	14.6	9.9	15.8	.13	.19	.16	.20	2.9	8.0	2.2	6.3
10	4.8	15.7	-3.7	14.0	24.0	16.8	26.7	.19	.25	.21	.26	5.4	11.7	4.0	10.4
09	6.3	12.4	-5.4	24.4	45.7	27.5	41.3	.27	.37	.29	.35	8.8	23.0	7.3	18.0

Meter	Dist. (km)	K.E. ($\text{Cm}^2 \cdot \text{Sec}^{-2}$)			K.E. ($\text{Cm}^2 \cdot \text{Sec}^{-2}$)			Total			K.E. Ratio (Fluc. / Total)			
		U	V	Mean	10-14	18-24	Fluc.	10-14	18-24	K.E.	U	V	Total	
15	0.8	84	57	92	87	49	54	141	.27	.30	.45	.49	.35	.38
14	1.4	166	18	172	167	12	17	184	.03	.04	.46	.56	.07	.09
13	1.9	191	19	197	192	13	18	210	.02	.04	.46	.57	.06	.08
12	2.8	207	33	232	227	8	13	240	.02	.03	.13	.18	.04	.05
11	3.5	246	36	274	267	8	15	282	.01	.03	.14	.22	.03	.05
10	4.8	245	37	267	257	15	25	282	.03	.05	.23	.36	.05	.09
09	6.3	176	62	212	194	26	44	238	.07	.13	.22	.33	.11	.18

TABLE 4. Episode 3.

Meter	Dist. (km)	Mean (Cm . Sec ⁻¹)		Variance (Cm ² . Sec ⁻²)		Turbulence Coefficient		Diffusivity (x 10 ⁴ Cm ² .Sec ⁻¹)	
		U	V	U	V	U	V	Ax	Ay
15	0.8	13.4	-2.9	35.7	38.0	95.0	97.2	.32	.33
14	1.4	18.6	-4.0	7.4	9.0	21.8	23.0	.14	.15
13	1.9	19.6	-3.7	6.1	7.5	19.9	20.4	.12	.13
12	2.8	19.8	-8.1	3.7	4.5	8.1	8.6	.09	.10
11	3.5	20.5	-8.3	6.7	7.9	8.1	8.8	.11	.12
09	6.3	11.7	-3.0	16.9	19.1	38.1	41.6	.28	.30

Meter	Dist. (km)	K.E. (Cm ² .Sec ⁻²)			K.E. (Cm ² . Sec ⁻²)			Total			K.E. Ratio (Fluc./ Total)			
		Mean		Fluc.	K.E.		Fluc.	K.E.		U	V	Ratio		
		U	V	10-14	18-24	10-14	18-24	10-14	18-24	10-14	18-24	10-14	18-24	
15	0.8	172	62	169	166	65	68	234	.10	.11	.77	.79	.28	.29
14	1.4	253	24	262	261	15	16	277	.01	.02	.45	.47	.05	.06
13	1.9	281	20	288	287	13	14	301	.01	.01	.49	.50	.04	.05
12	2.8	277	51	322	321	6	7	328	.01	.01	.08	.08	.02	.02
11	3.5	314	51	358	357	7	8	365	.01	.01	.08	.09	.02	.02
09	6.3	136	40	149	146	27	30	176	.06	.07	.47	.52	.16	.17

APPENDIX A

Appendix A

Numerical Filtering Technique

In order to define a nonstationary mean flow it was necessary to process the time series current data with a numerical low-pass filter. This had the effect of removing high-frequency oscillations from the data, while leaving the distribution of the remaining frequencies essentially unchanged. Subsequent differencing of the original and filtered series resulted in a new series of fluctuations which had only the high frequency oscillations remaining.

Filtering was accomplished by using a method developed by Graham (1963). It involved calculating a set of $2N + 1$ weights $\{w_i\}$ $i = 0, \pm 1, \dots, \pm N$ as follows:

$$w_i = \phi_i / \sum_{j=-N}^N \phi_j$$

$$\text{where } \phi_j = \frac{1}{2\pi j\Delta t} \frac{[\sin 2\pi j\Delta t f_t + \sin 2\pi j\Delta t f_c]}{[1 - 4(f_t - f_c)^2 (j\Delta t)^2]}$$

Δt = sampling interval

f_t = lowest frequency passed with zero gain

f_c = highest frequency passed with unit gain

Note 1: $\phi_0 = \lim_{i \rightarrow 0} \phi_i = f_t + f_c$

Note 2: $w_i = w_{-i}$

Each point u_i of the original series was then filtered by evaluating $F(u_i)$ where

$$F(u_i) = \sum_{j=-N}^N w_j u_{i+j} = w_0 u_i + \sum_{j=1}^N w_j (u_{i+j} + u_{i-j})$$

This resulted in a new time series $\{f_i\}$ which had frequencies greater than f_t removed, while frequencies less than f_c remained unchanged.

Due to the nature of the filter function F we required N extra points to be available from both ends of each episode in order to evaluate F at all points.

If $\{u_i\}$ and $\{f_i\}$ are respectively the unfiltered and filtered series, $i = 1, 2, \dots, m$, then it can be shown that:

$$\bar{f} = \bar{u} + b$$

where $a = \sum_{k=-N}^N w_k$

$$\text{and } b = \frac{1}{m} \sum_{k=1}^N w_k \left(\sum_{i=1}^k (u_{i+m} - u_{i+m-k}) - (u_i - u_{i-k}) \right)$$

By definition we have that $\bar{f} = \bar{u}$, therefore we corrected the filtered velocities by setting

$$f_i = f_i + \bar{u} - \bar{f} = f_i + (1-a)\bar{u} - b$$

As noted above, the fluctuation time series has only high frequency oscillations remaining in its power spectrum. This series may be obtained directly from the data using a high-pass filter as follows:

Given weights $\{w_i\}$ as before, we define a set of high-pass filter weights $\{\psi_i\}$:

$$\psi_i = \begin{cases} 1-w_0 & i=0 \\ -w_i & i \neq 0 \end{cases}$$

The fluctuation u'_i for point u_i of the original series is

$$u'_i = u_i - f_i$$

$$= u_i - (w_0 u_i + \sum_{j=1}^N w_j (u_{i+j} + u_{i-j}) - b) \text{ since } a = 1$$

$$= (1 - w_0) u_i + \sum_{j=1}^N - w_j (u_{i+j} + u_{i-j}) + b$$

$$= \psi_0 u_i + \sum_{j=1}^N \psi_j (u_{i+j} + u_{i-j}) + b$$

now $b = \sum_{j=1}^N w_k c_k$

$$= - \sum_{j=1}^N \psi_k c_k$$

$$= -b'$$

therefore $u'_i = \psi_0 u_i + \sum_{j=1}^N \psi_j (u_{i+j} + u_{i-j}) - b'$

Thus, by subjecting the data to a high pass filter and correcting with the term b' we obtain identical results.

Following the above scheme, we used two different low-pass filters to generate a nonstationary mean flow. One had a cut-off range from 10 - 14 hours, while the other cut-off was from 18 - 24 hours. Seventy-two weights were used for both filters, thus requiring 24 hours of extra data from both ends of each episode.

The amplitude response curves for these filters are shown in

figures A1 and A2. Figure A3 shows the superimposed spectral density plots of the unfiltered and two filtered series for meter 09 during the period from July 20 to September 19. These show how motions with periods less than the lower cut-off limit have been effectively removed. This result is substantiated further in figure A4 which is the superimposed plots of the original and filtered time series for meter 09 over a portion of this interval. Of particular interest is the obvious removal of the inertial oscillation by the 18-24 hour filter.

In an effort to quantify the performance of the filters we have plotted the normalized integrals of the spectral densities. These are defined as follows:

Let $D(f)$ be the K. E. density at frequency f .

$$I(f) = \int_0^f D(f) df / \int_0^\infty D(f) df$$

Thus $I(f)$ is the fraction of energy in motions with frequencies less than f , and a plot of $I(f)$ vs f allows one to calculate the fraction of energy in any given frequency band. Fig. A5 shows the three curves for the unfiltered and two filtered series.

In the filtered series with a 10 - 14 hr filter cut-off virtually 100% of the energy is in oscillations with periods greater than 10 hours. The corresponding value for the unfiltered series is 93%. Similarly, for the 18 - 24 hour filter, in excess of 99% of the energy is in periods greater than 18 hours, while the unfiltered series has a corresponding value of 77%.

A

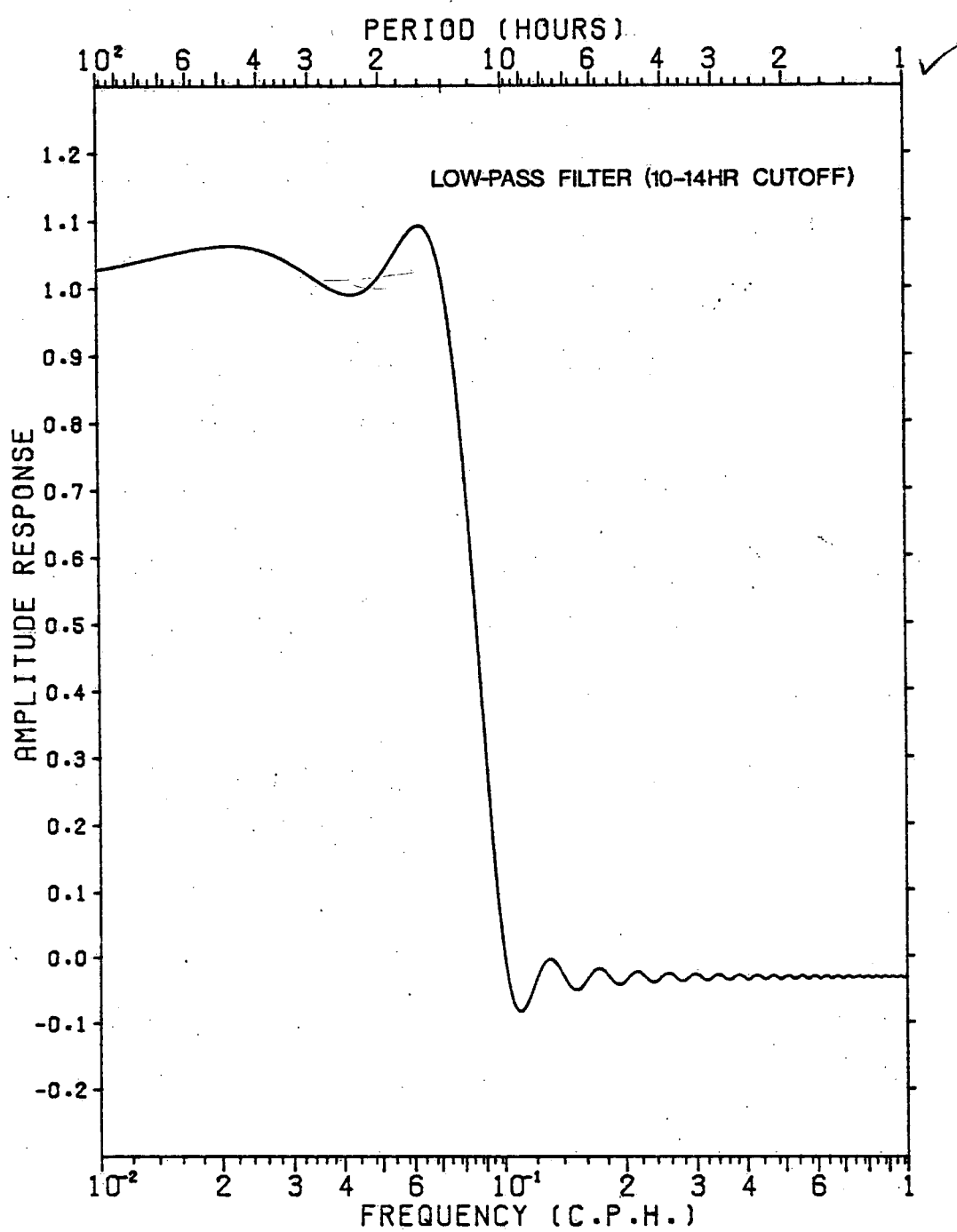


Figure A1.

B

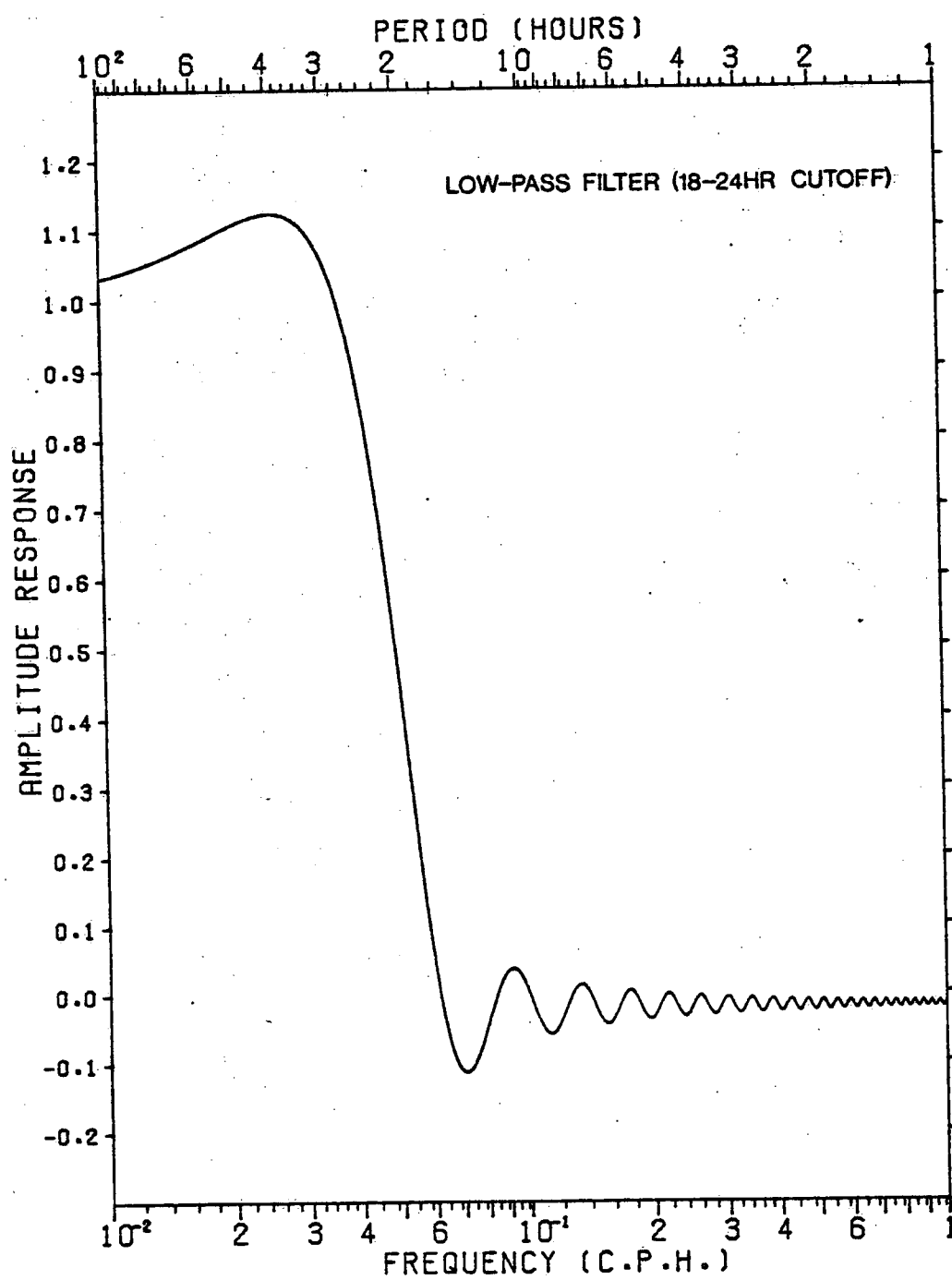


Figure A2.

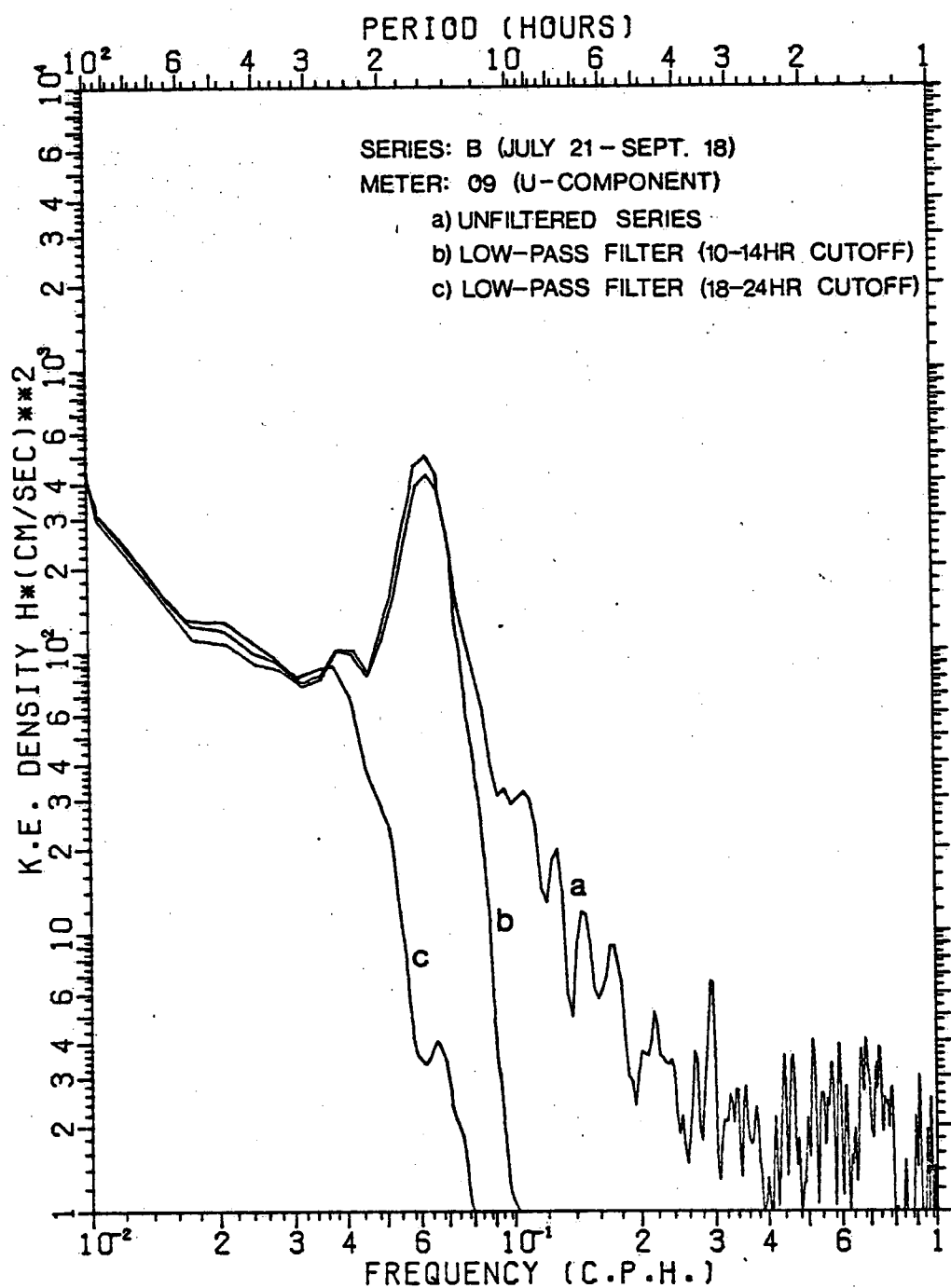


Figure A3.

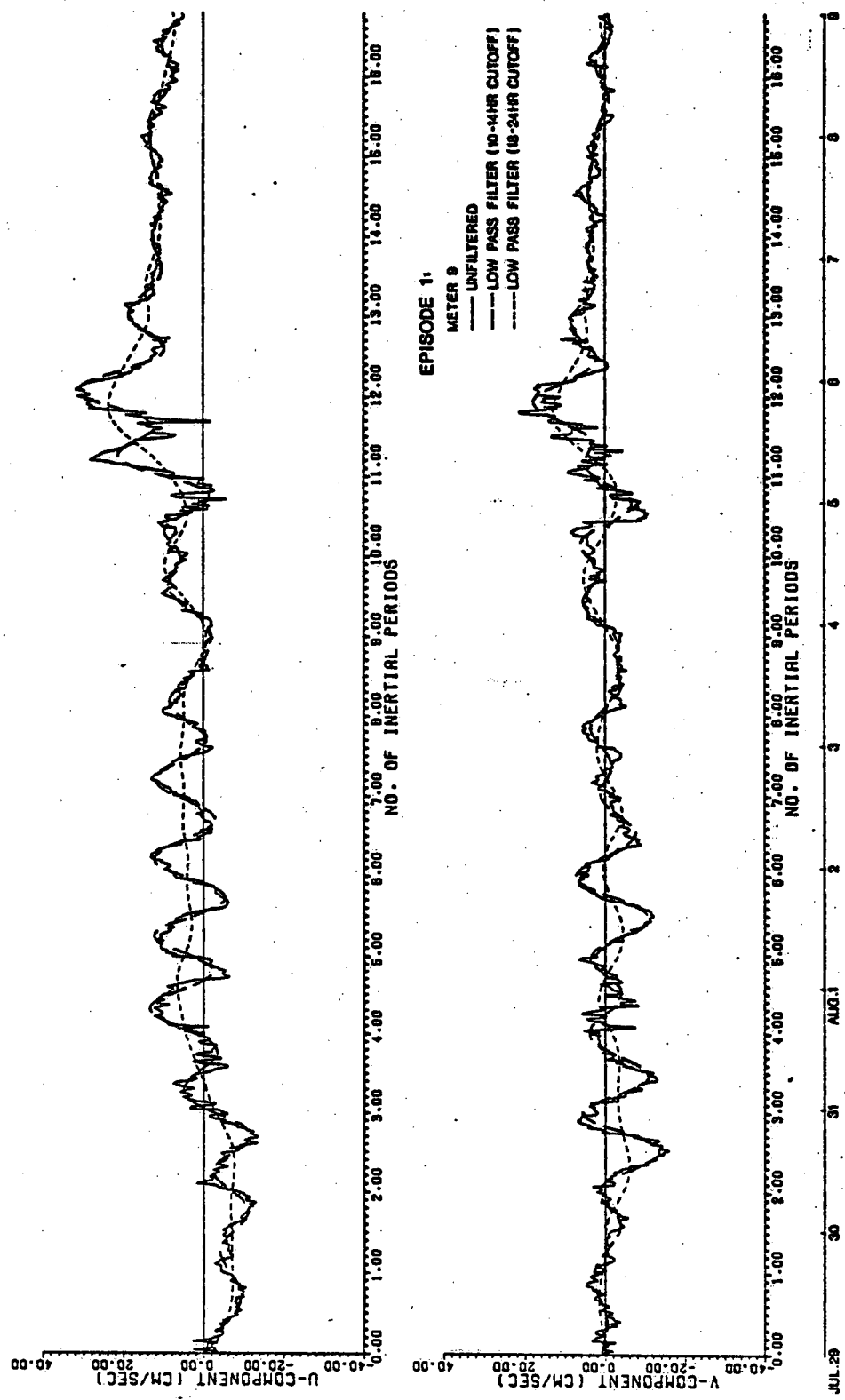


Figure A4.

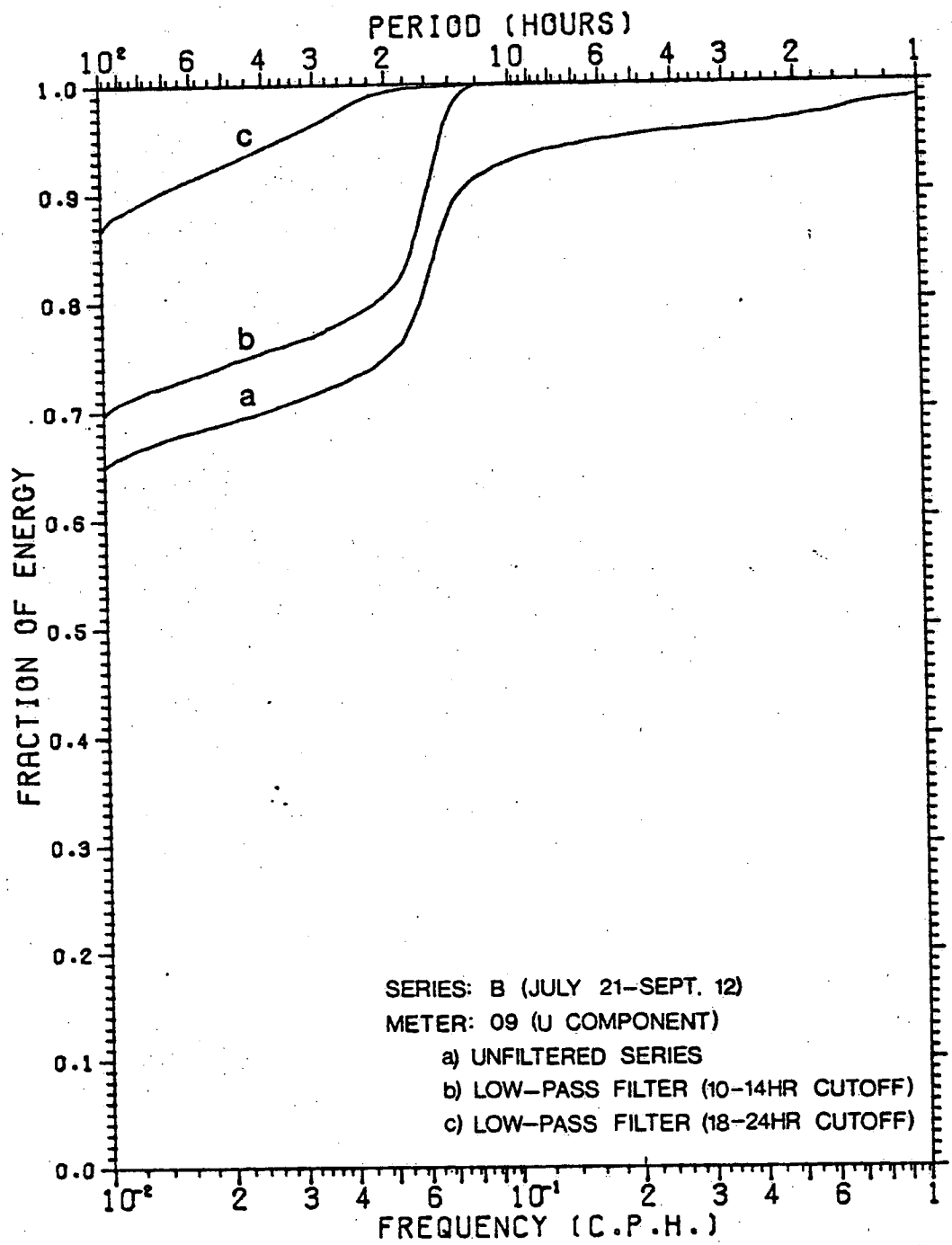
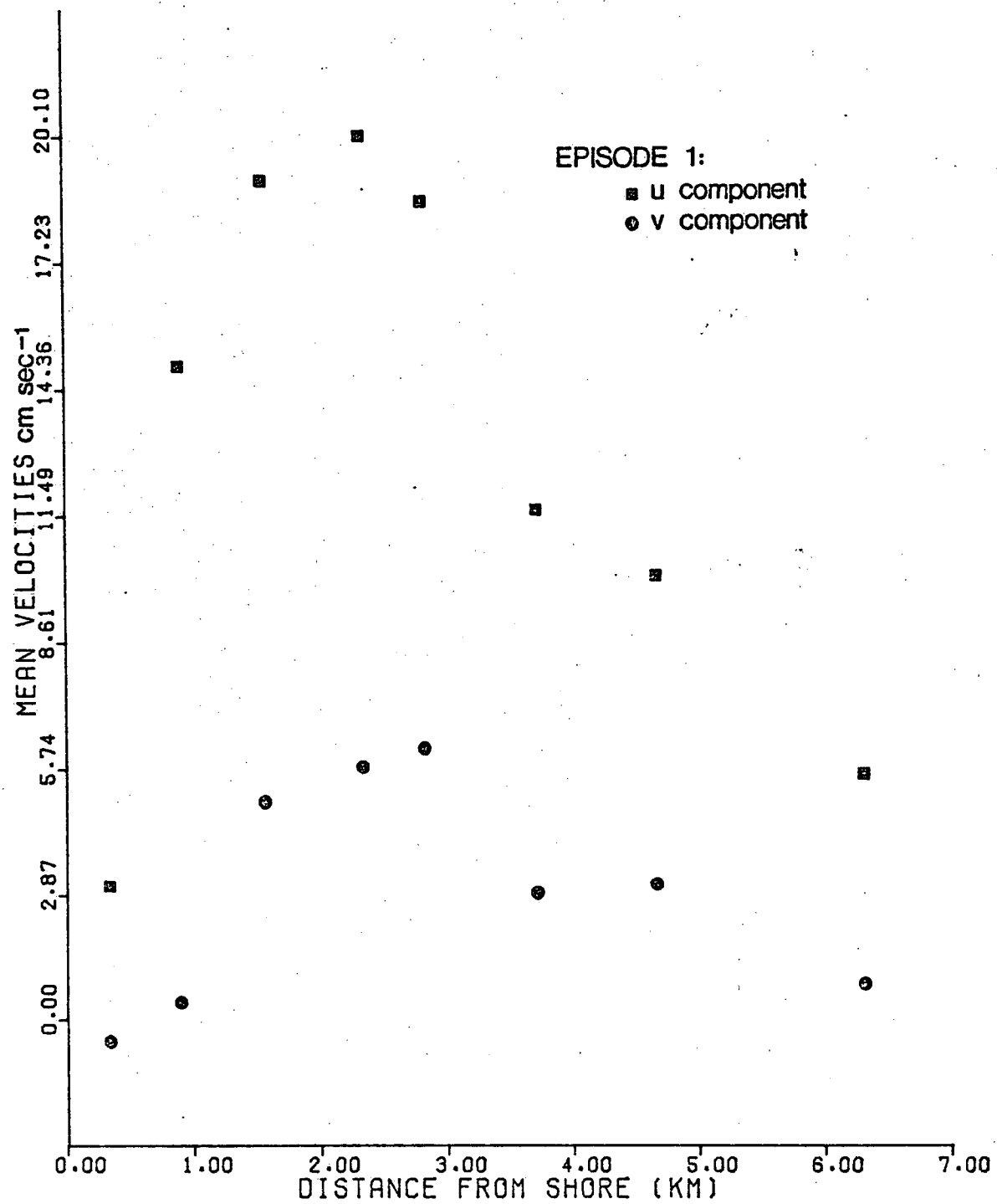
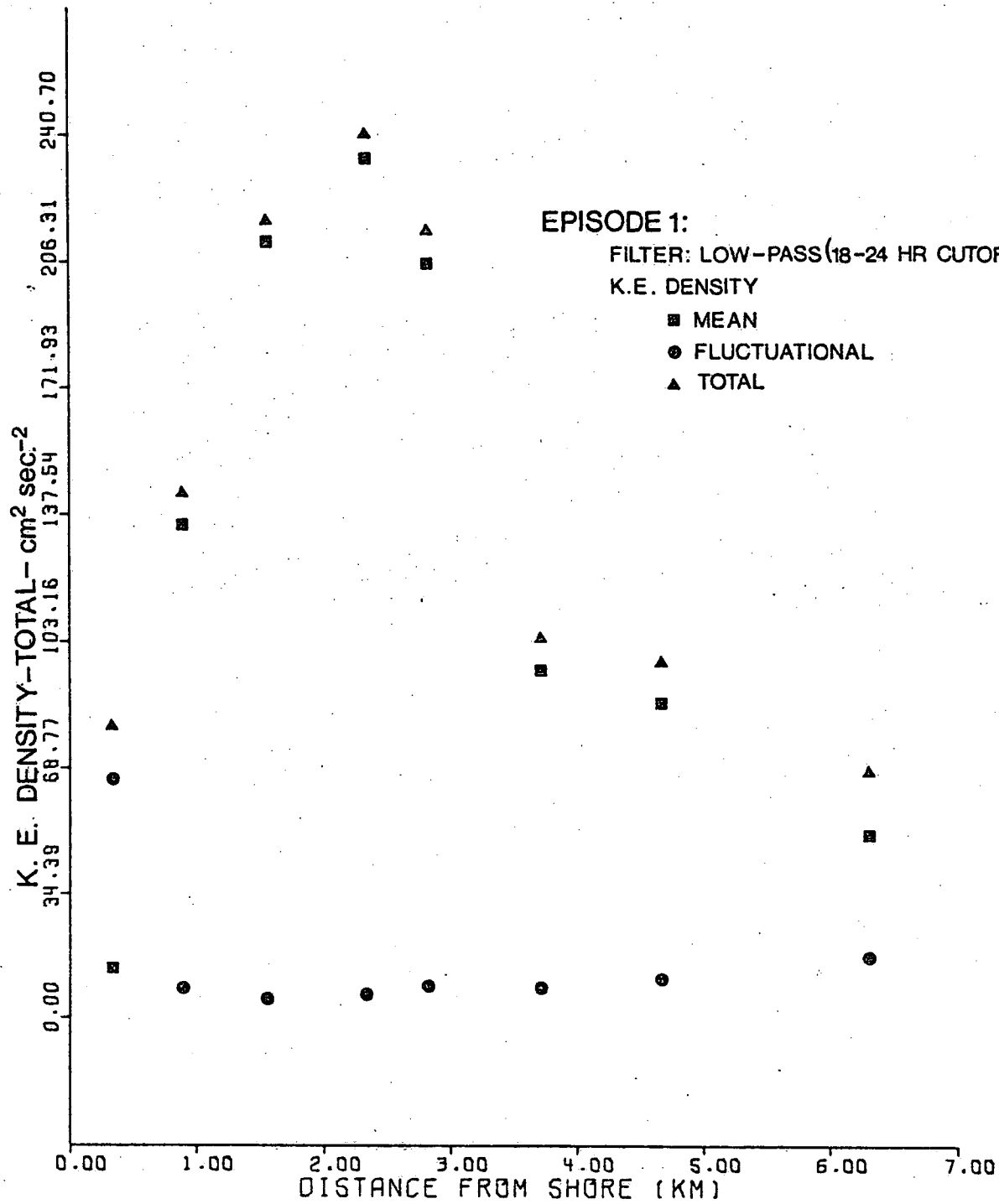
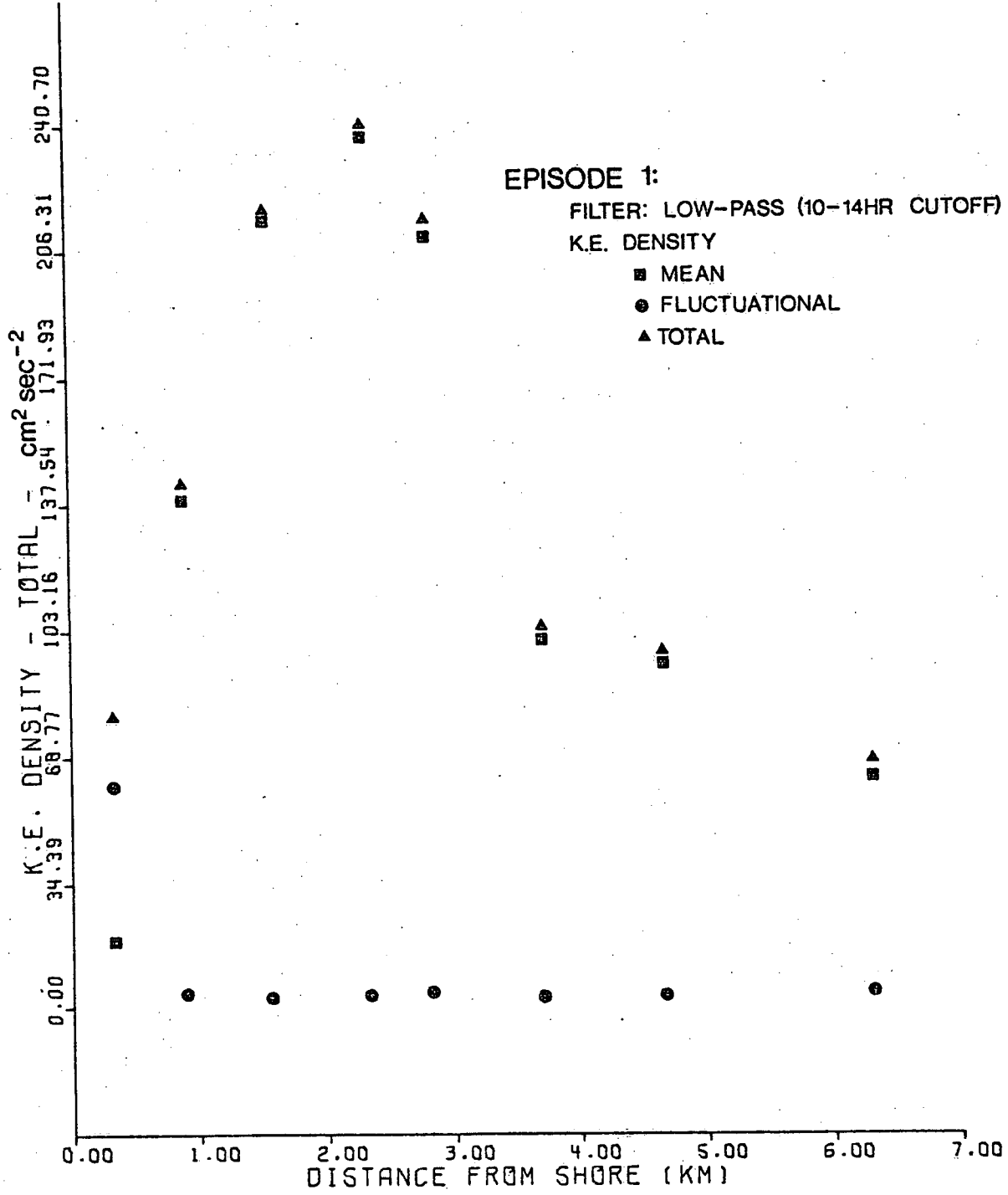


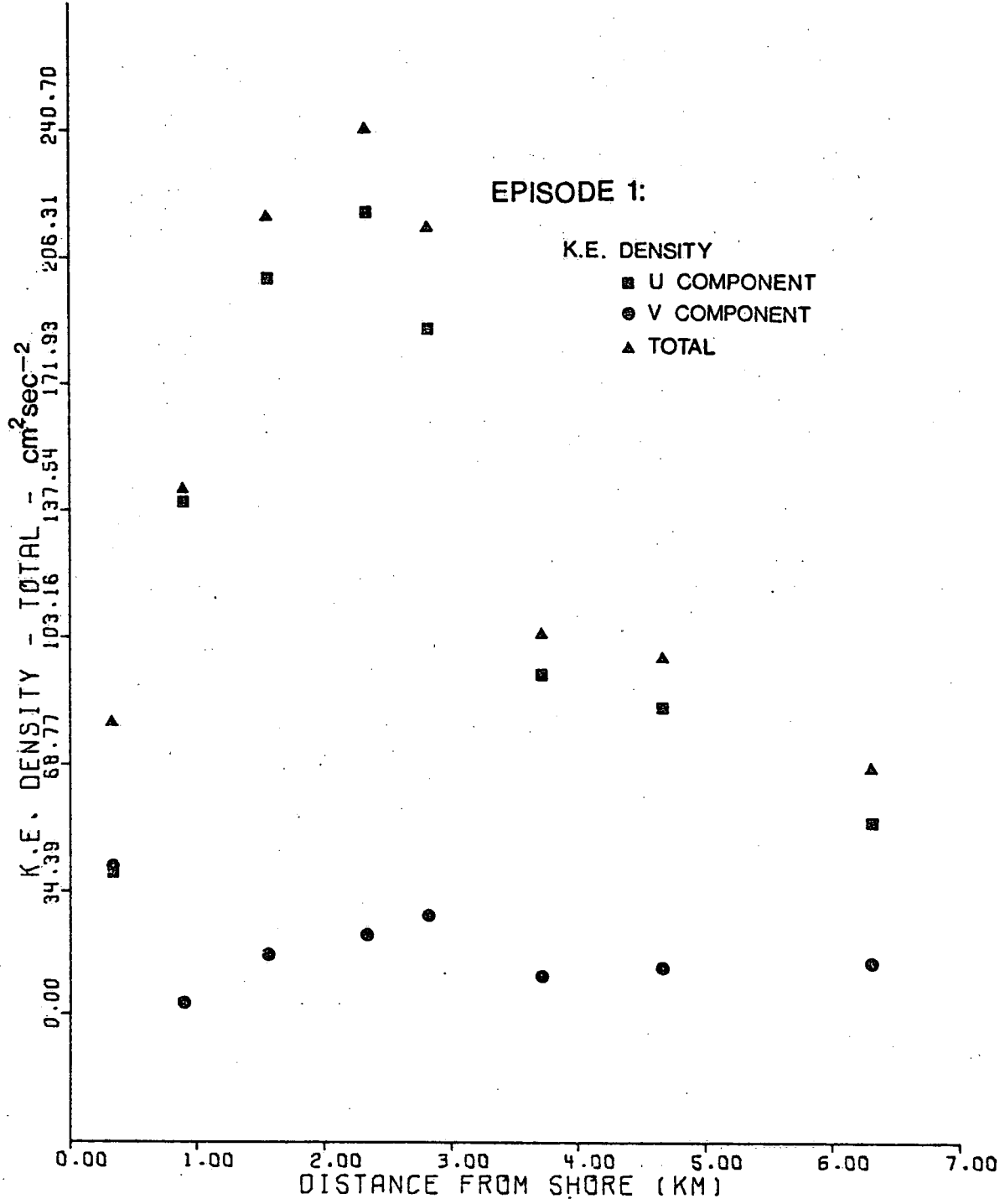
Figure A5.

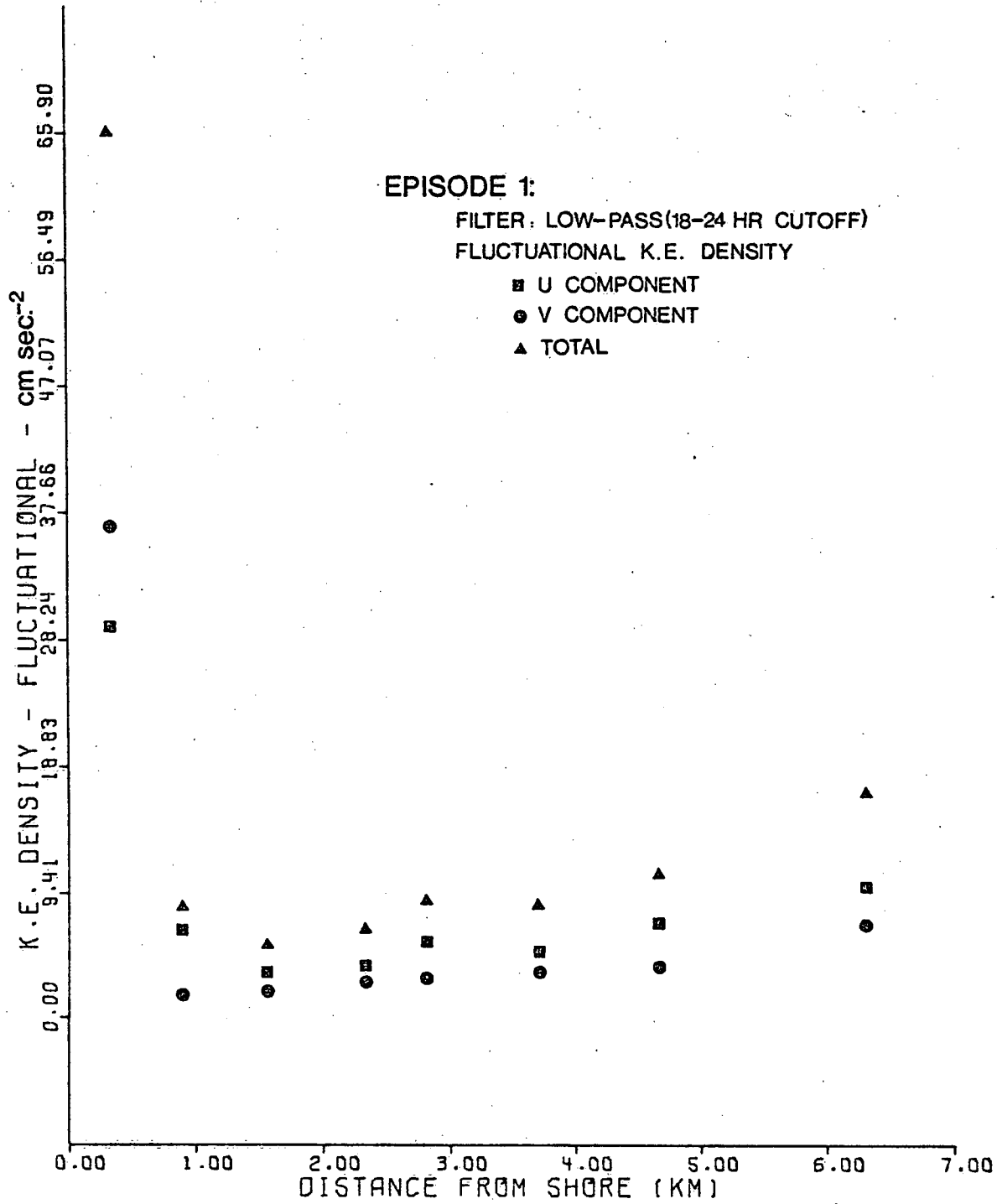
APPENDIX B

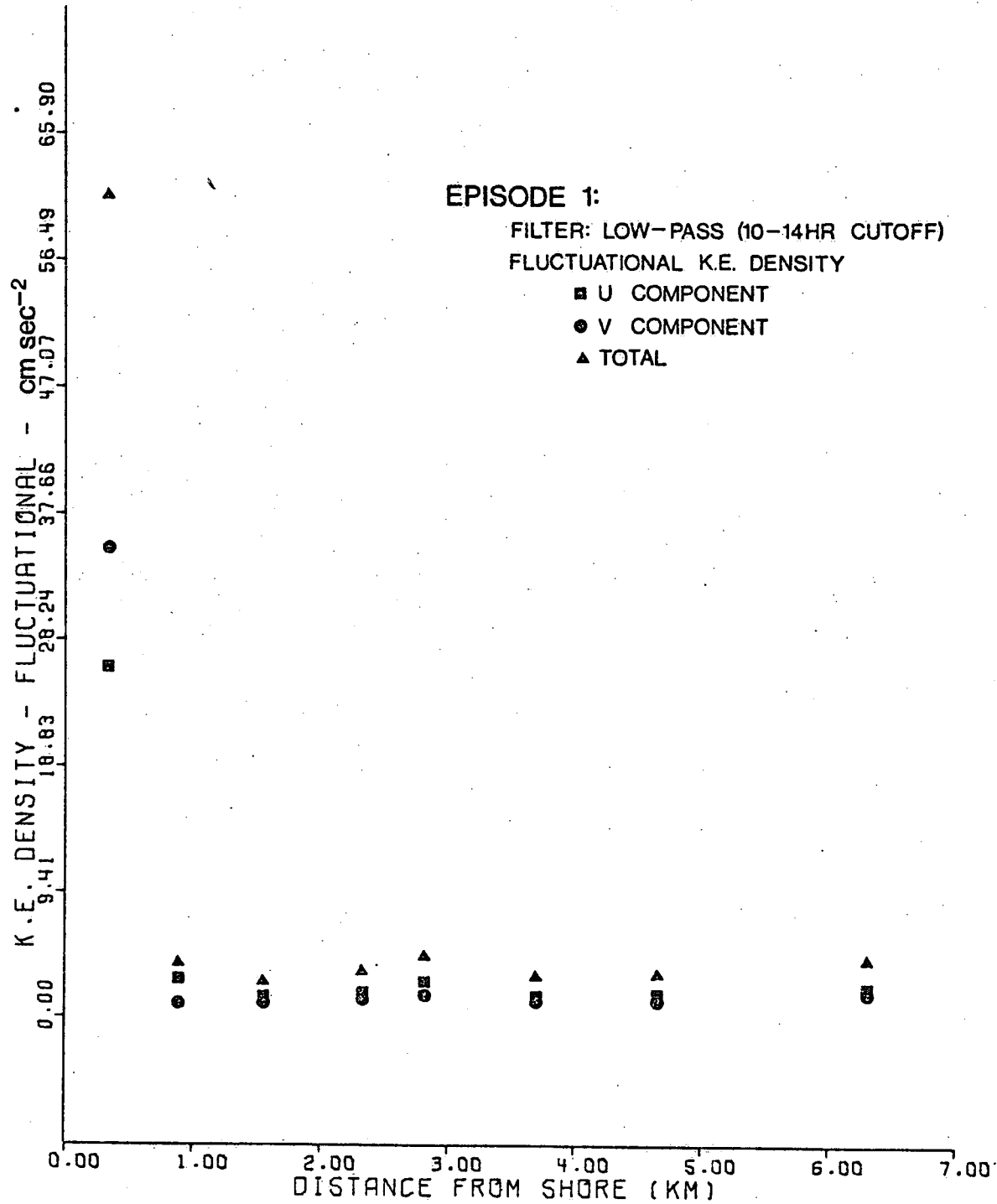


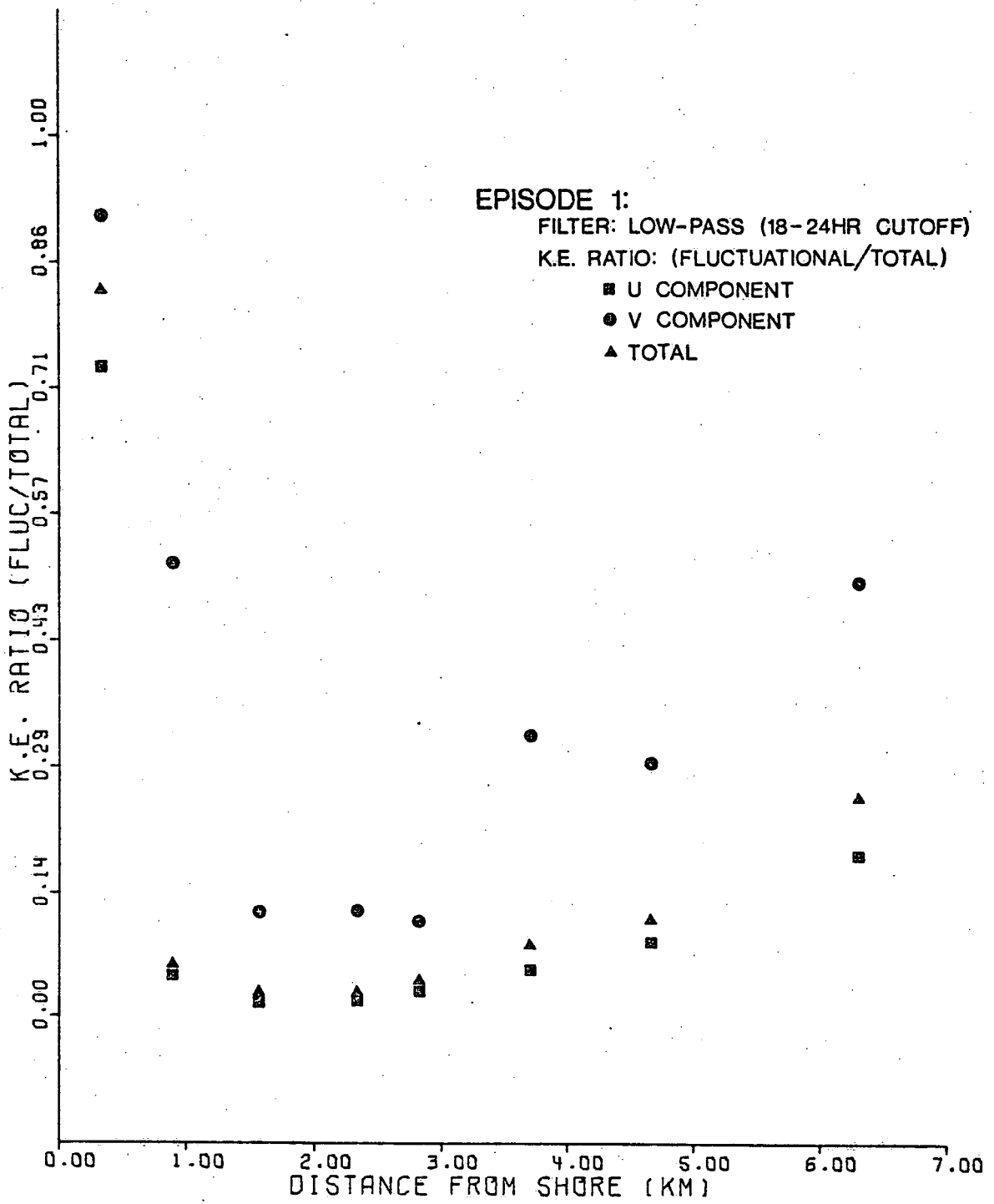


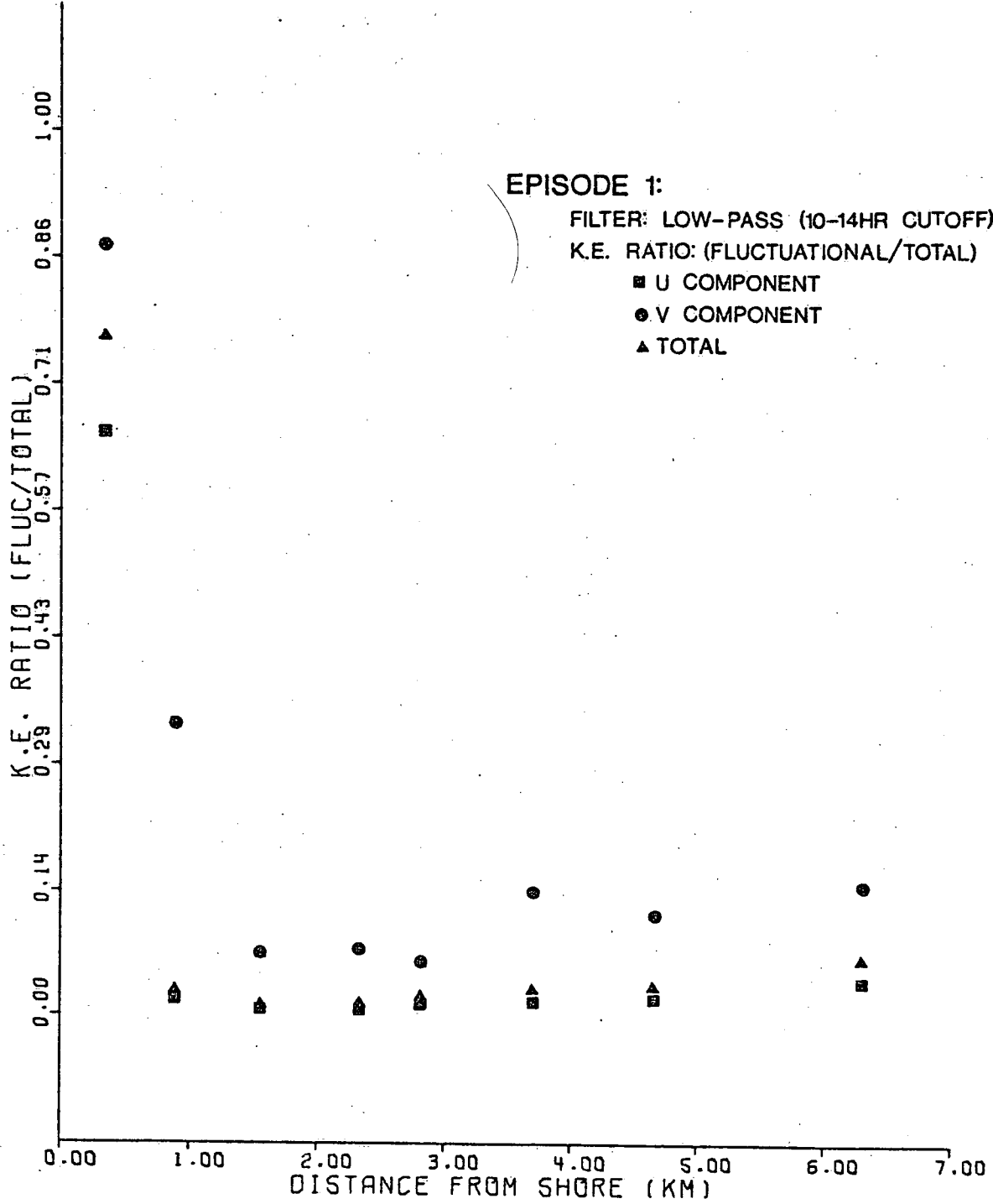


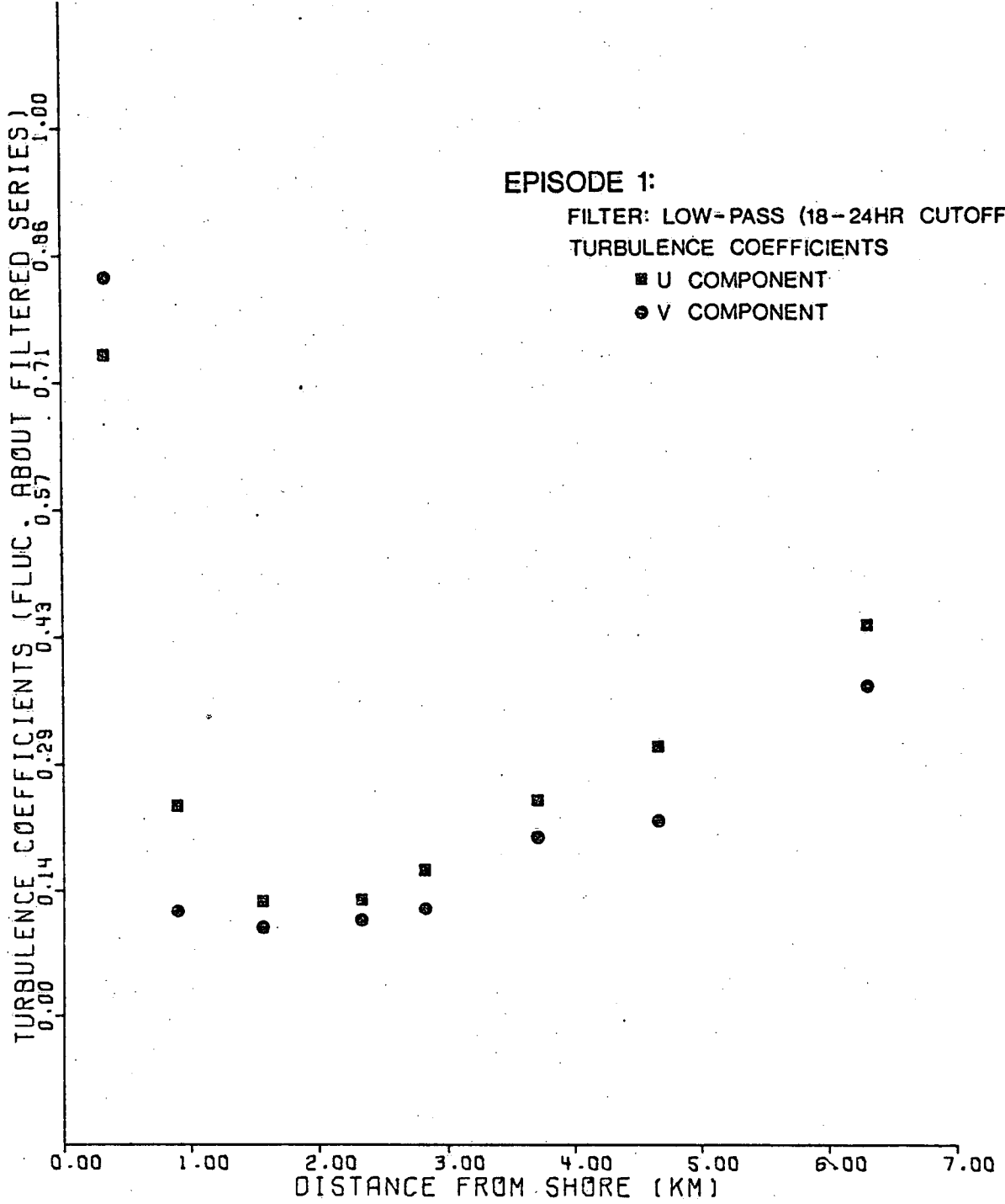


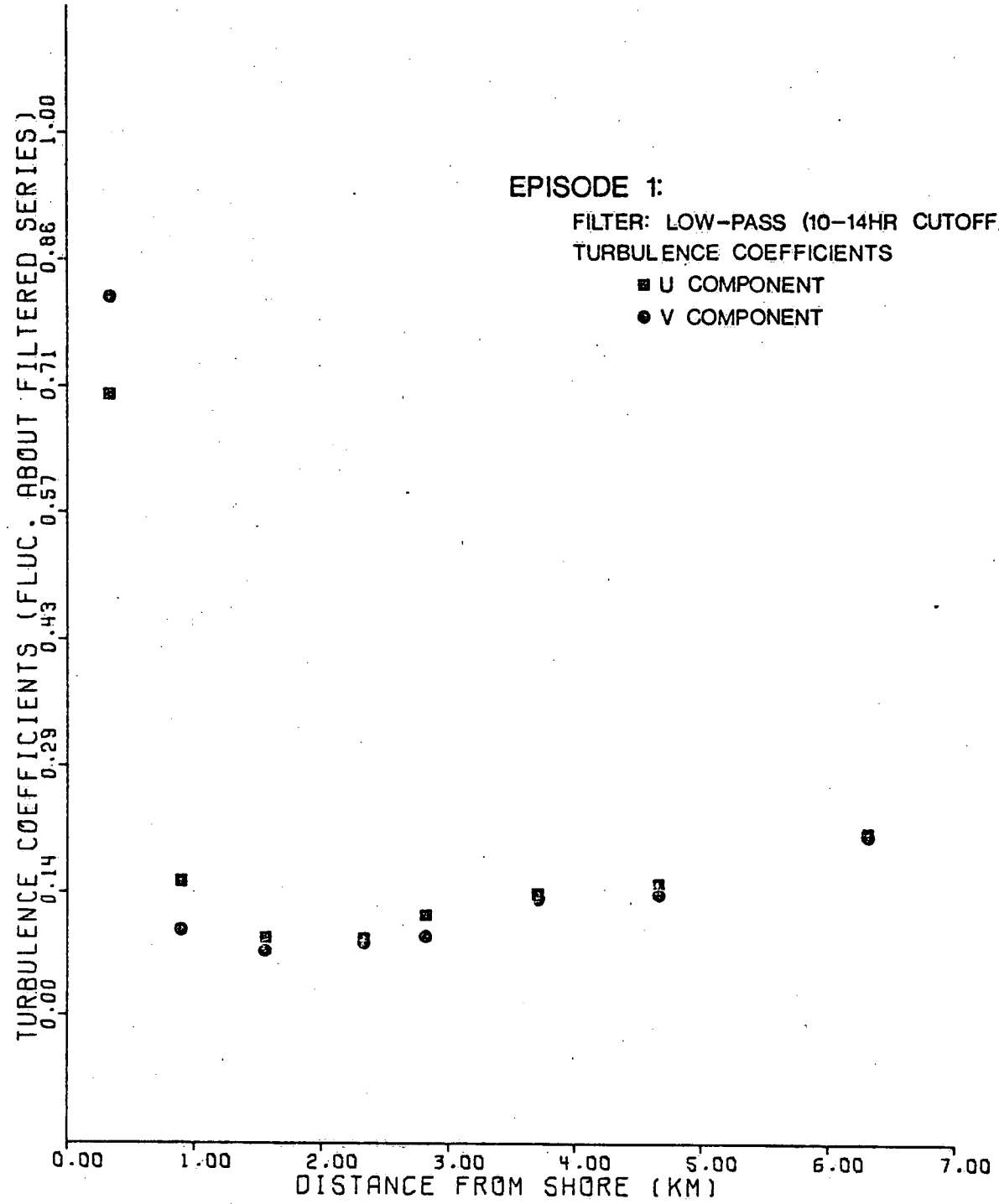








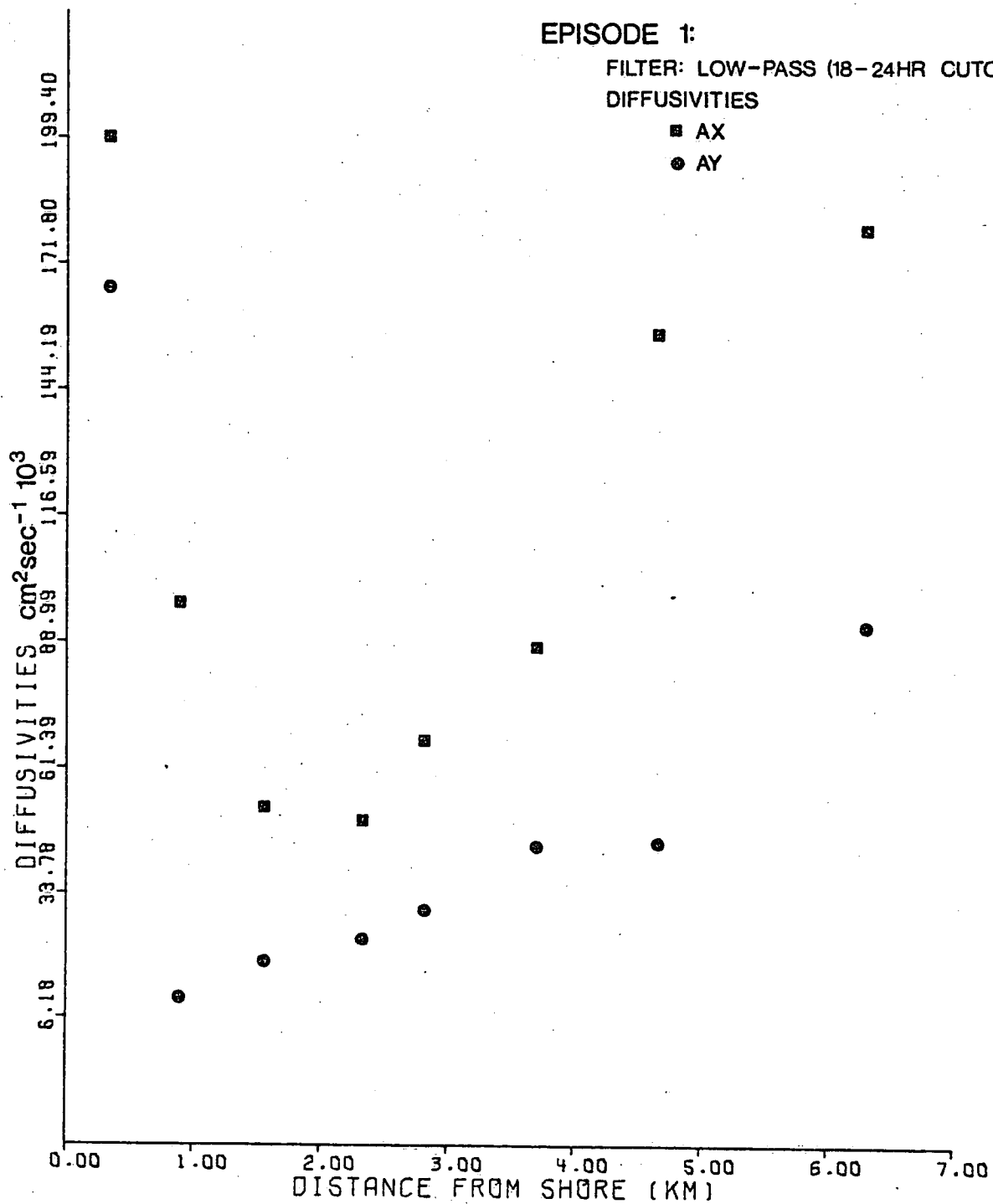




EPISODE 1:

FILTER: LOW-PASS (18-24HR CUTOFF)
DIFFUSIVITIES

- AX
- AY



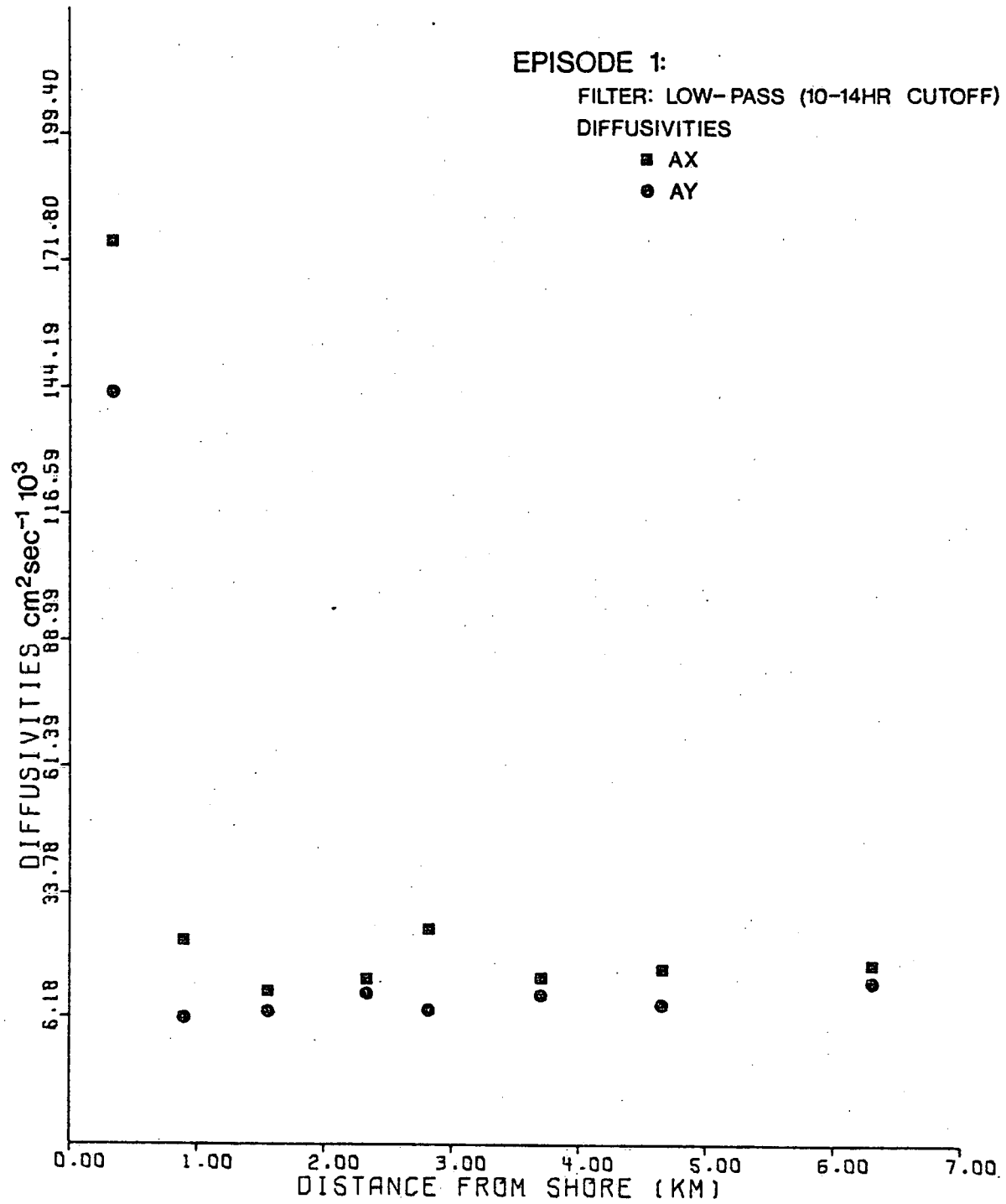
EPISODE 1:

FILTER: LOW-PASS (10-14HR CUTOFF)

DIFFUSIVITIES

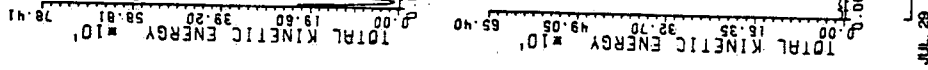
■ AX

● AY

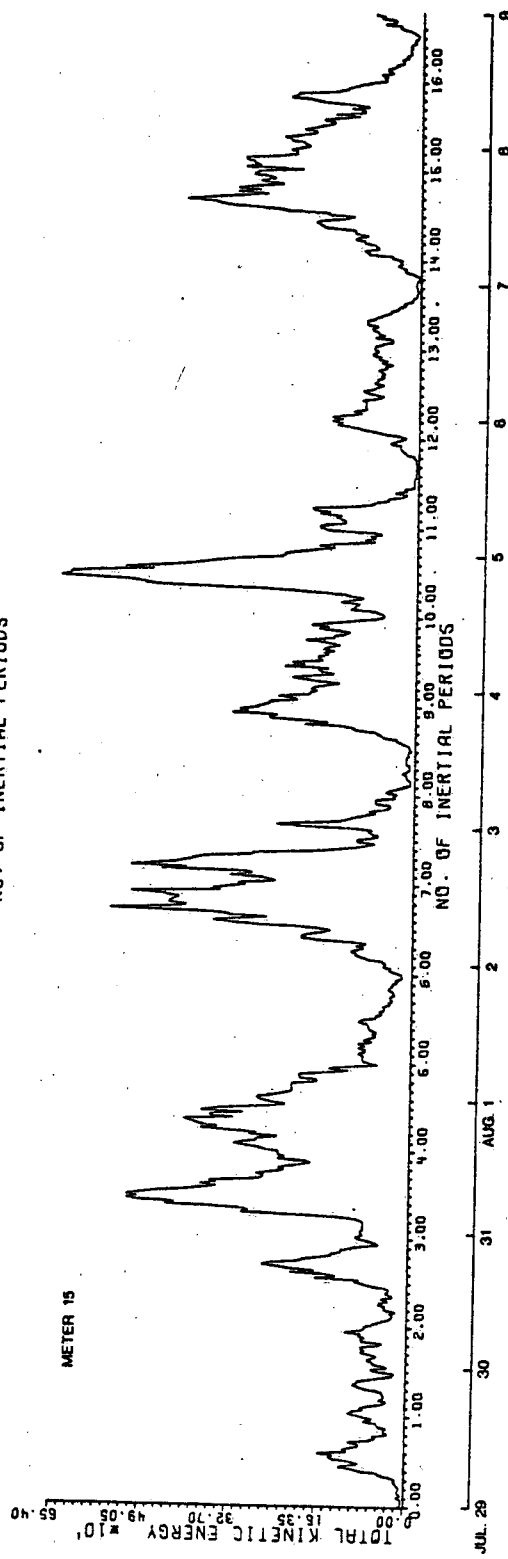


- EPISODE 1:

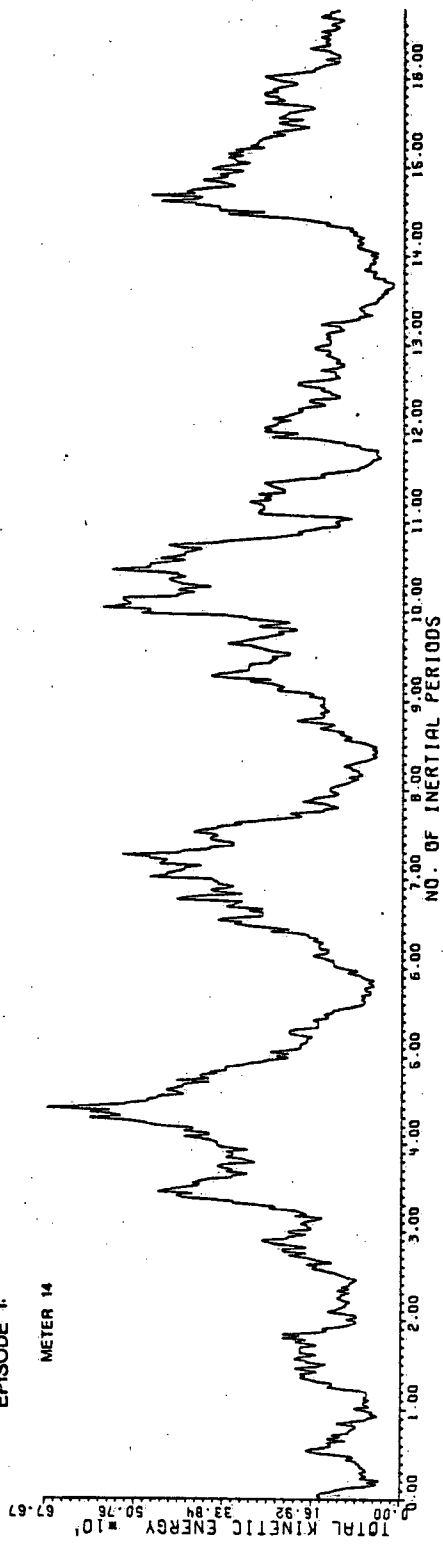
METER 18



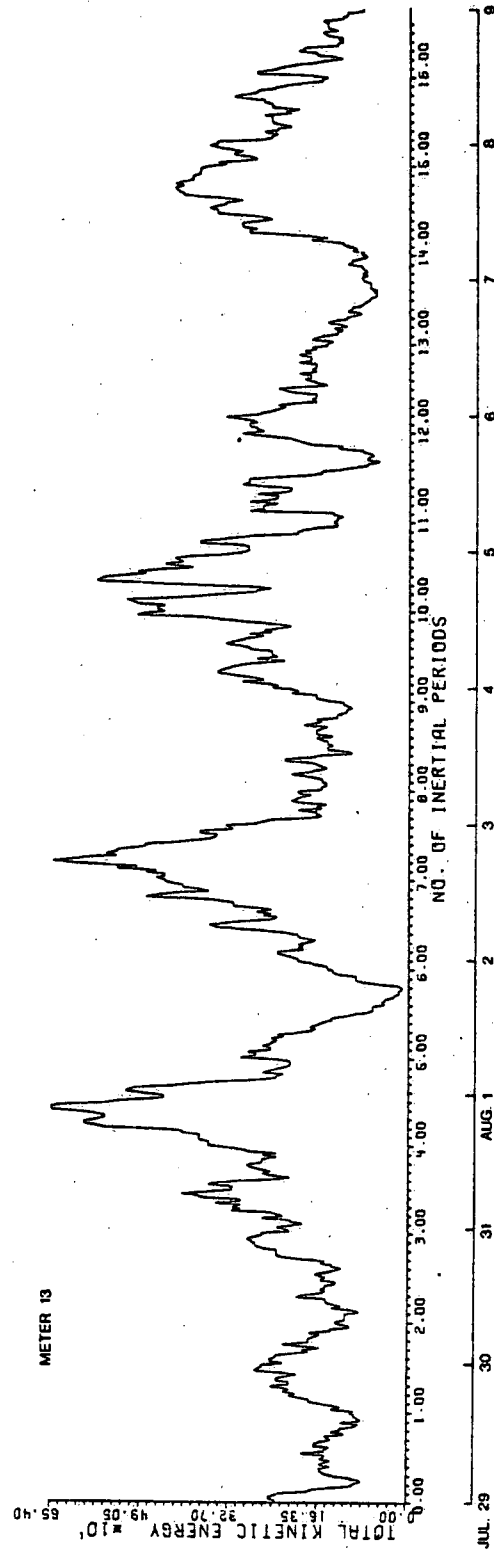
METER 15



EPISODE 1:
METER 14

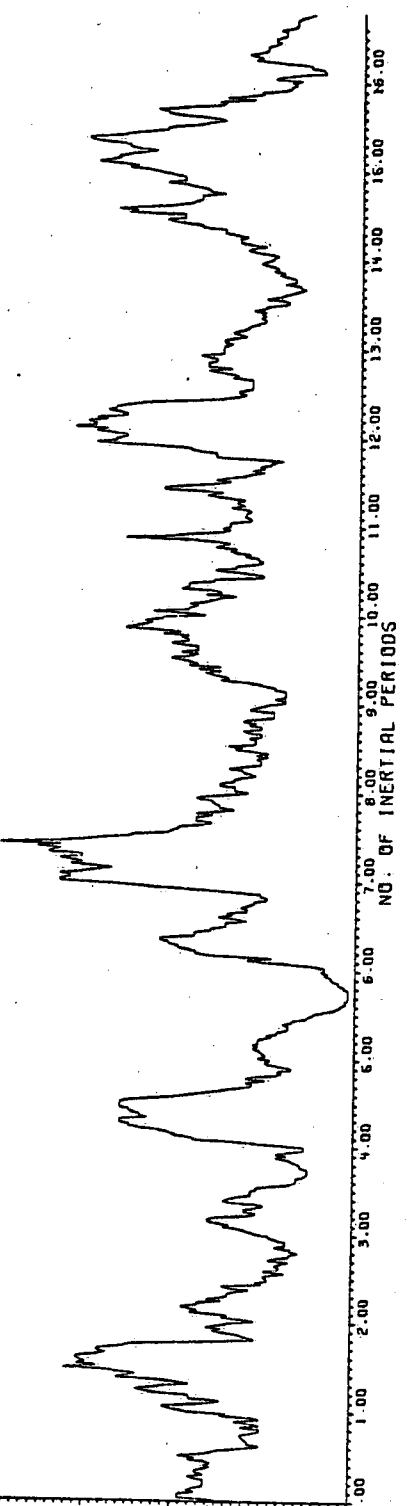


METER 13



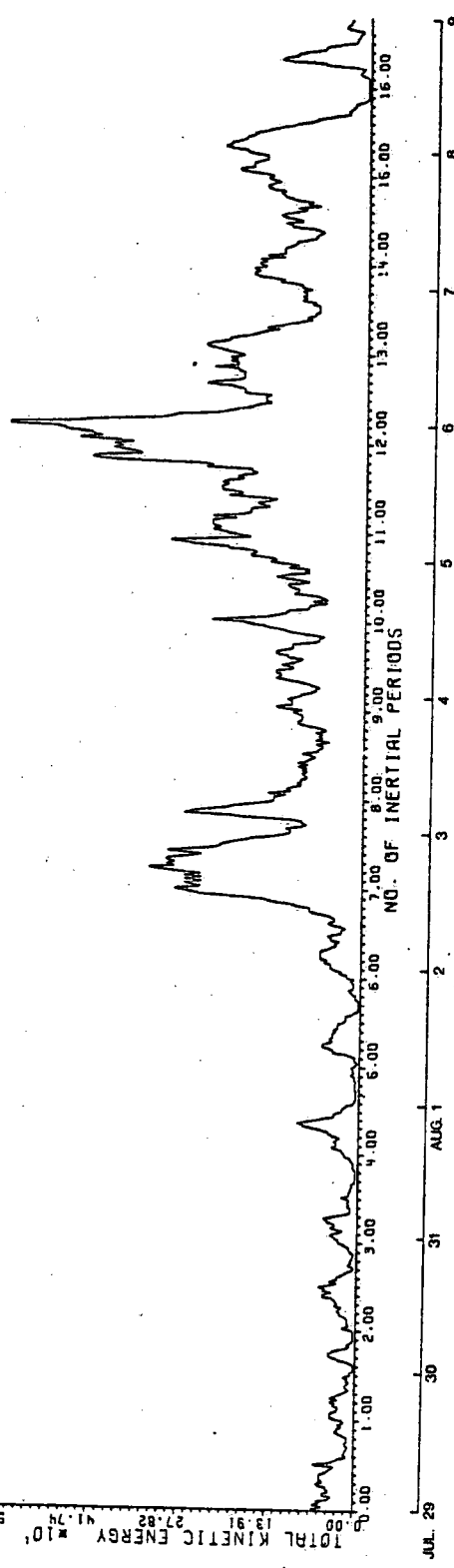
EPISODE 1:
METER 12

TOTAL KINETIC ENERGY 13.91 27.82 41.74 55.65
1.00 2.00 3.00 4.00 5.00 6.00 7.00 NO. OF INERTIAL PERIODS

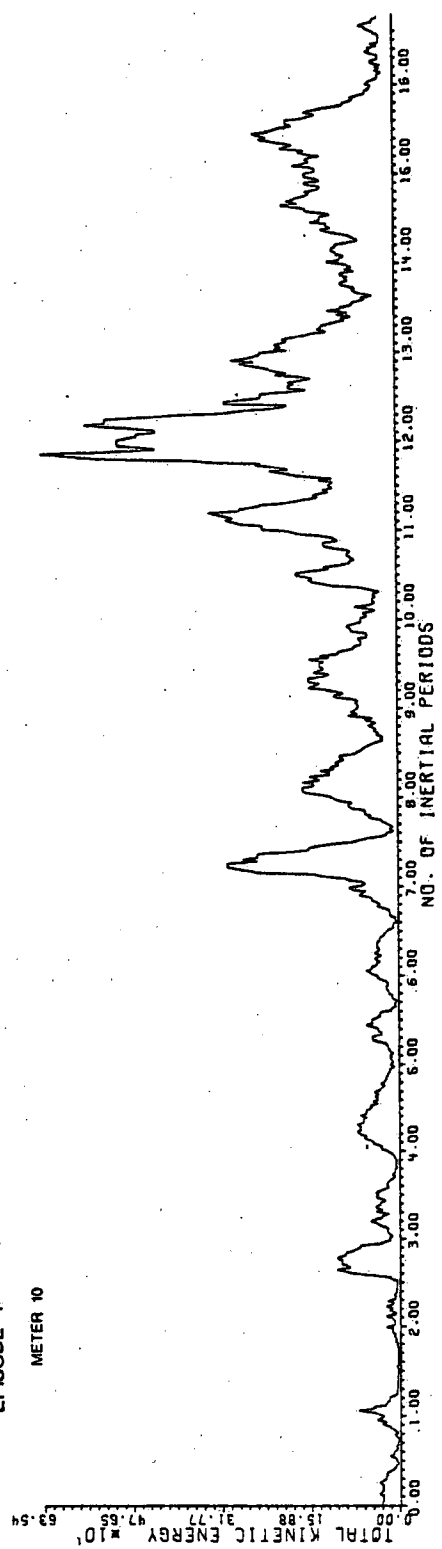


METER 11

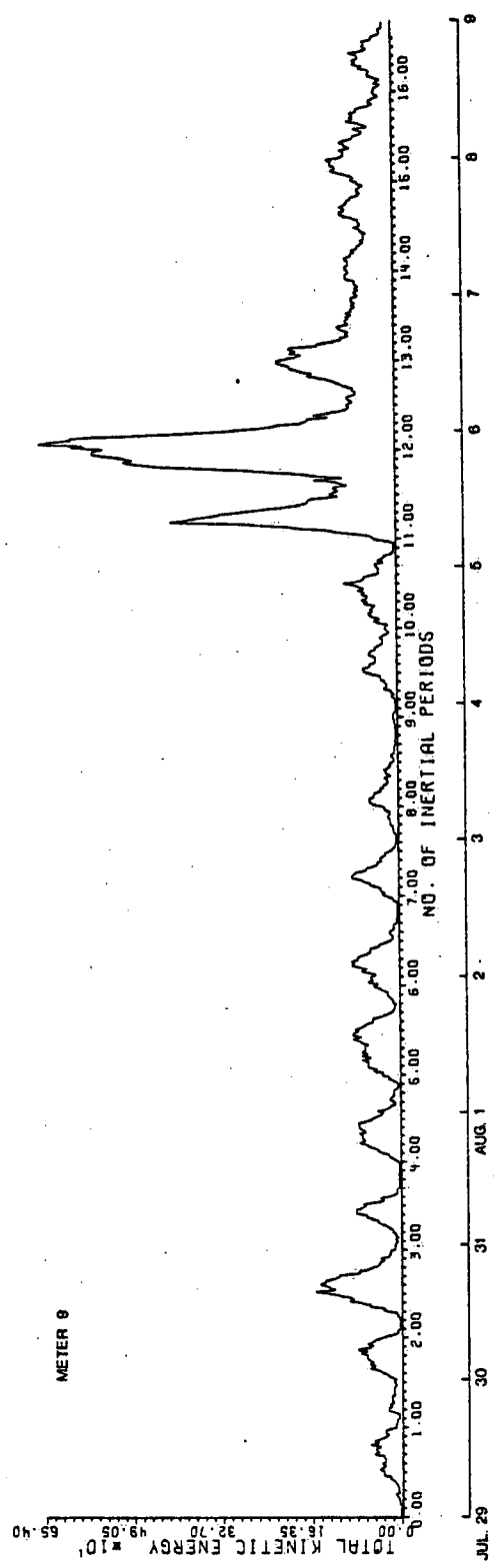
TOTAL KINETIC ENERGY 13.91 27.82 41.74 55.65
1.00 2.00 3.00 4.00 5.00 6.00 7.00 NO. OF INERTIAL PERIODS

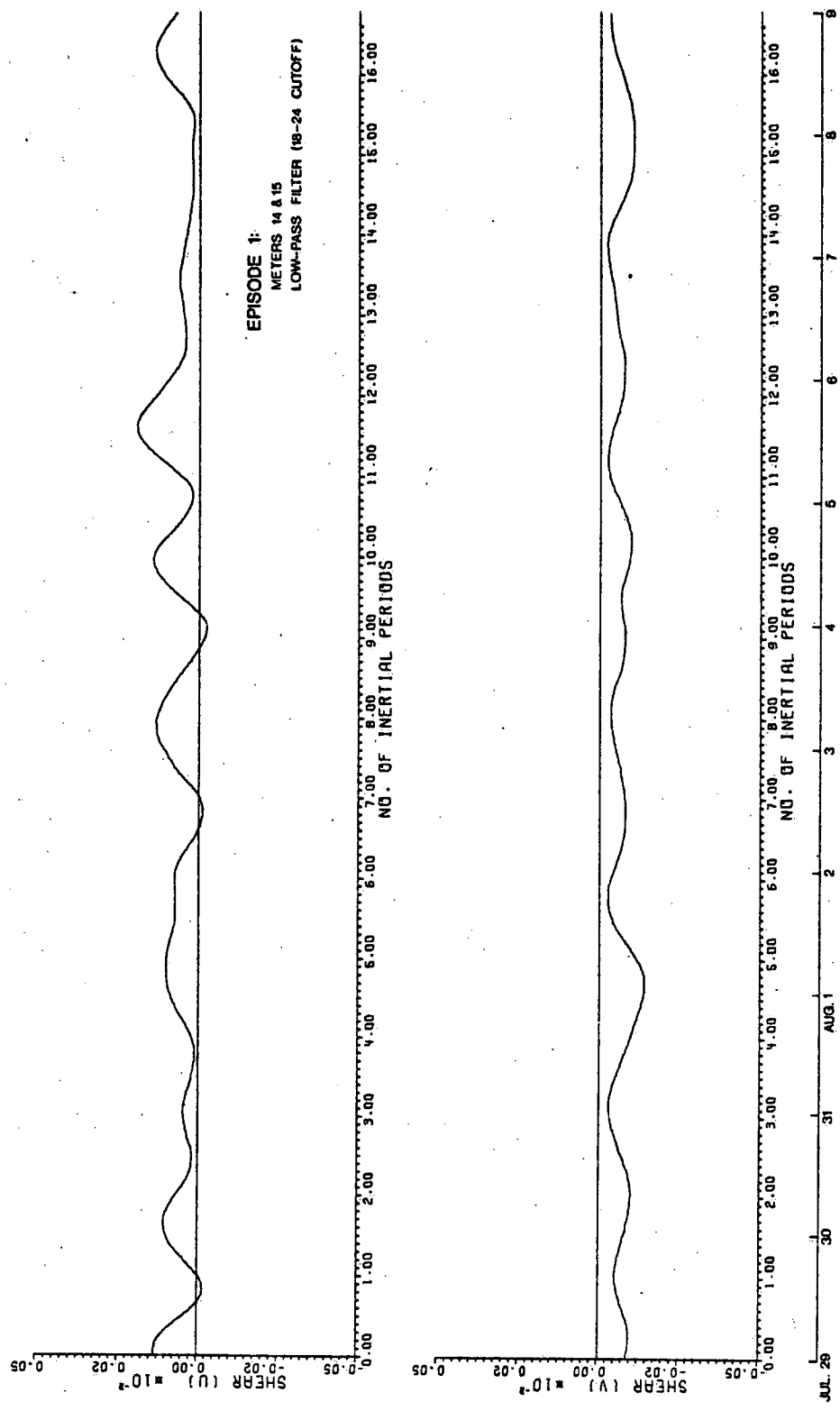


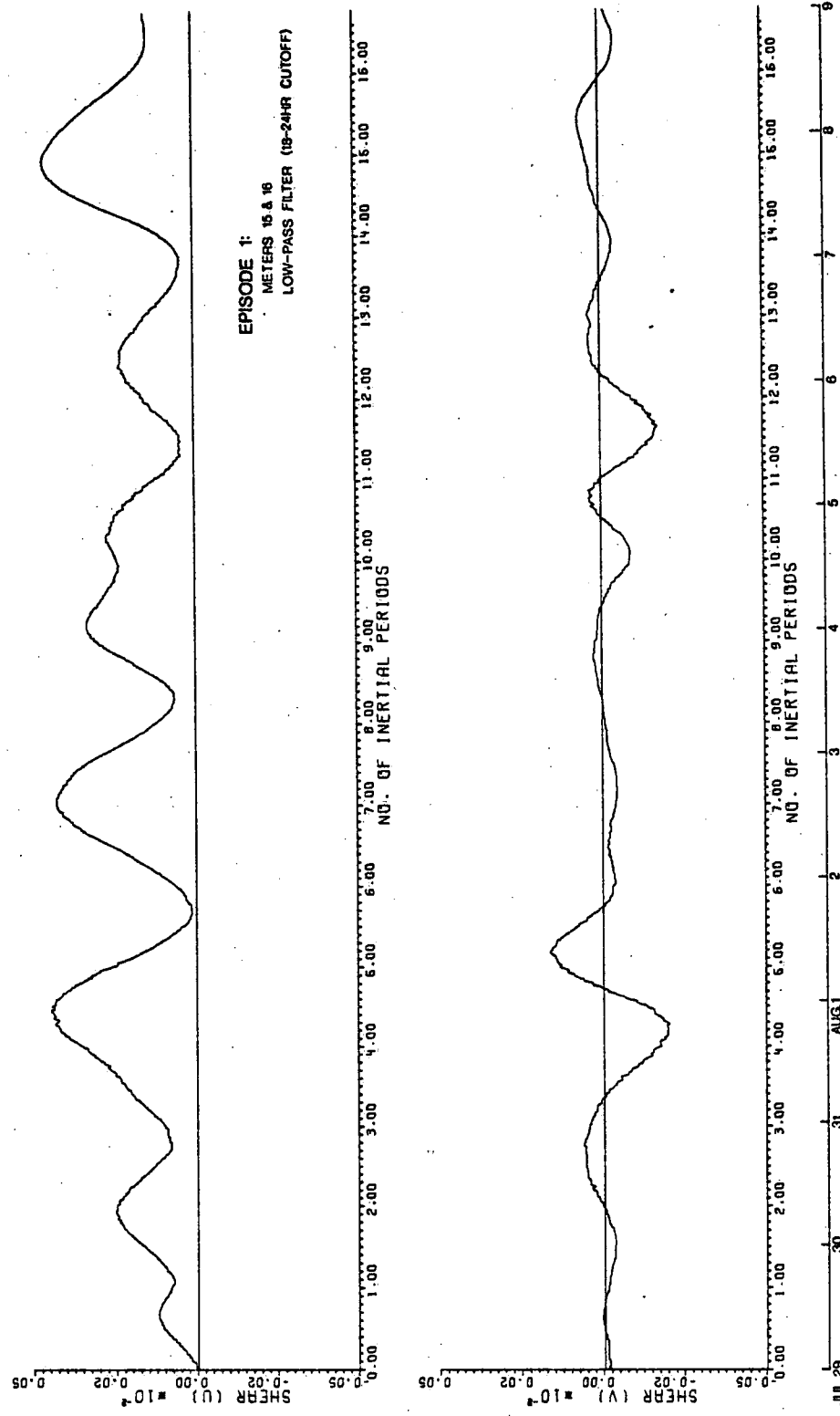
EPISODE 1:
METER 10



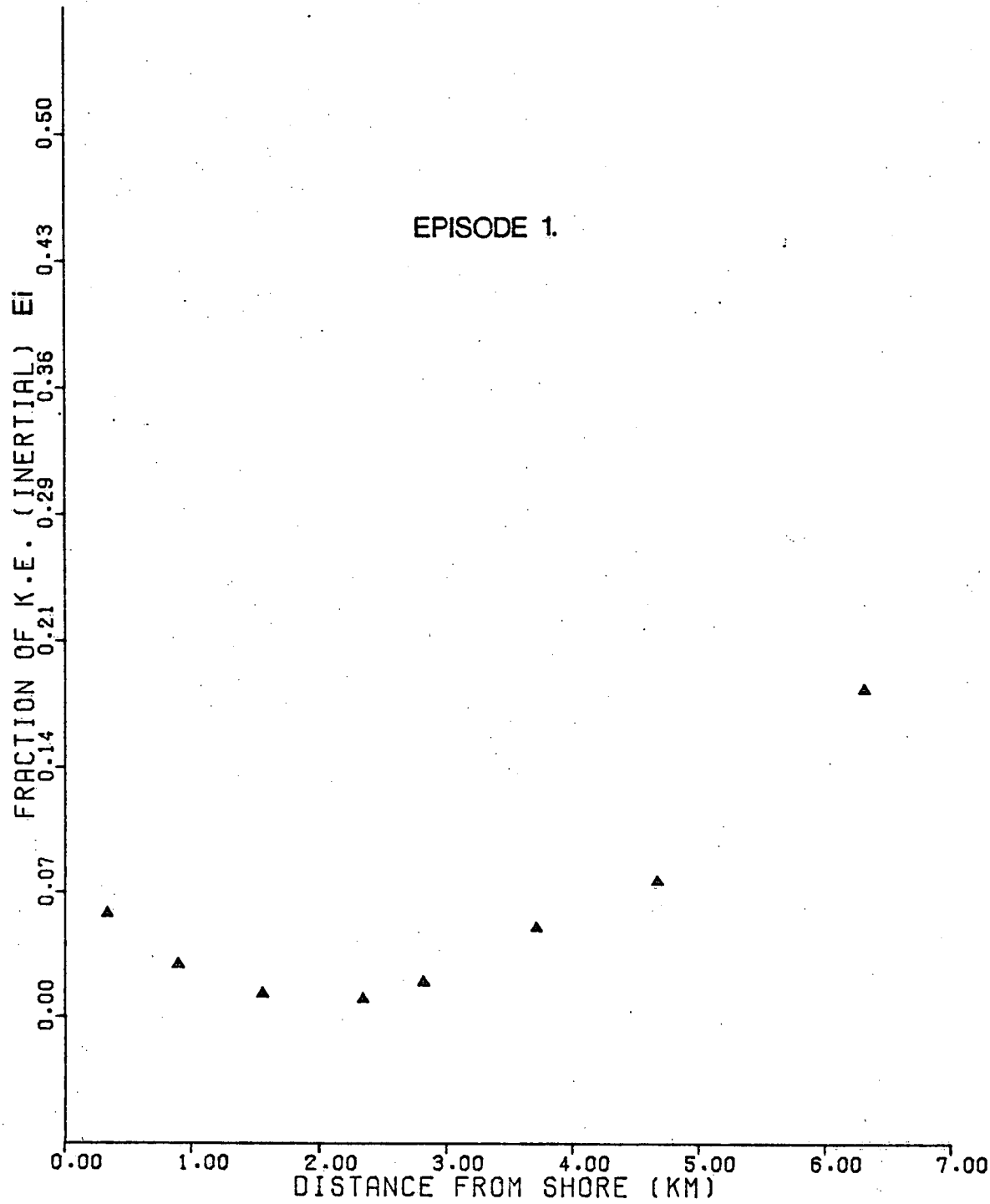
METER 9







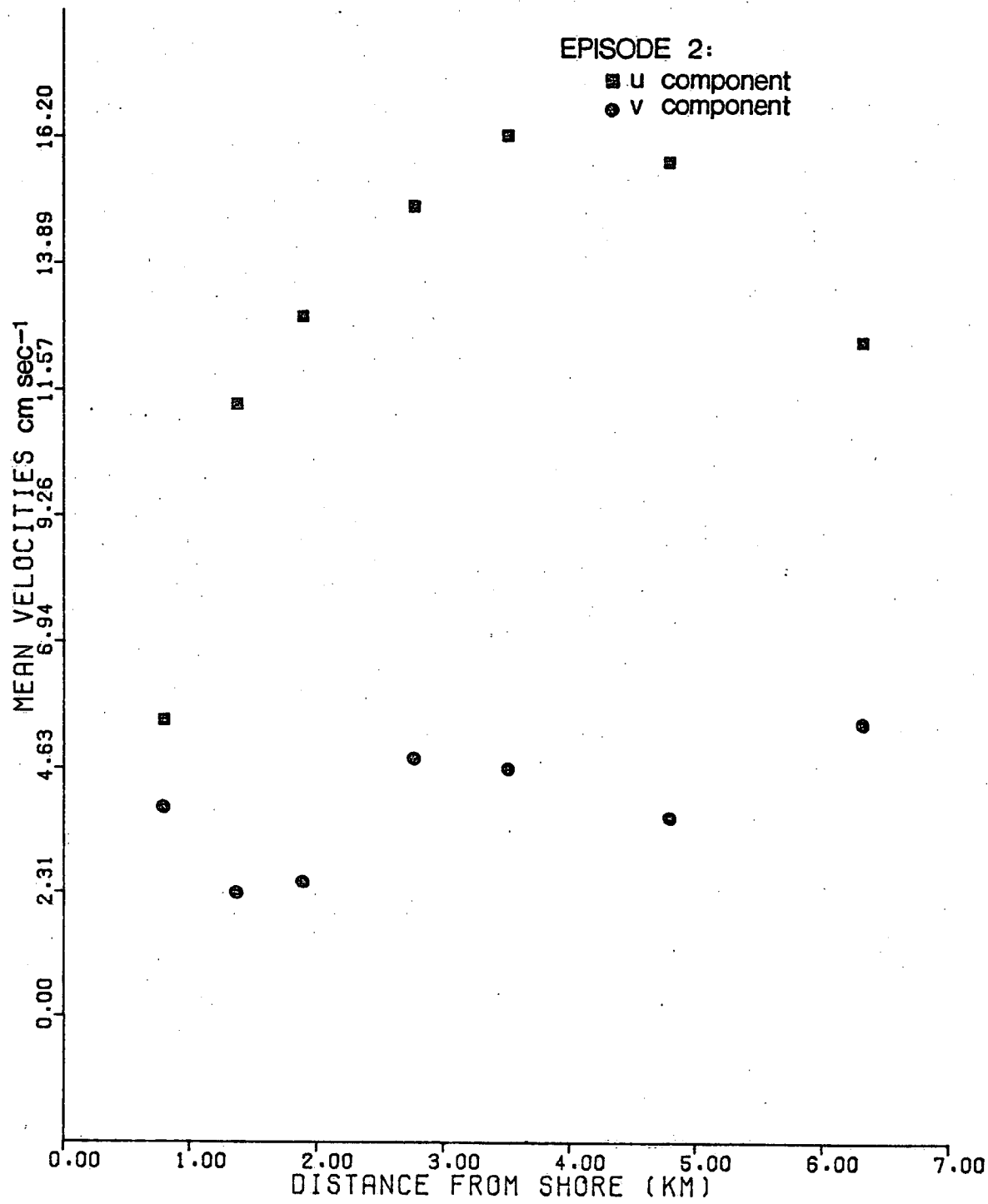
EPISODE 1.

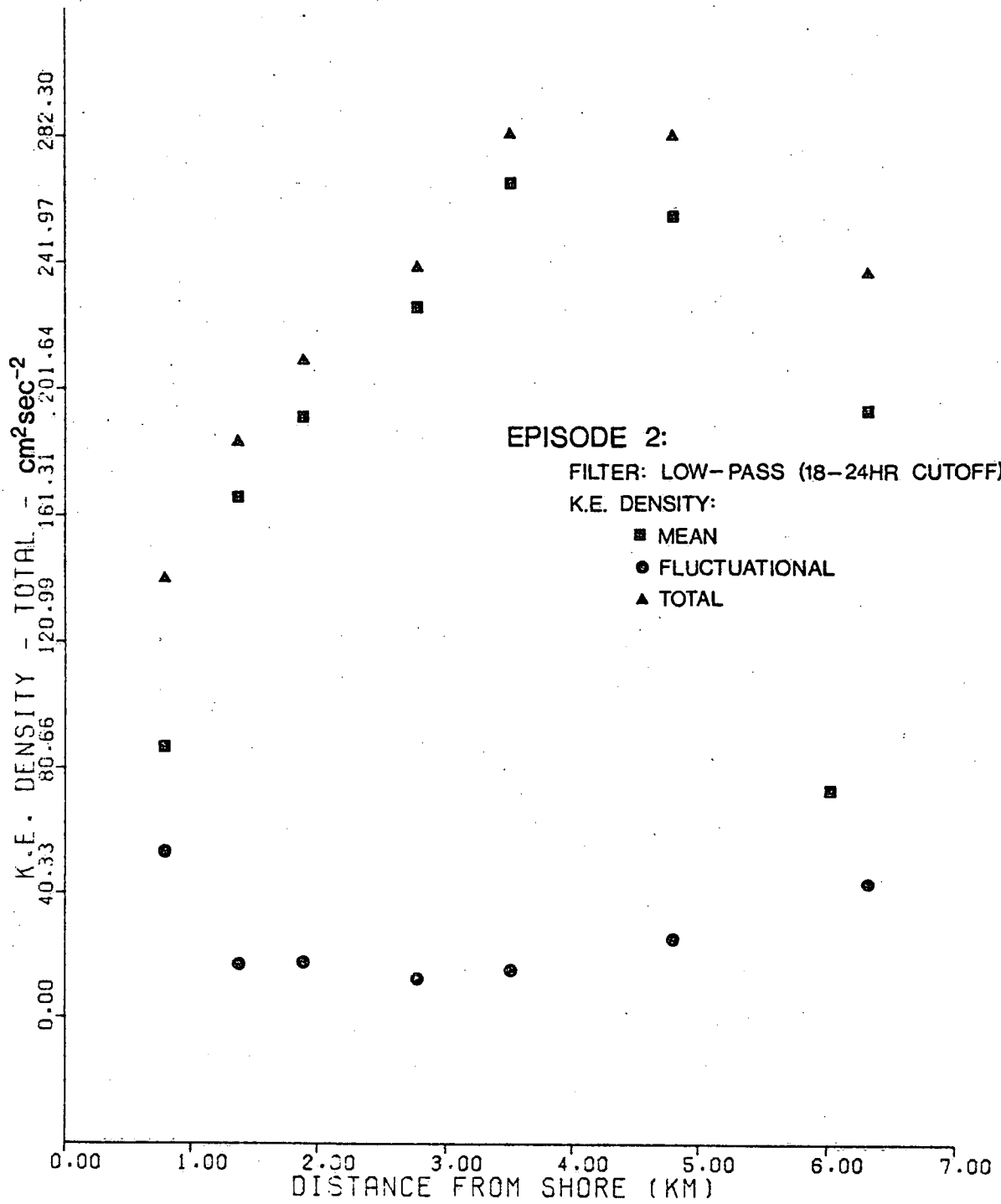


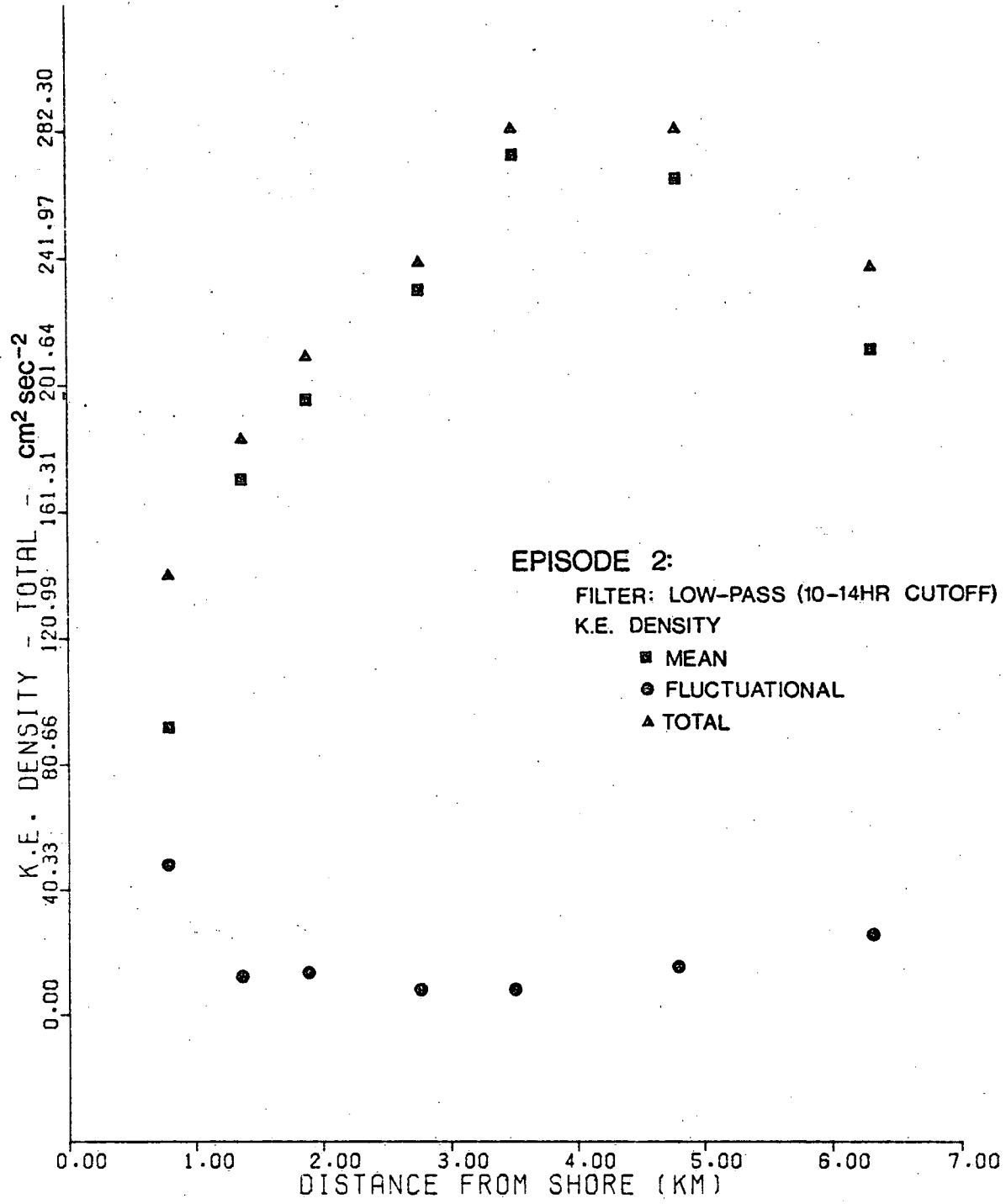
APPENDIX C

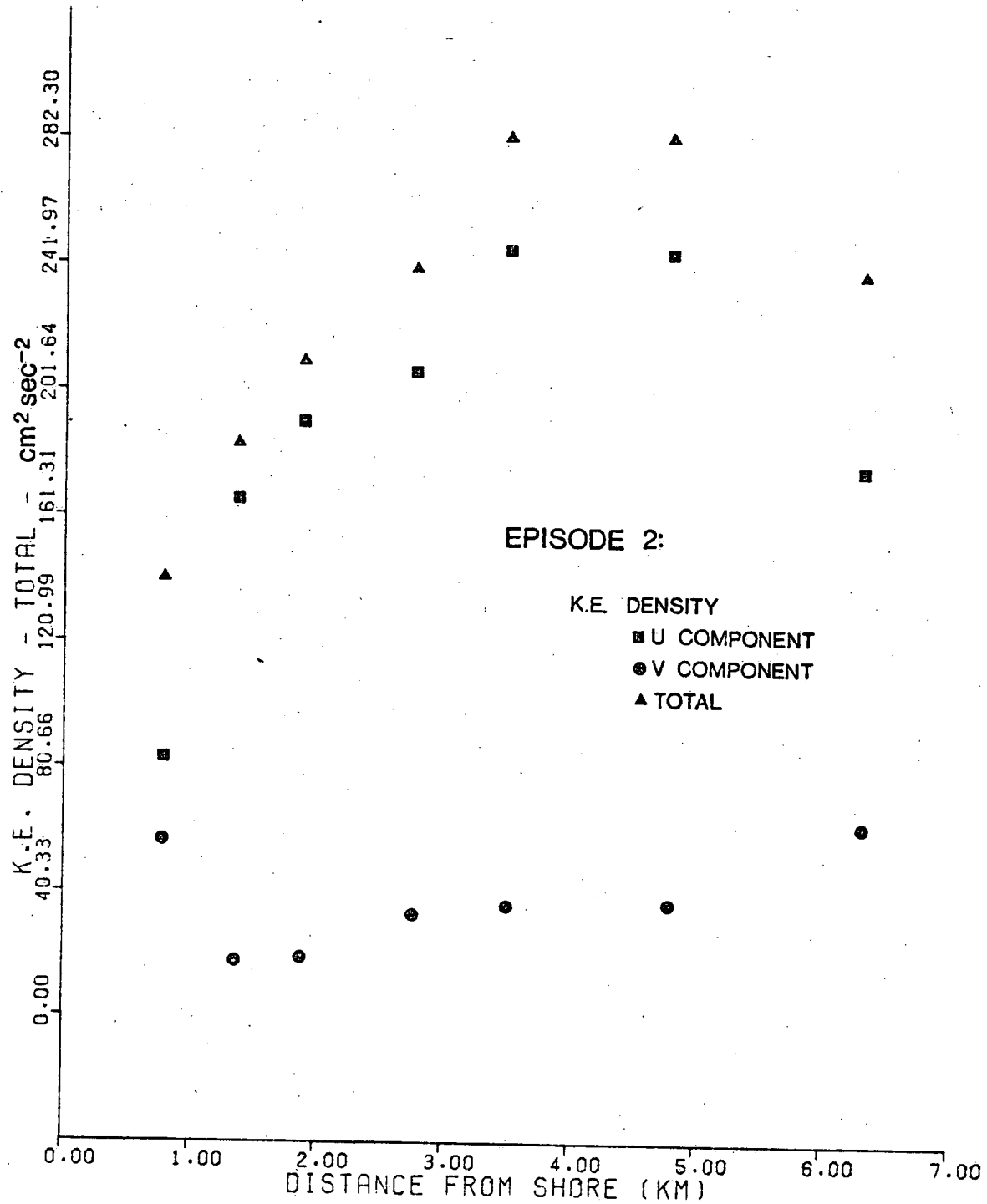
EPISODE 2:

■ u component
● v component









EPISODE 2:

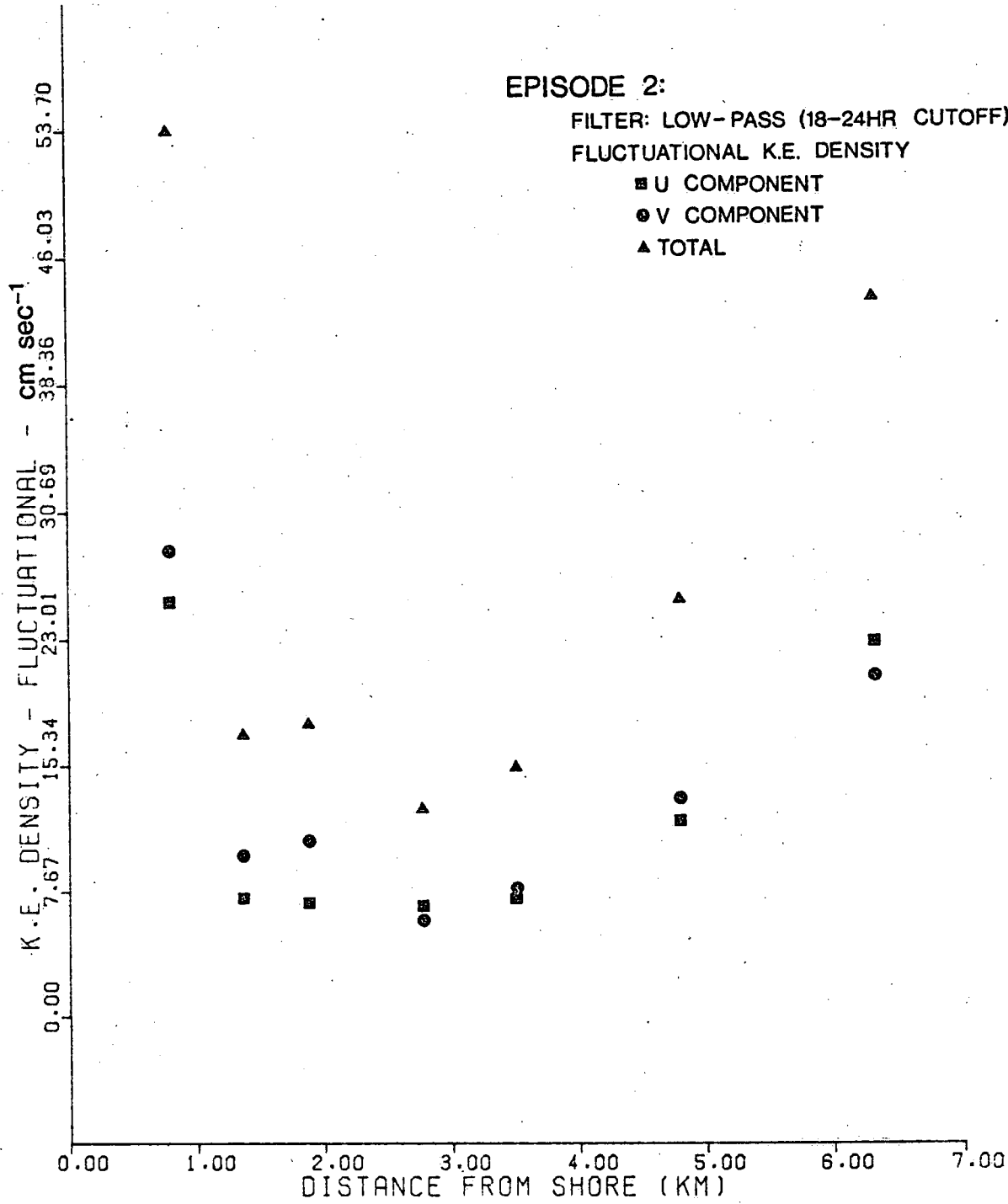
FILTER: LOW-PASS (18-24HR CUTOFF)

FLUCTUATIONAL K.E. DENSITY

■ U COMPONENT

● V COMPONENT

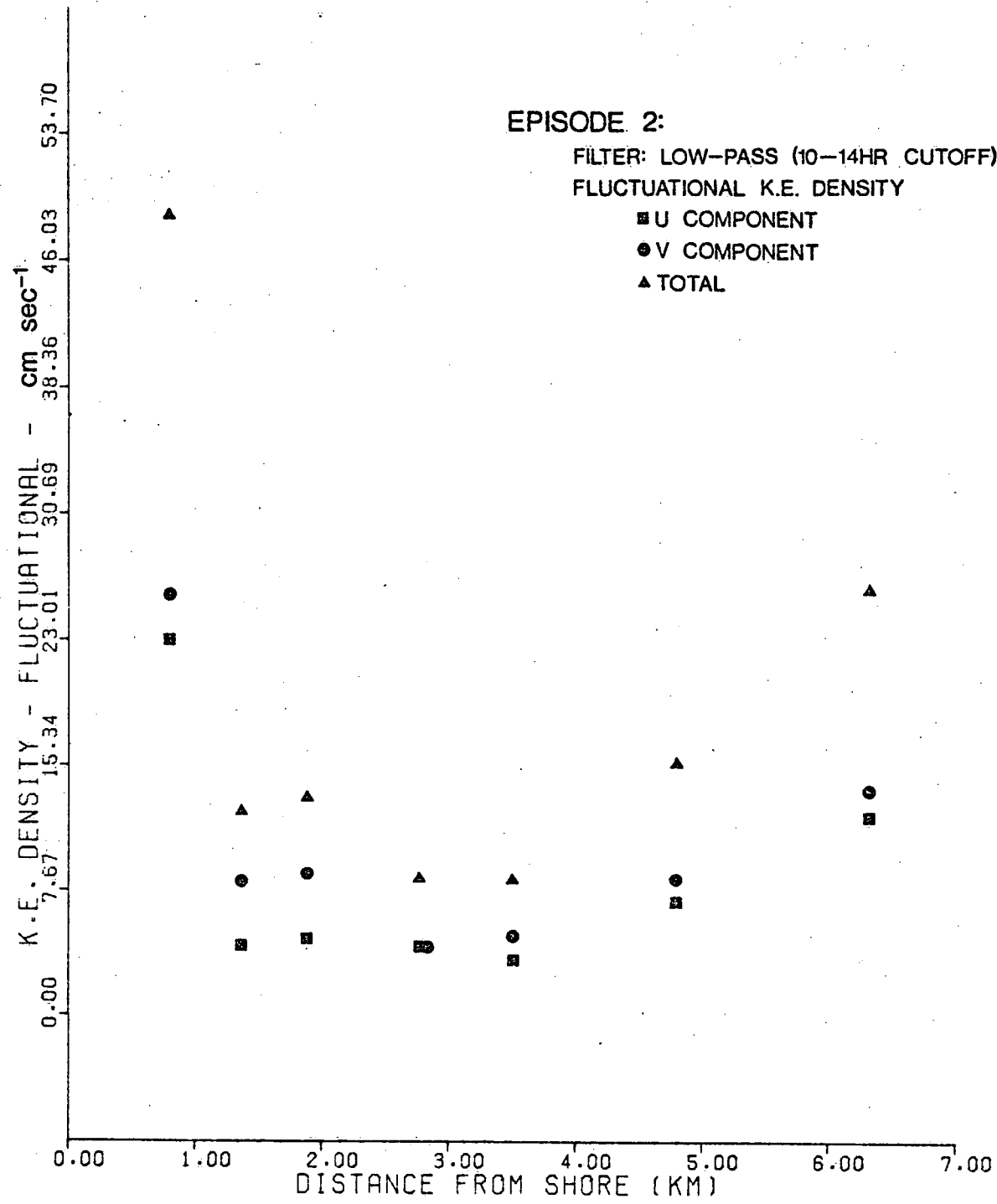
▲ TOTAL

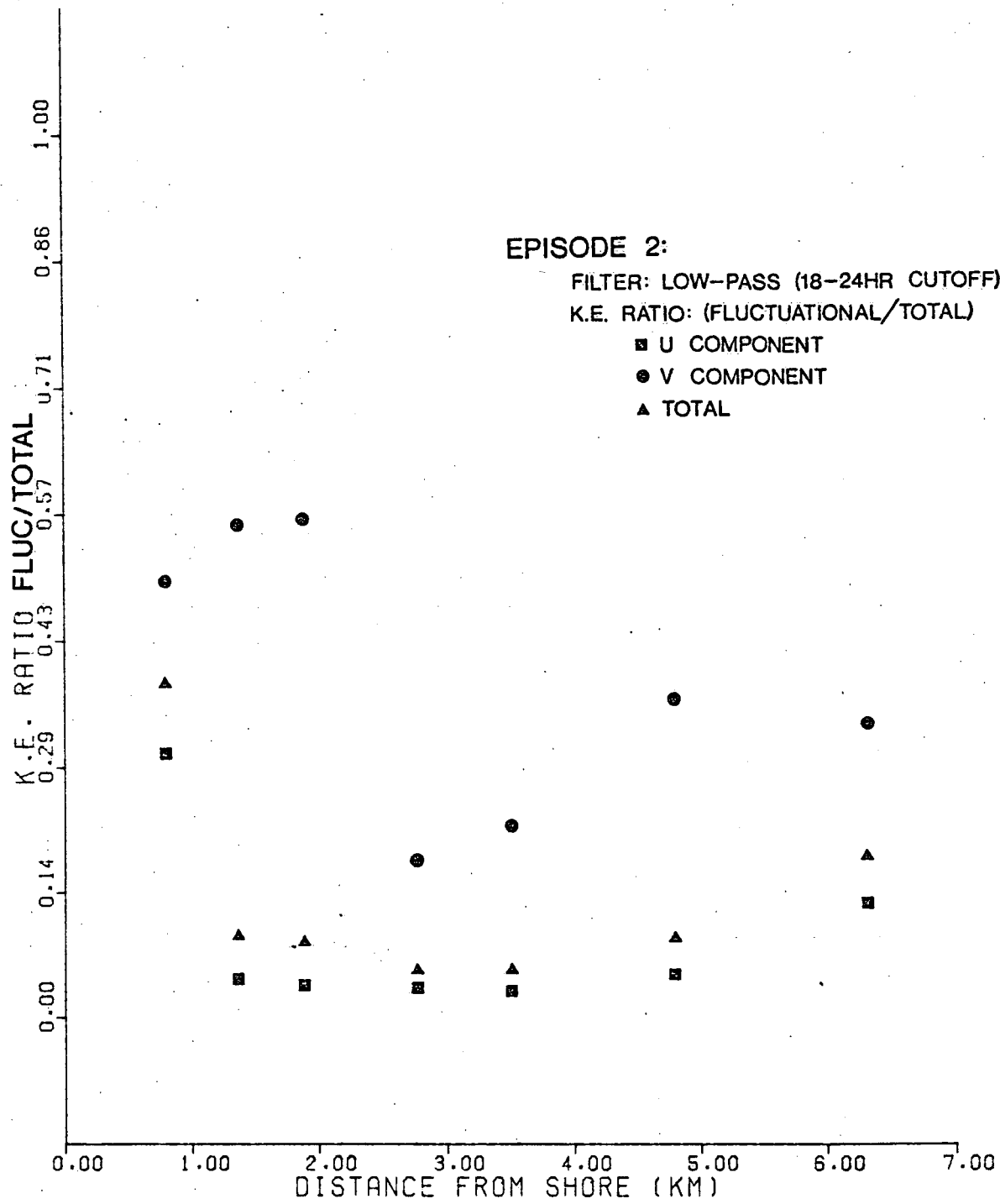


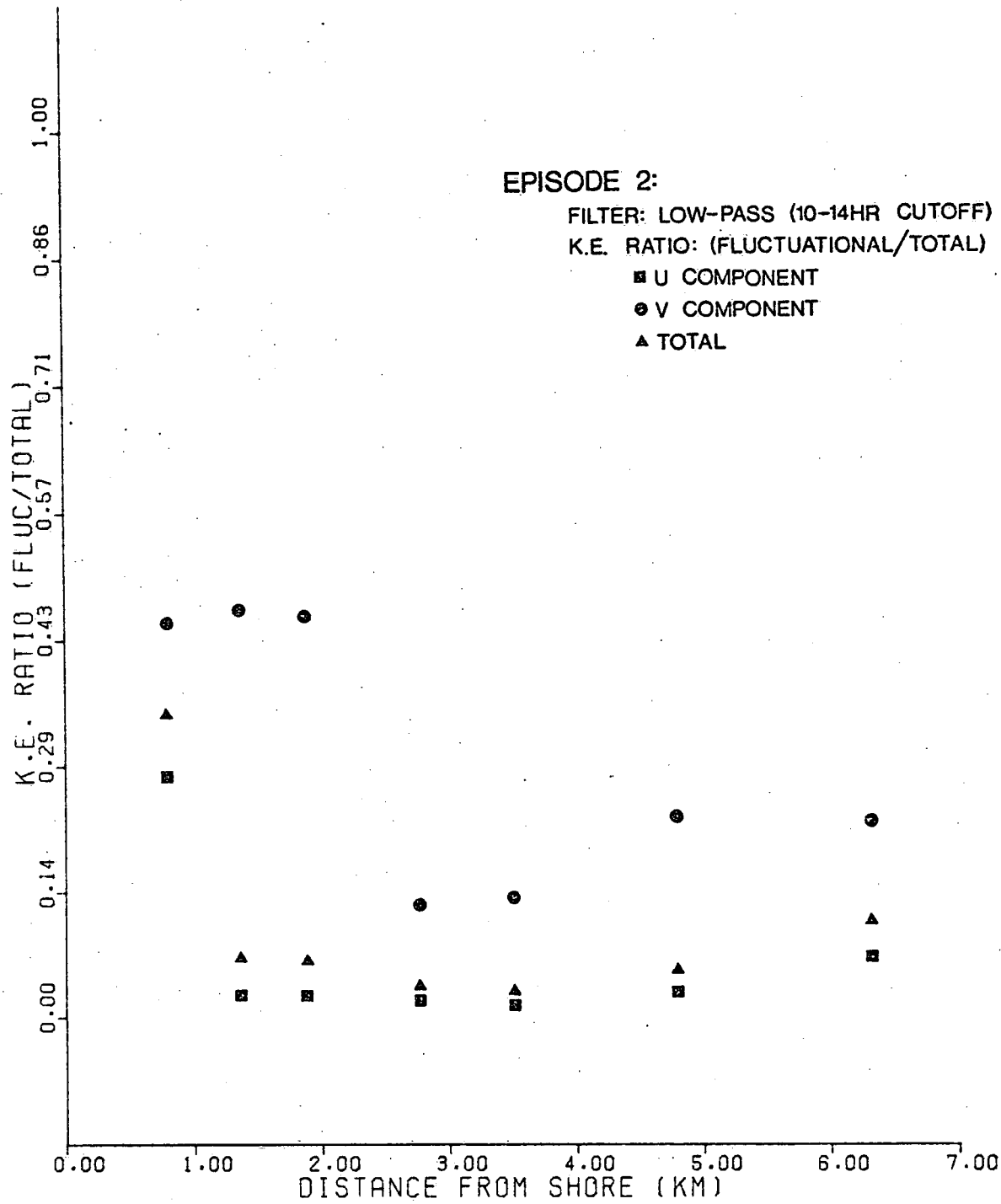
EPISODE 2:

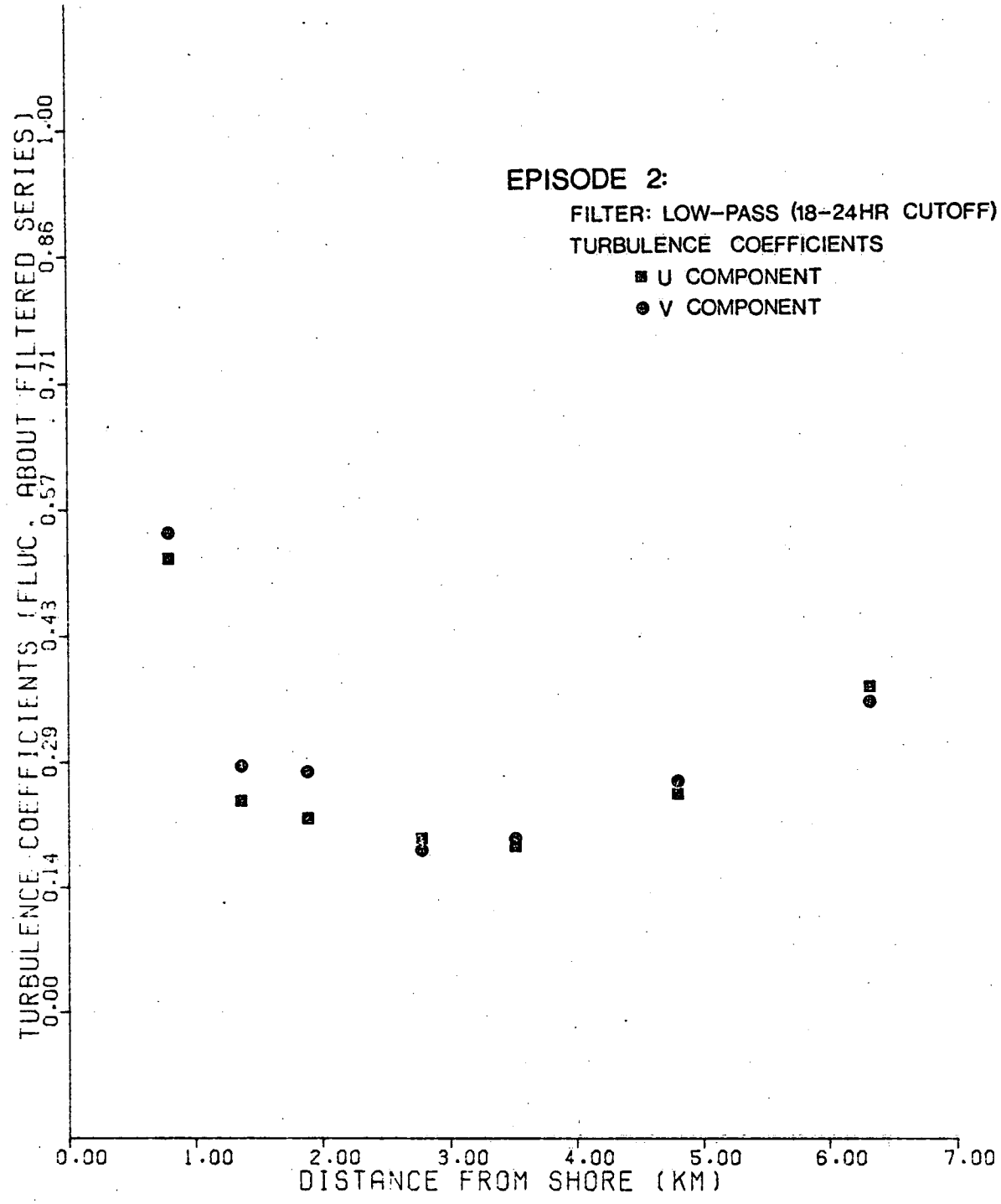
FILTER: LOW-PASS (10-14HR CUTOFF)
FLUCTUATIONAL K.E. DENSITY

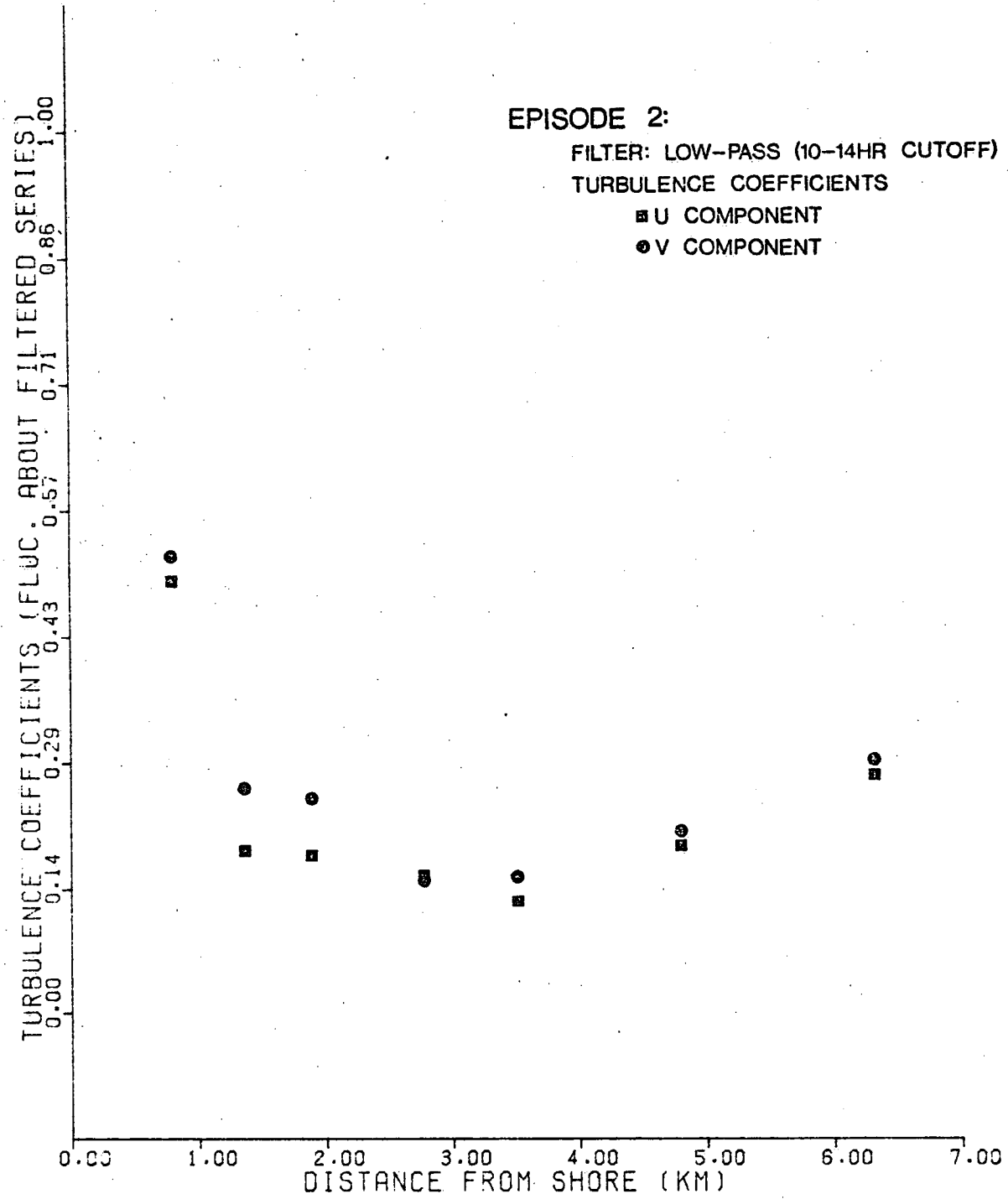
- U COMPONENT
- V COMPONENT
- ▲ TOTAL





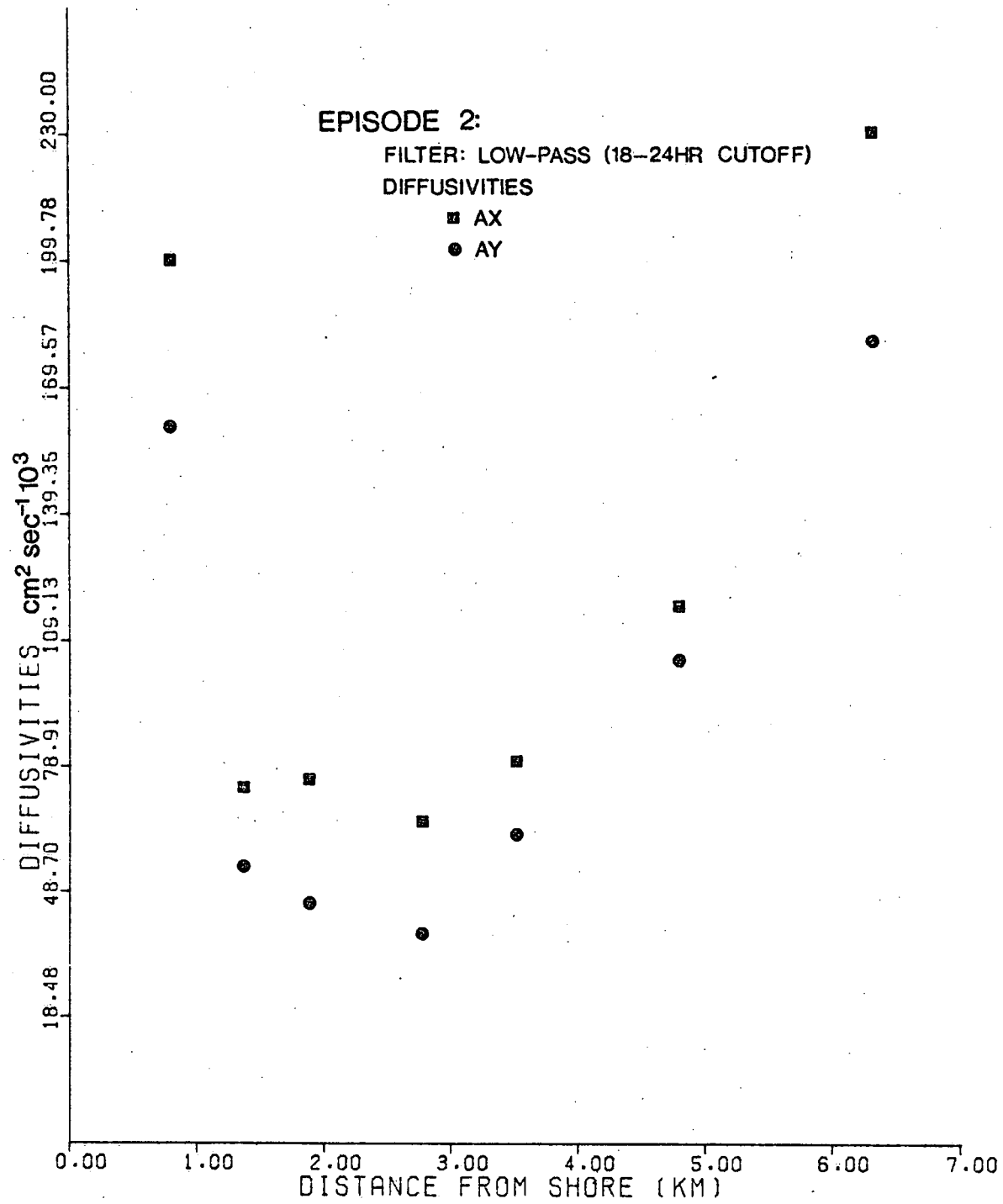






EPISODE 2:
FILTER: LOW-PASS (18-24HR CUTOFF)
DIFFUSIVITIES

■ AX
● AY



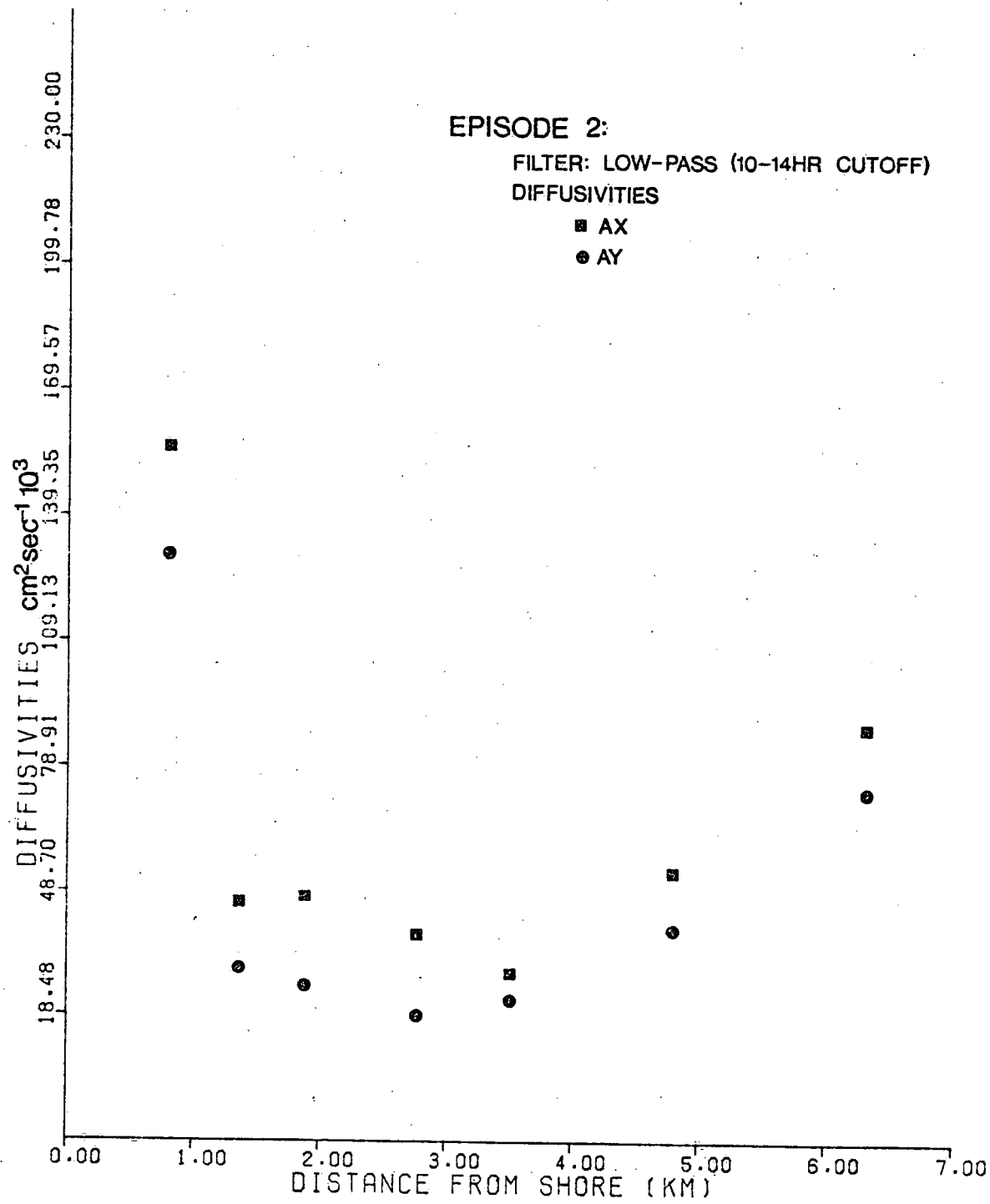
EPISODE 2:

FILTER: LOW-PASS (10-14HR CUTOFF)

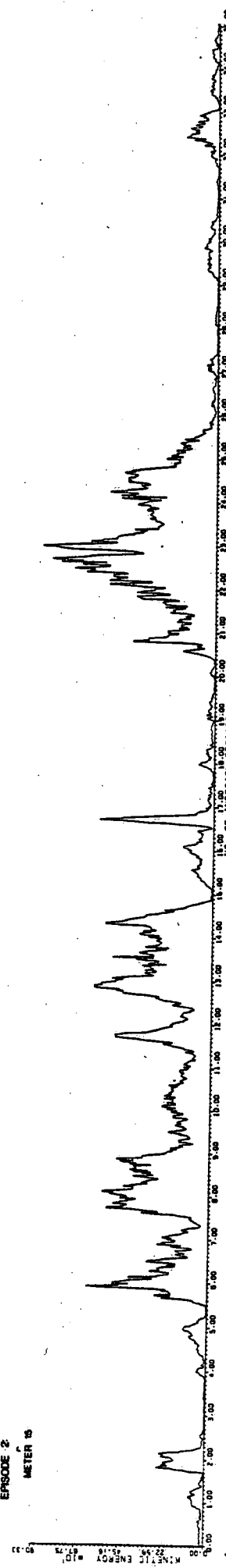
DIFFUSIVITIES

■ AX

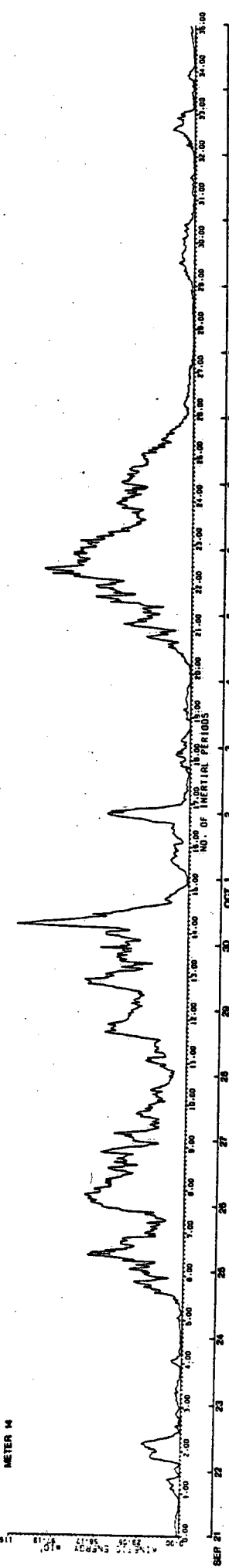
● AY



EPISODE 2
METER 10

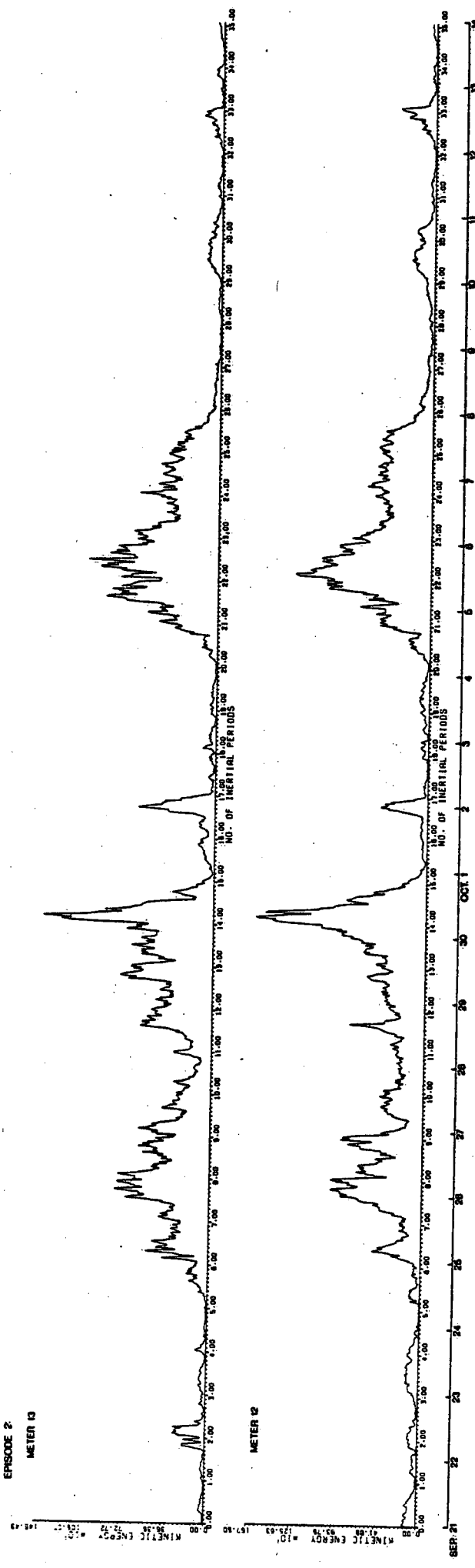


METER 11

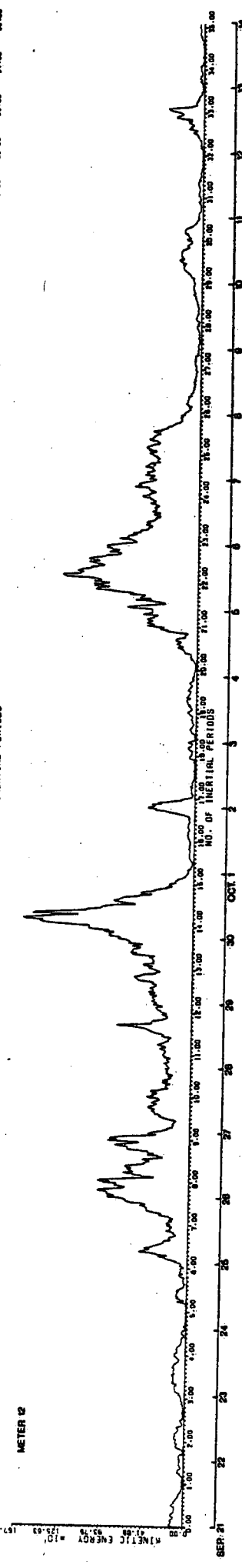


SER 2

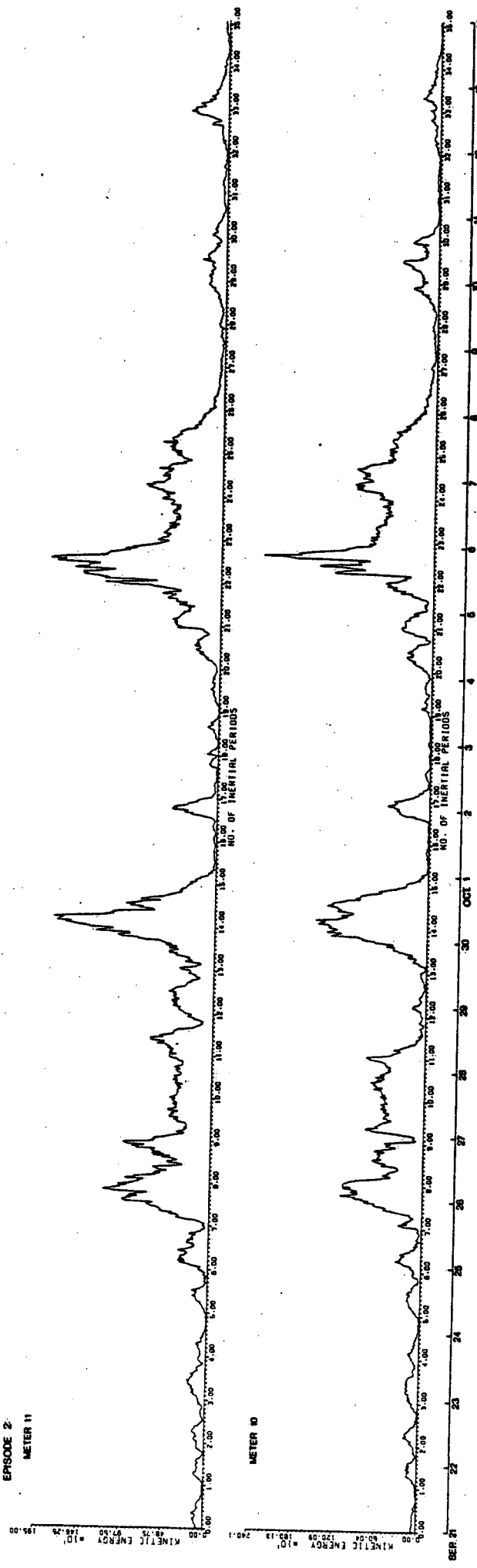
EPISODE 2
METER 13

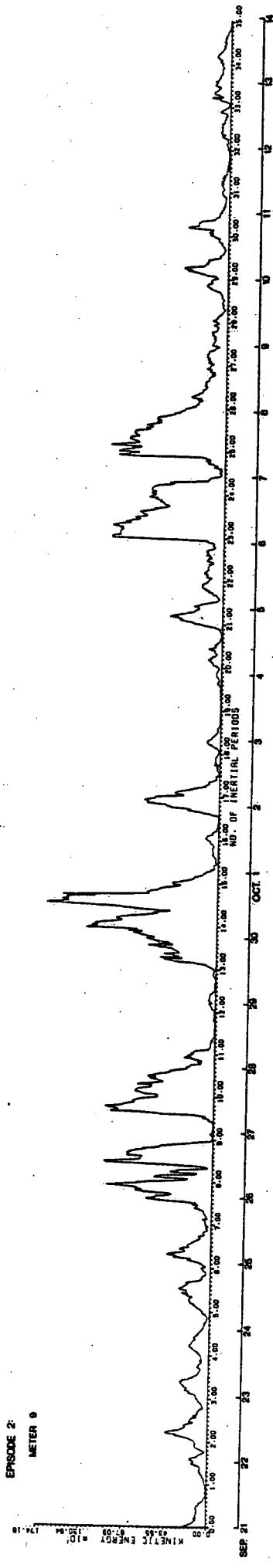


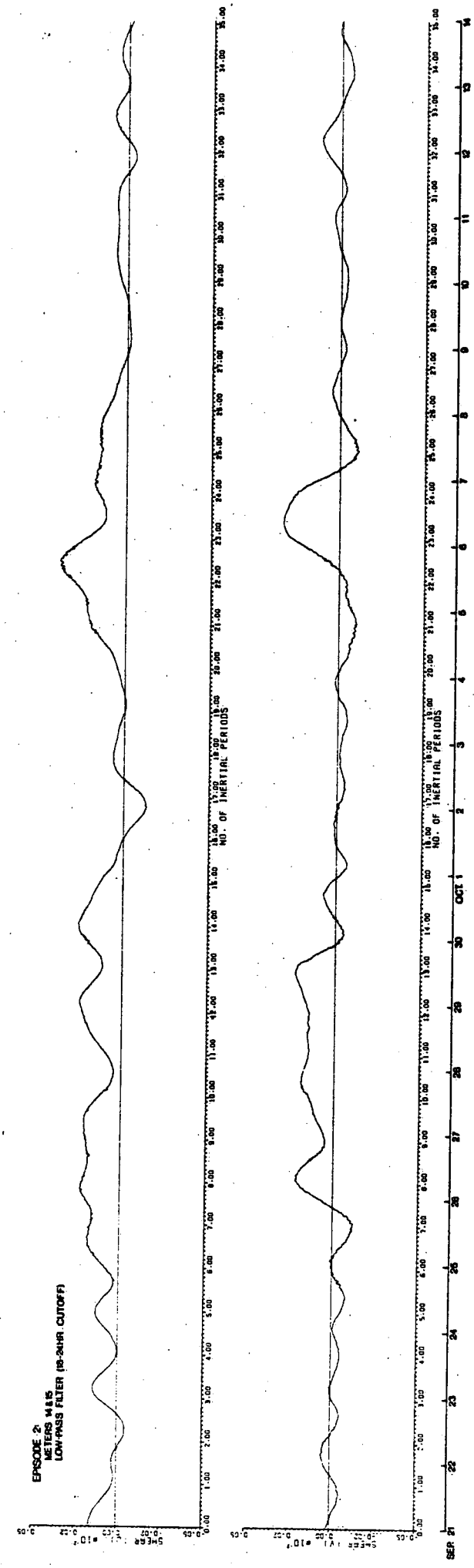
METER 12

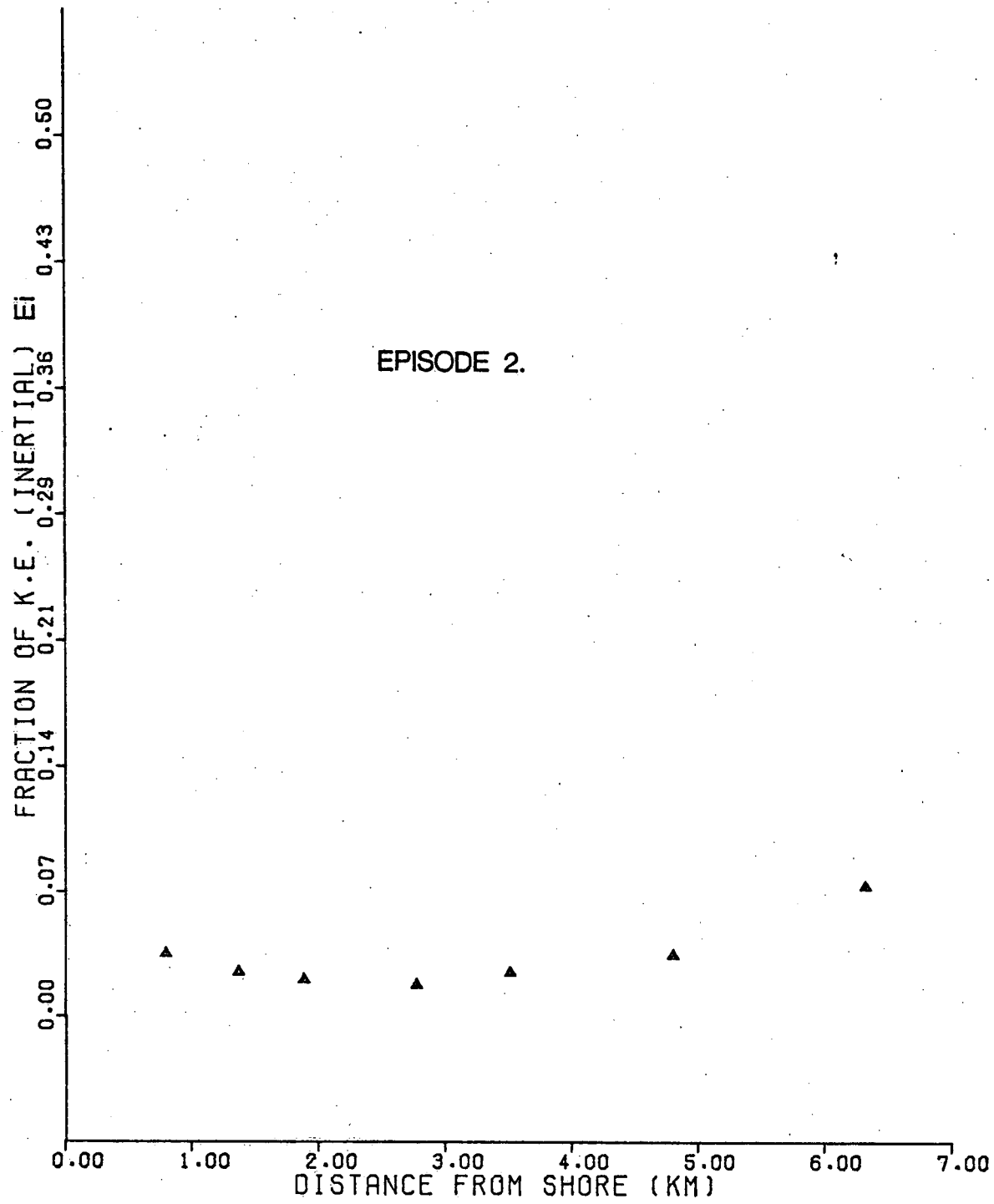


EPISODE 2
METER 11





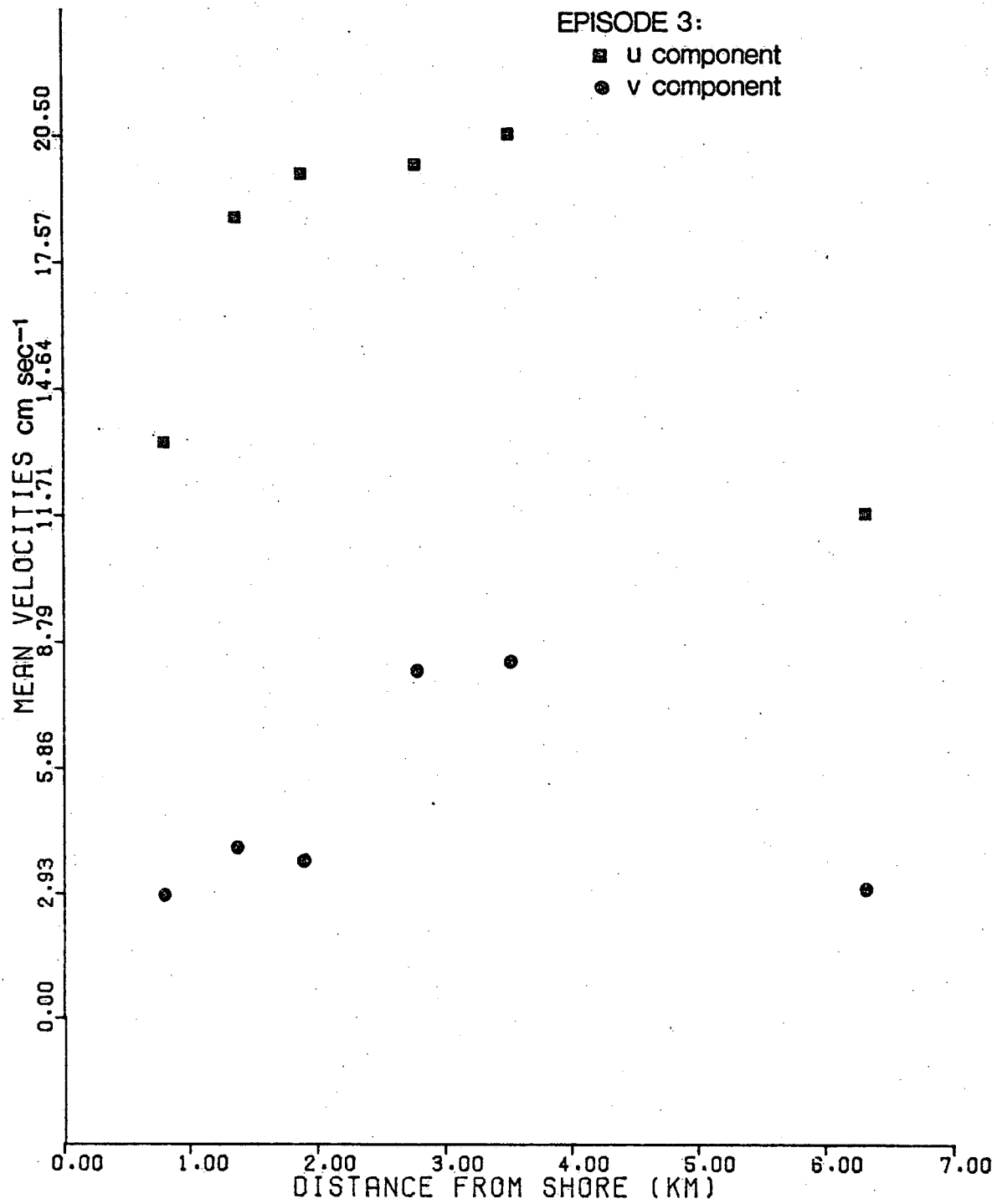


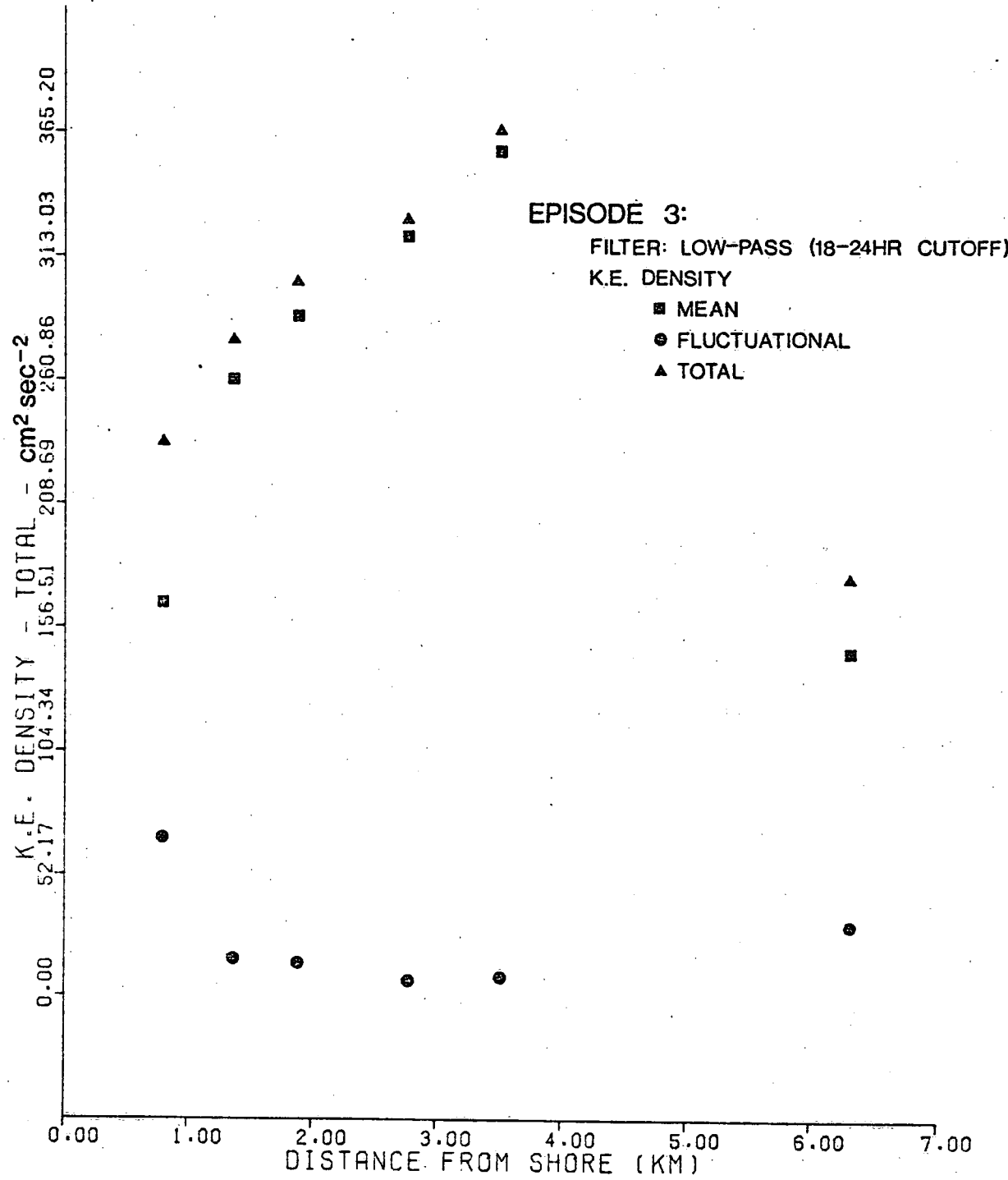


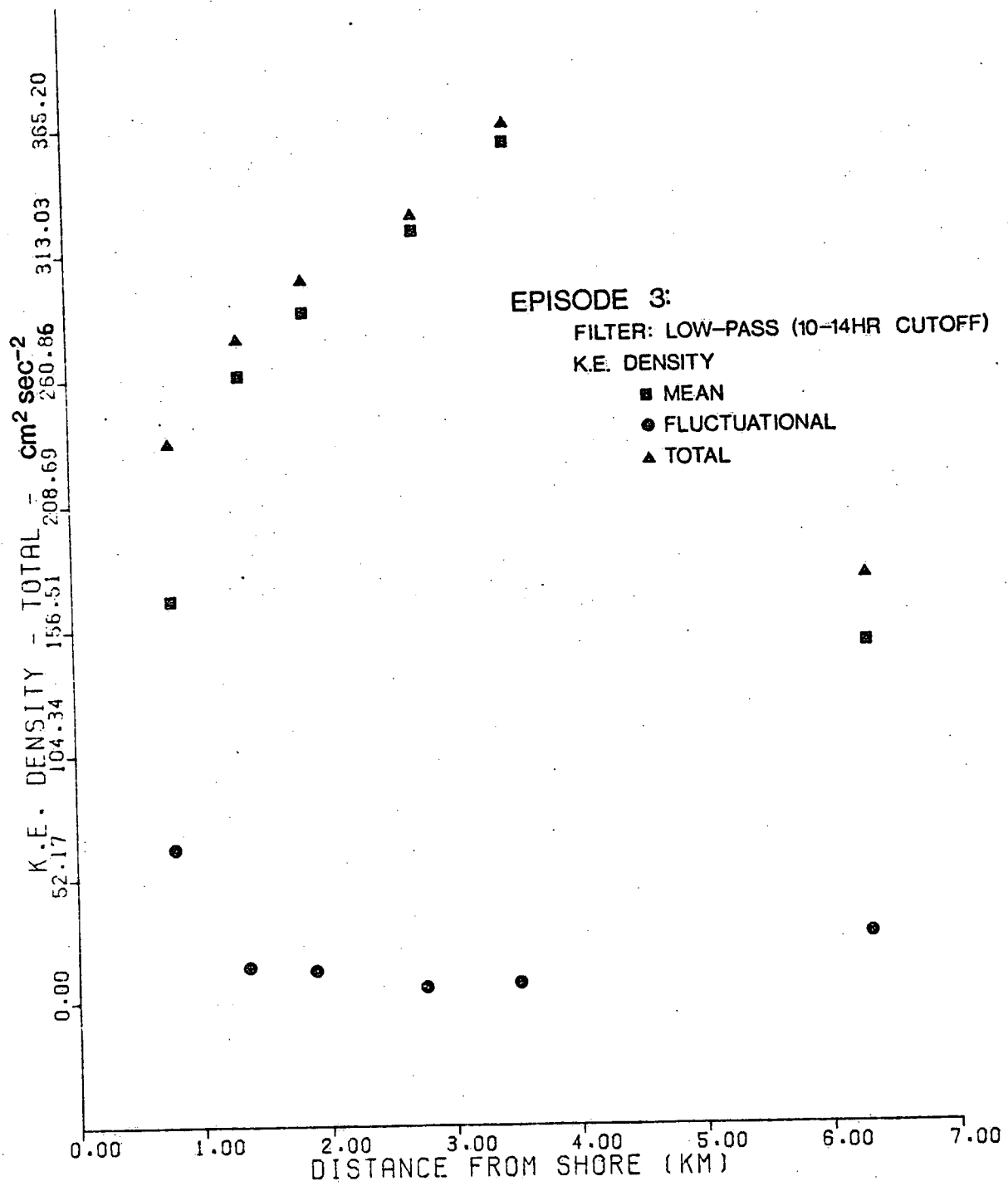
APPENDIX D

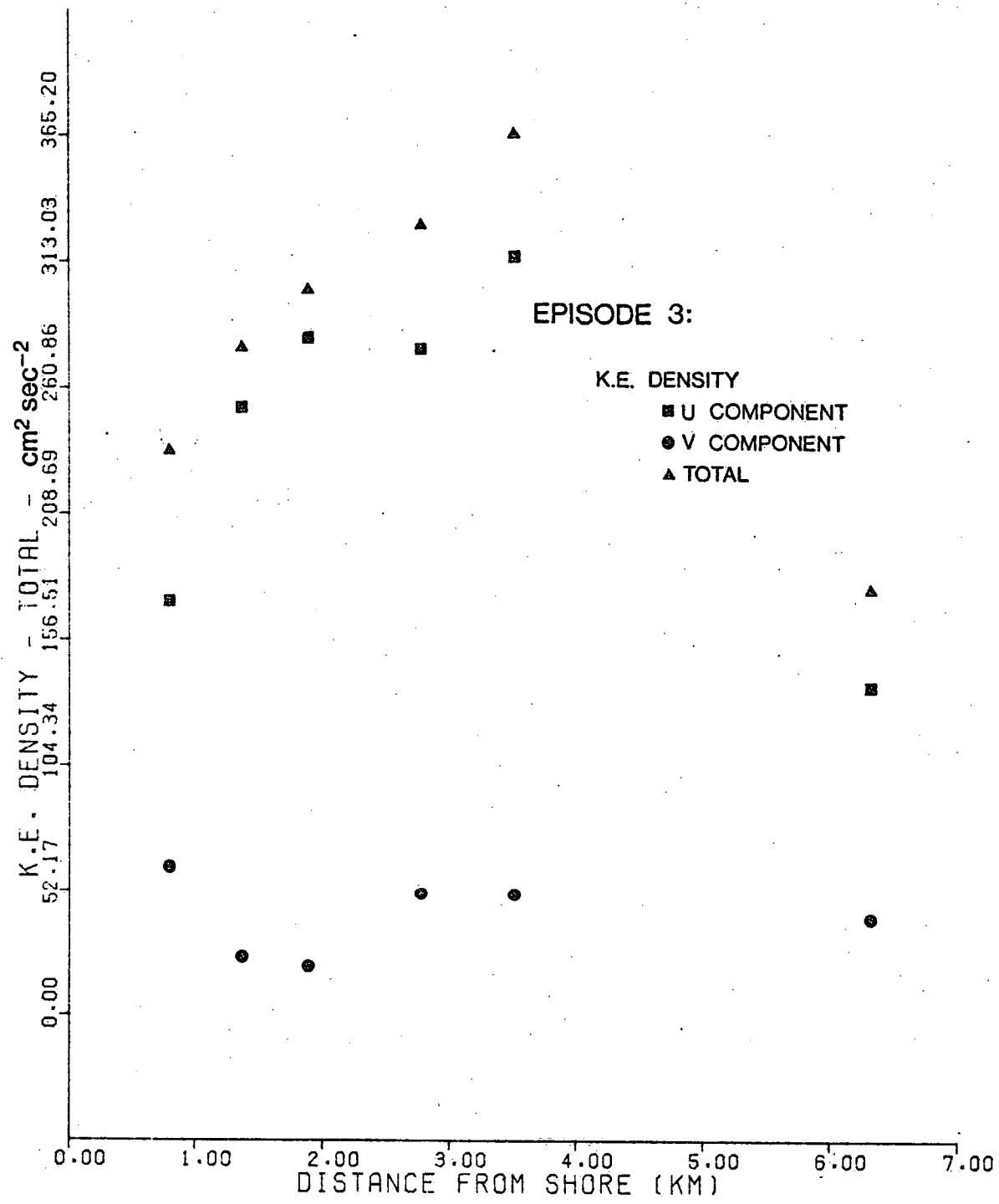
EPISODE 3:

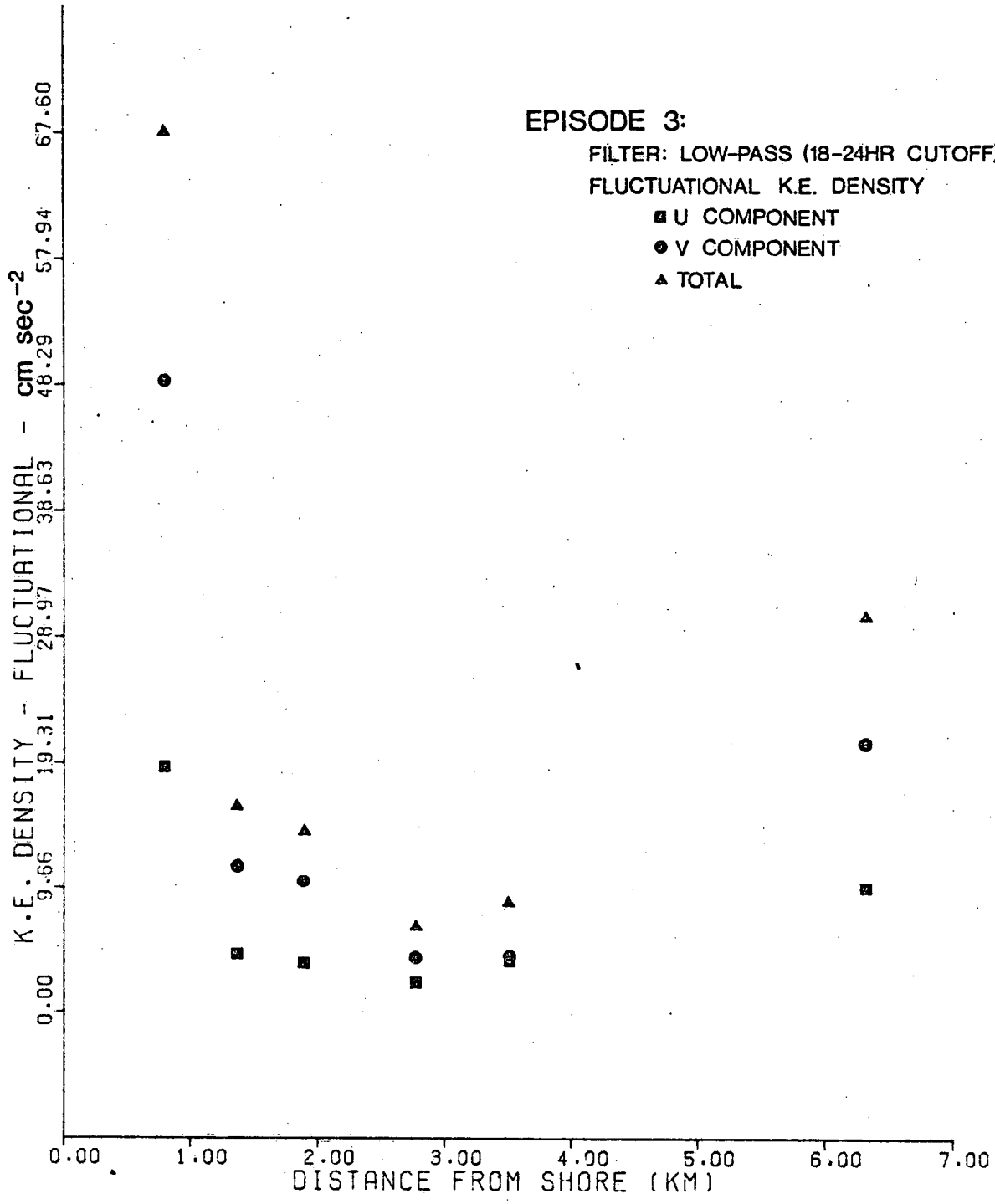
- u component
- v component

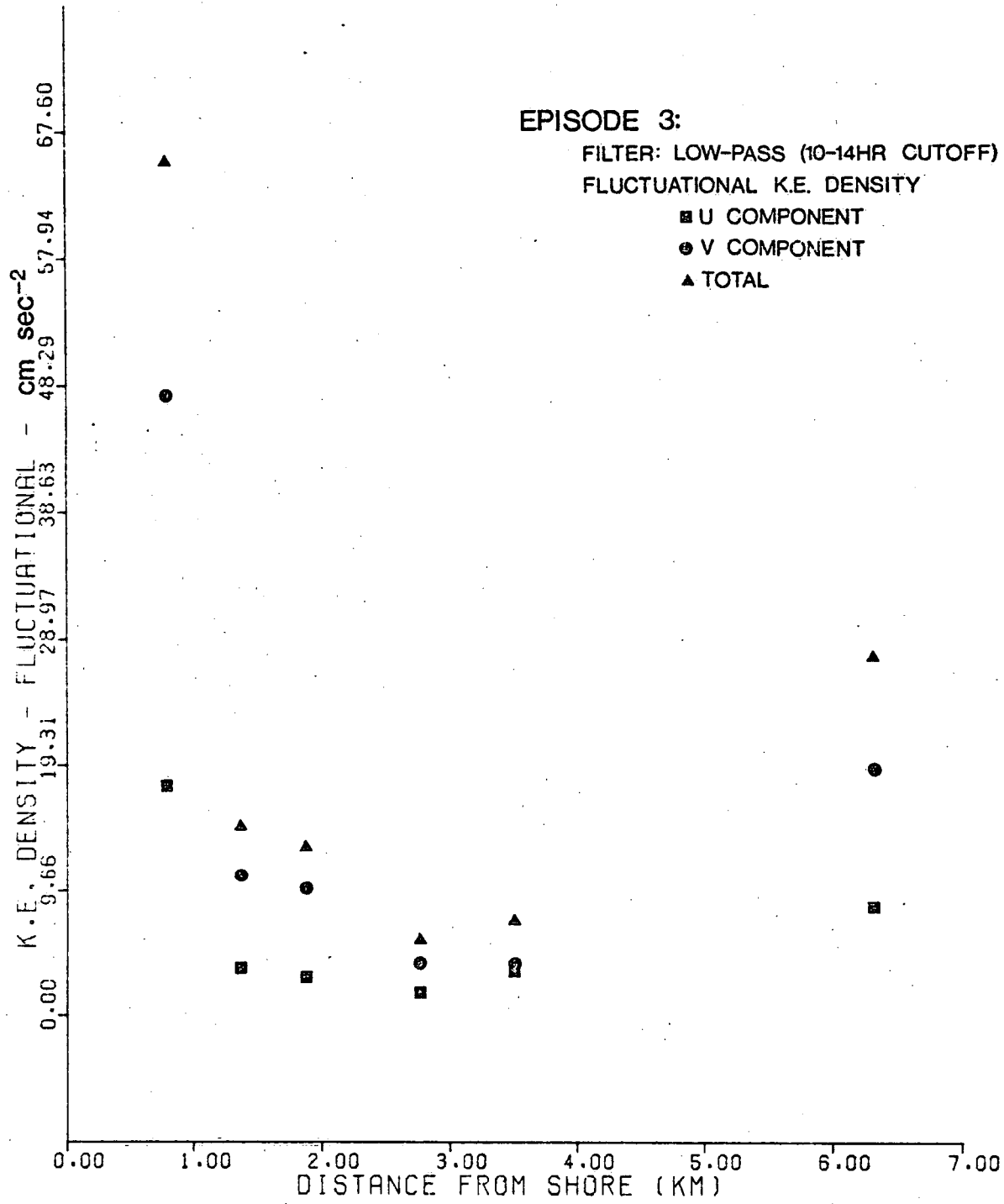


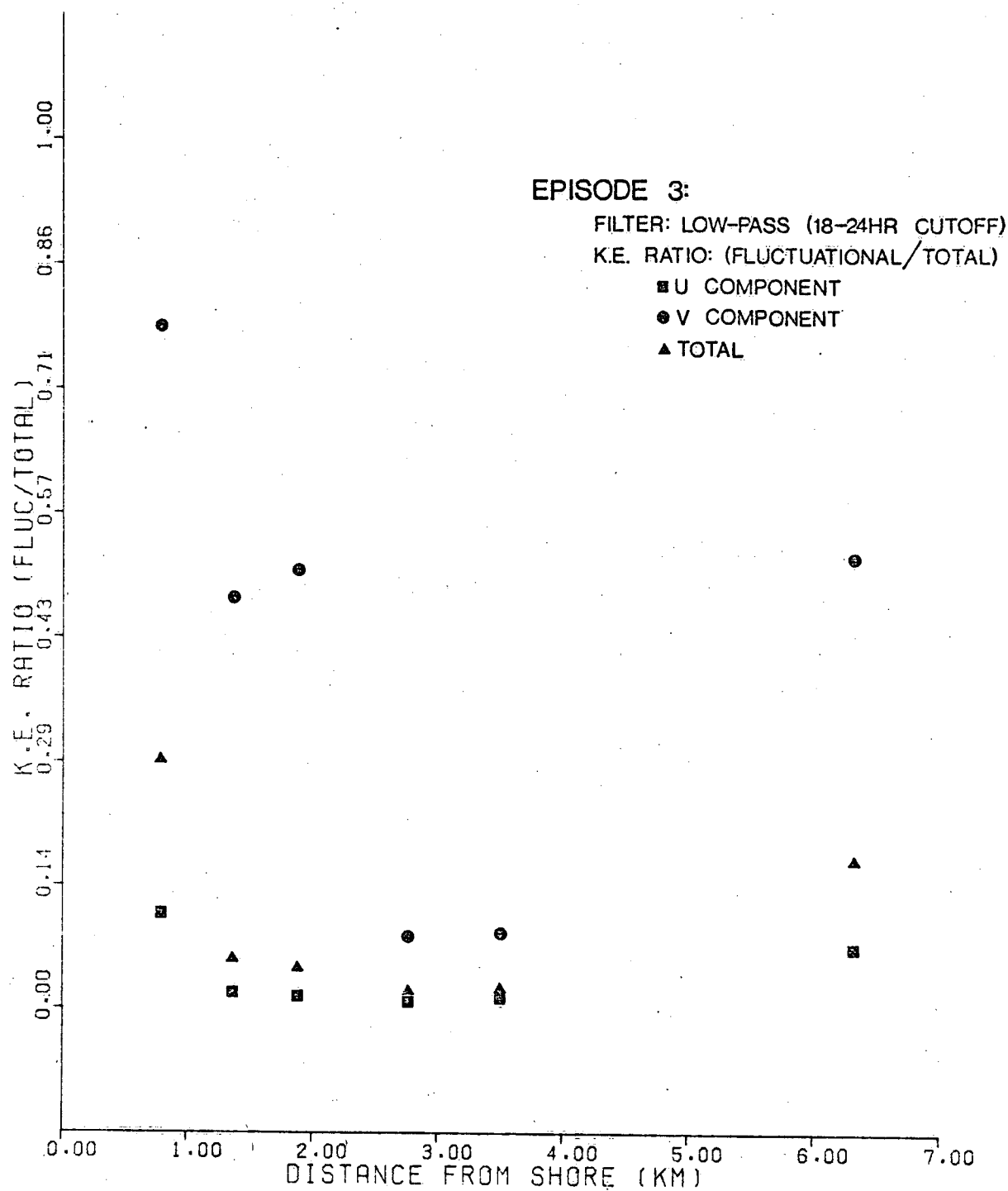












EPISODE 3:

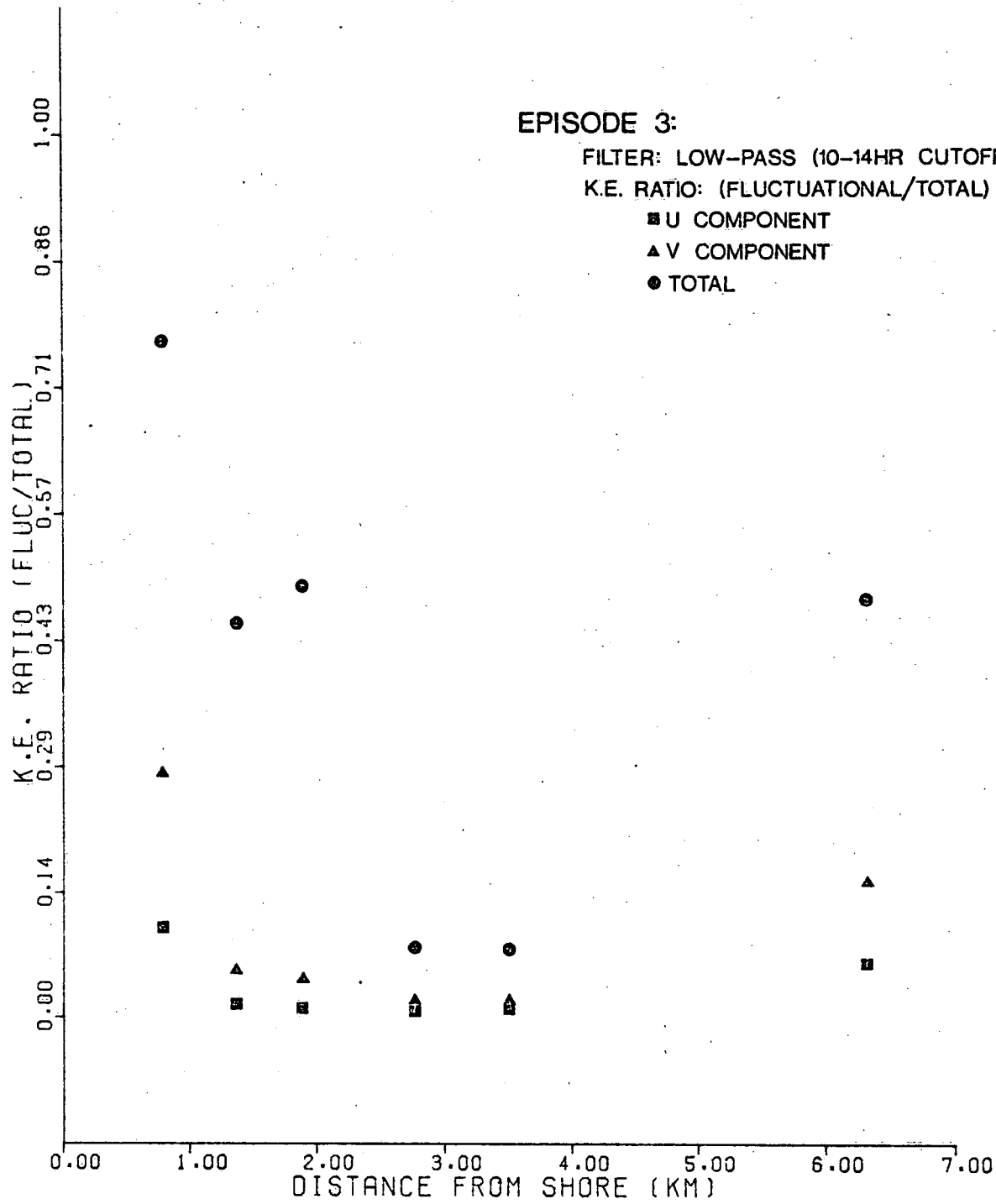
FILTER: LOW-PASS (10-14HR CUTOFF)

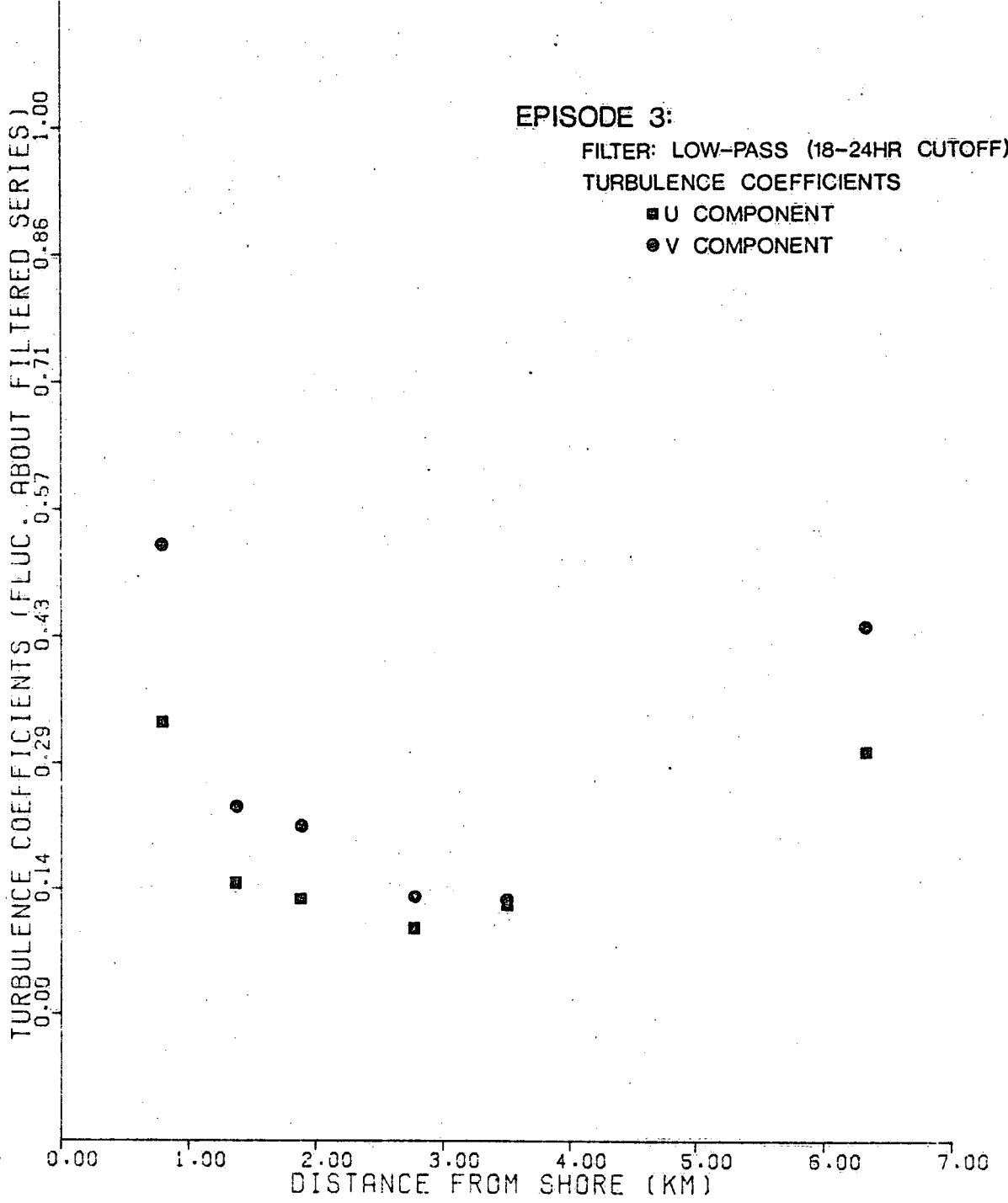
K.E. RATIO: (FLUCTUATIONAL/TOTAL)

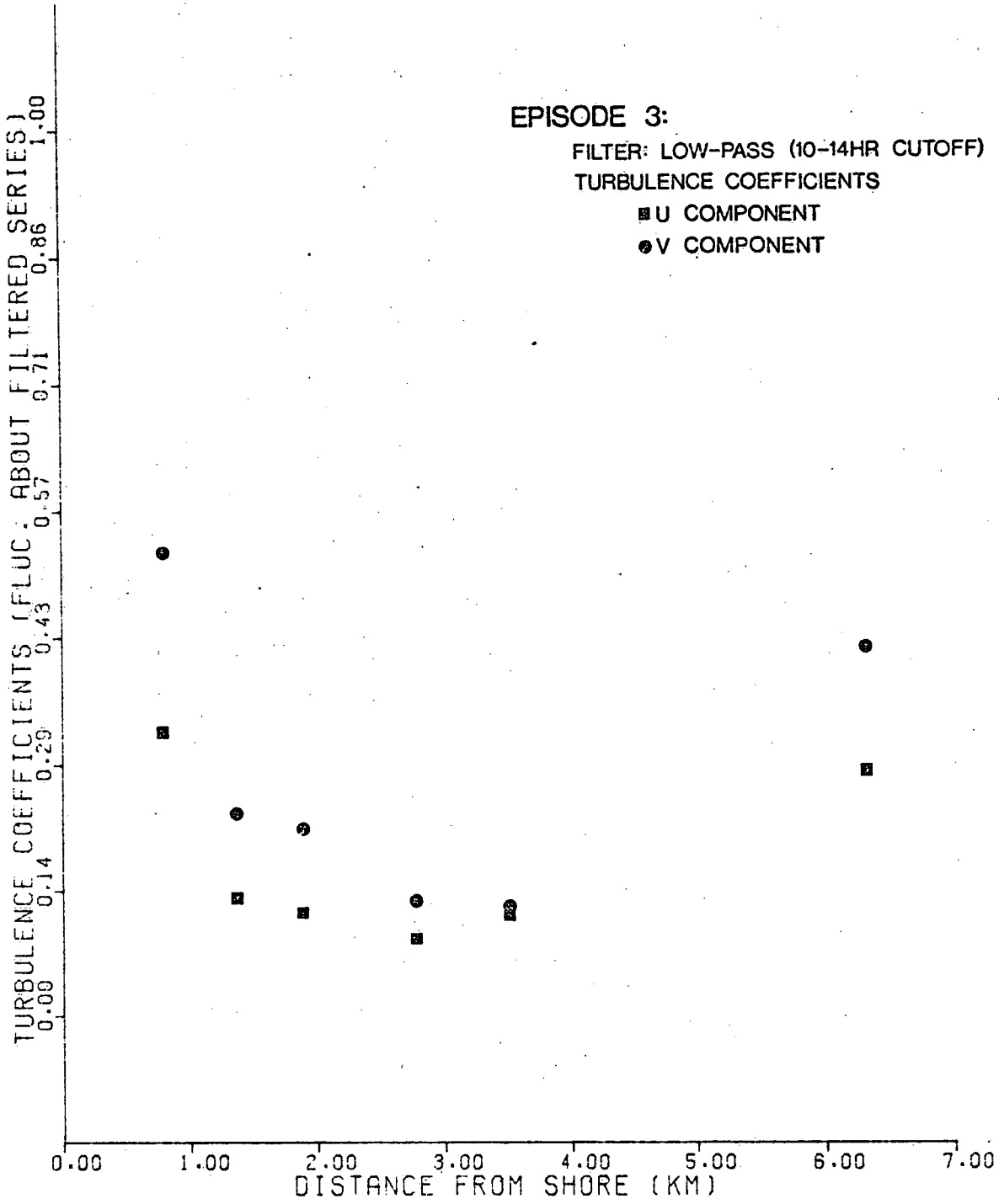
■ U COMPONENT

▲ V COMPONENT

● TOTAL



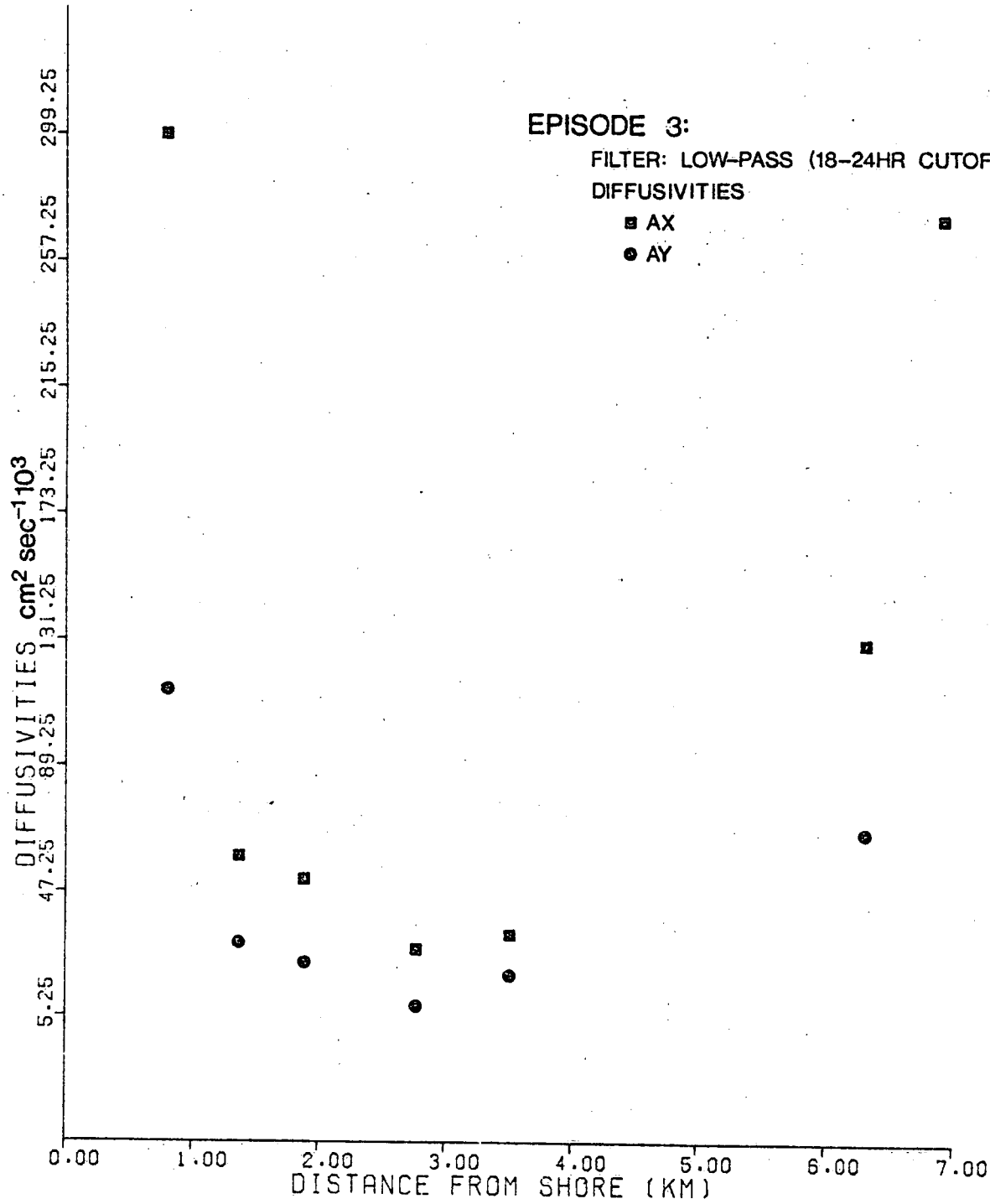




EPISODE 3:

FILTER: LOW-PASS (18-24HR CUTOFF)
DIFFUSIVITIES

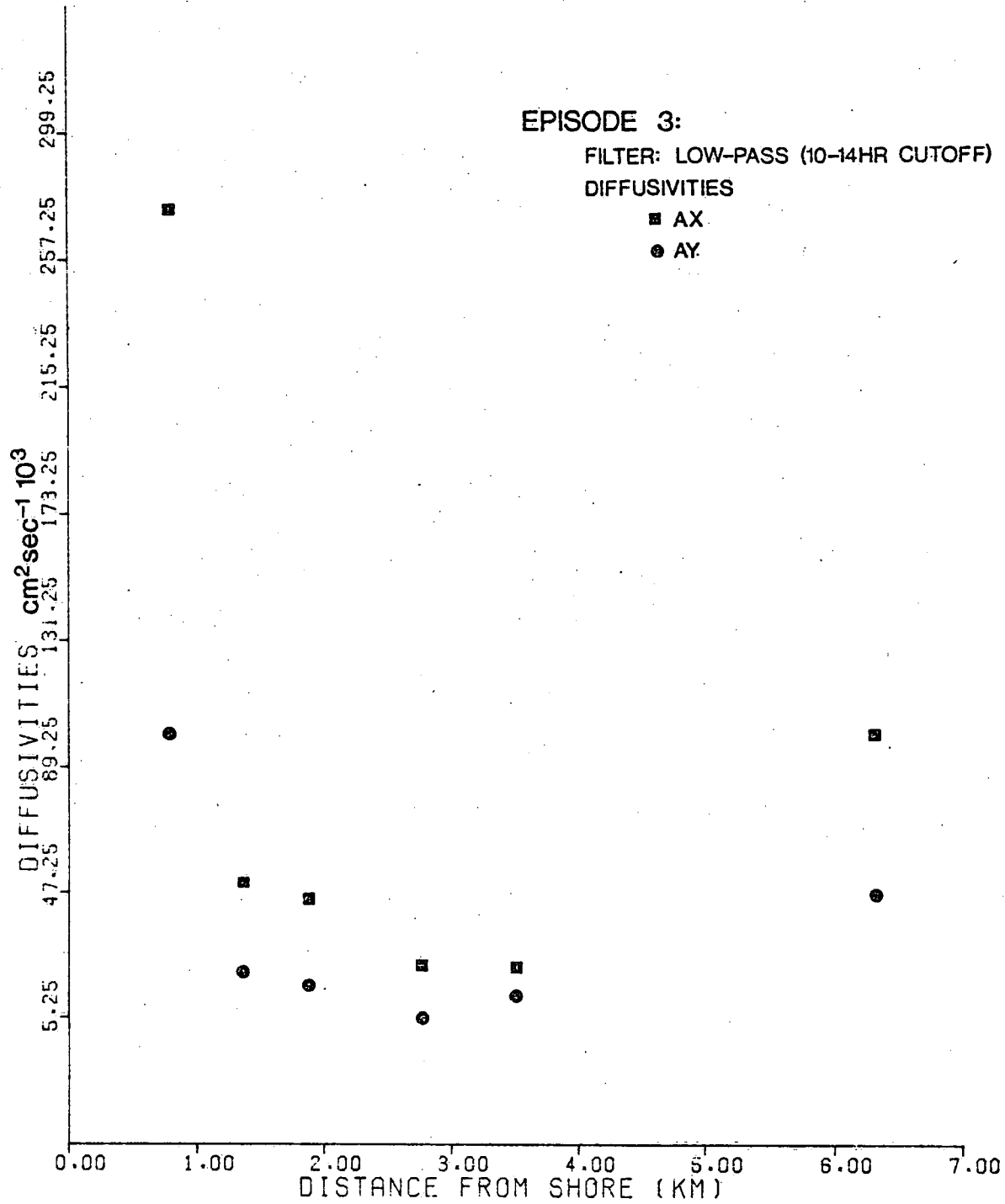
- AX
- AY



EPISODE 3:

FILTER: LOW-PASS (10-14HR CUTOFF)
DIFFUSIVITIES

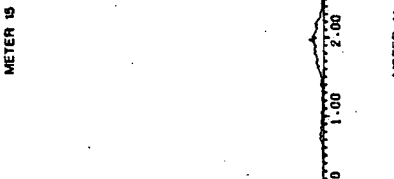
- AX
- AY



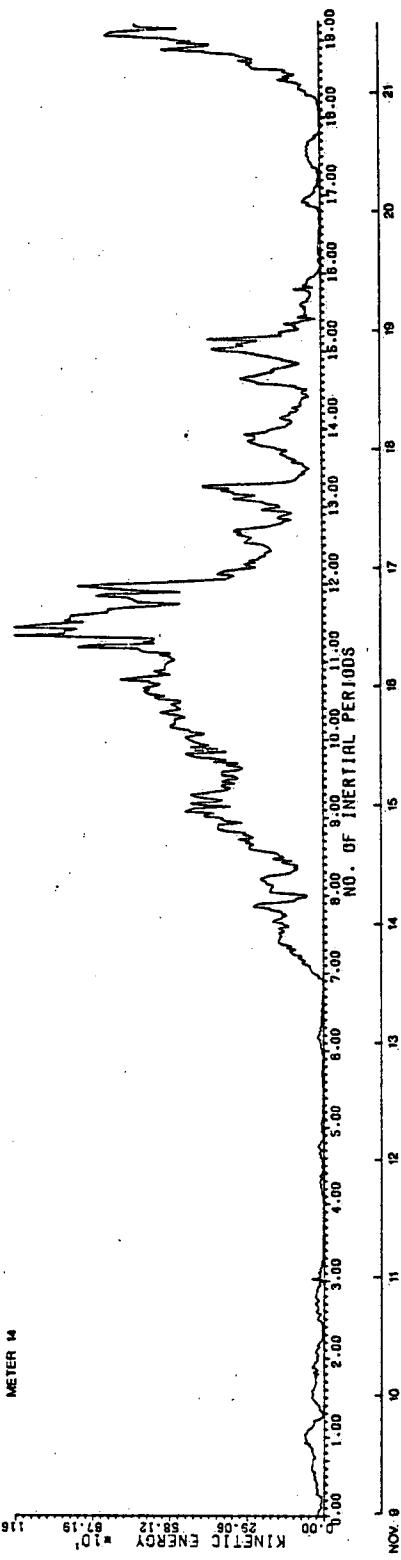
EPISODE 3:

METER 15

KINETIC ENERGY = 10¹² 29.06 58.12 67.19 116.25 NOV. 9 10 11 12 13 14 15 16 17 18 19 20 21



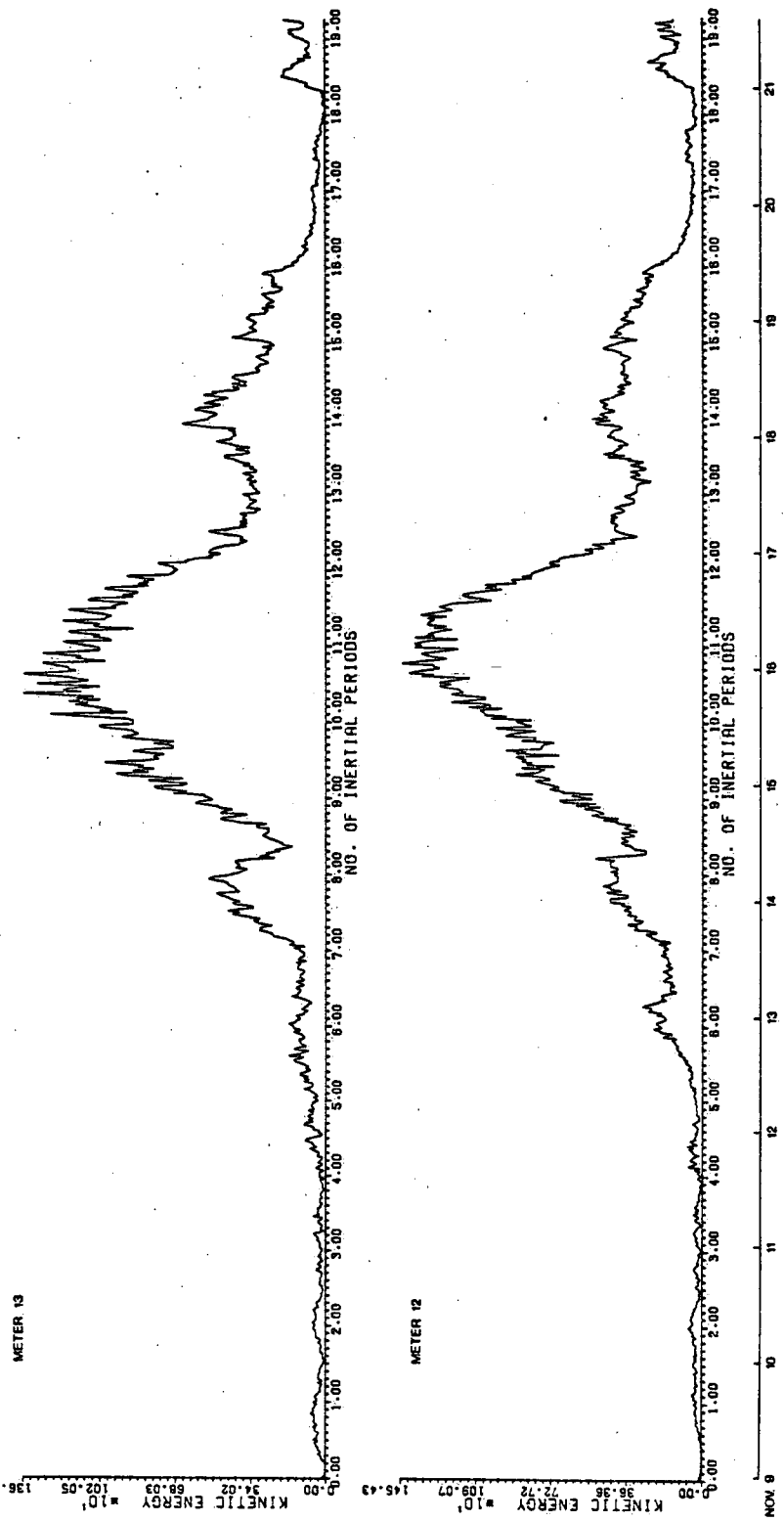
METER 14



EPISODE 3:

METER 13

KINETIC ENERGY = 10¹, 10², 10³, 10⁴, 10⁵, 10⁶, 10⁷, 10⁸, 10⁹, 10¹⁰, 10¹¹, 10¹², 10¹³, 10¹⁴, 10¹⁵, 10¹⁶, 10¹⁷, 10¹⁸, 10¹⁹, 10²⁰, 10²¹



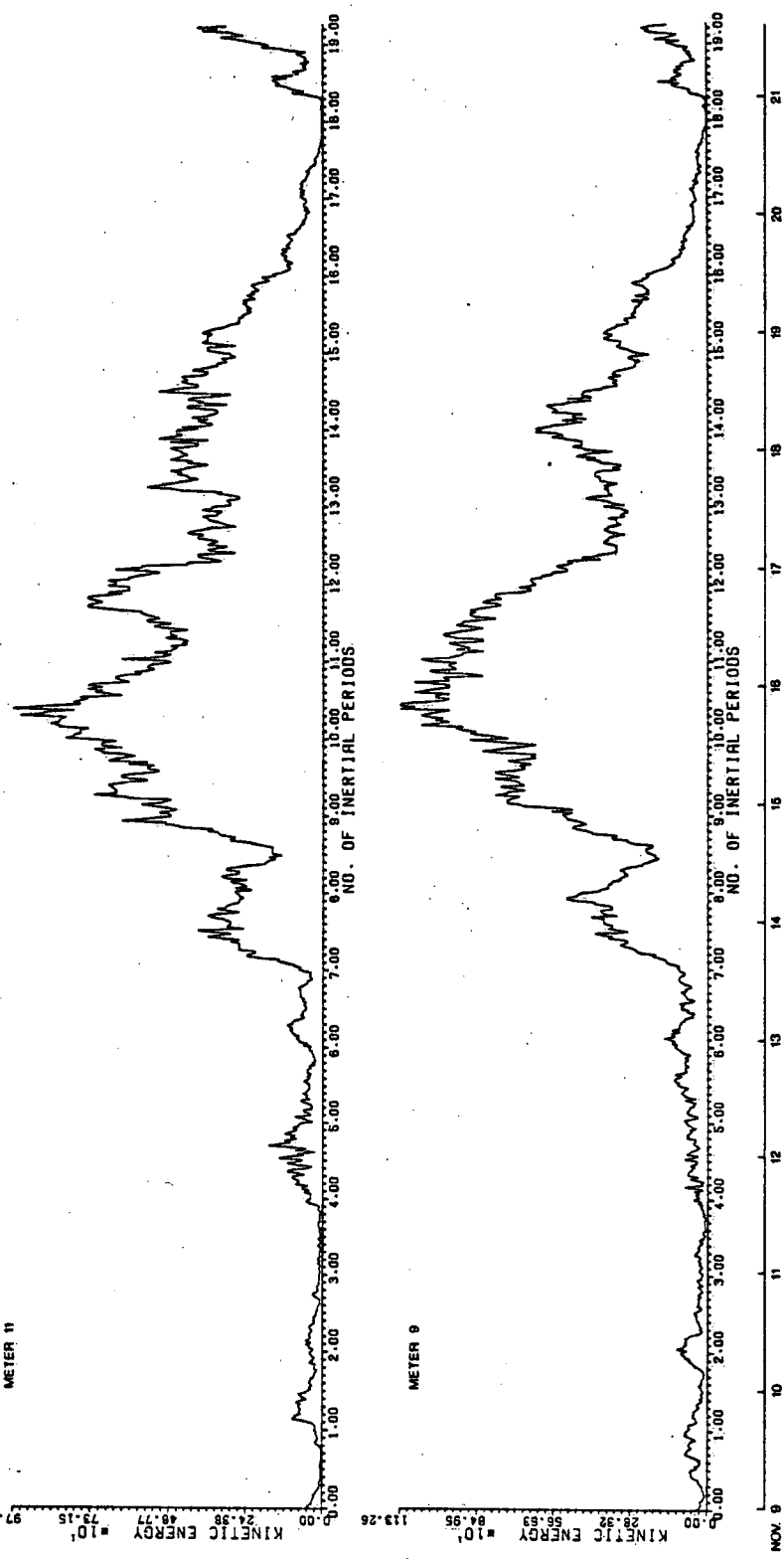
NOV 9 10 11 12 13 14 15 16 17 18 19 20 21

EPISODE 3

METER 11

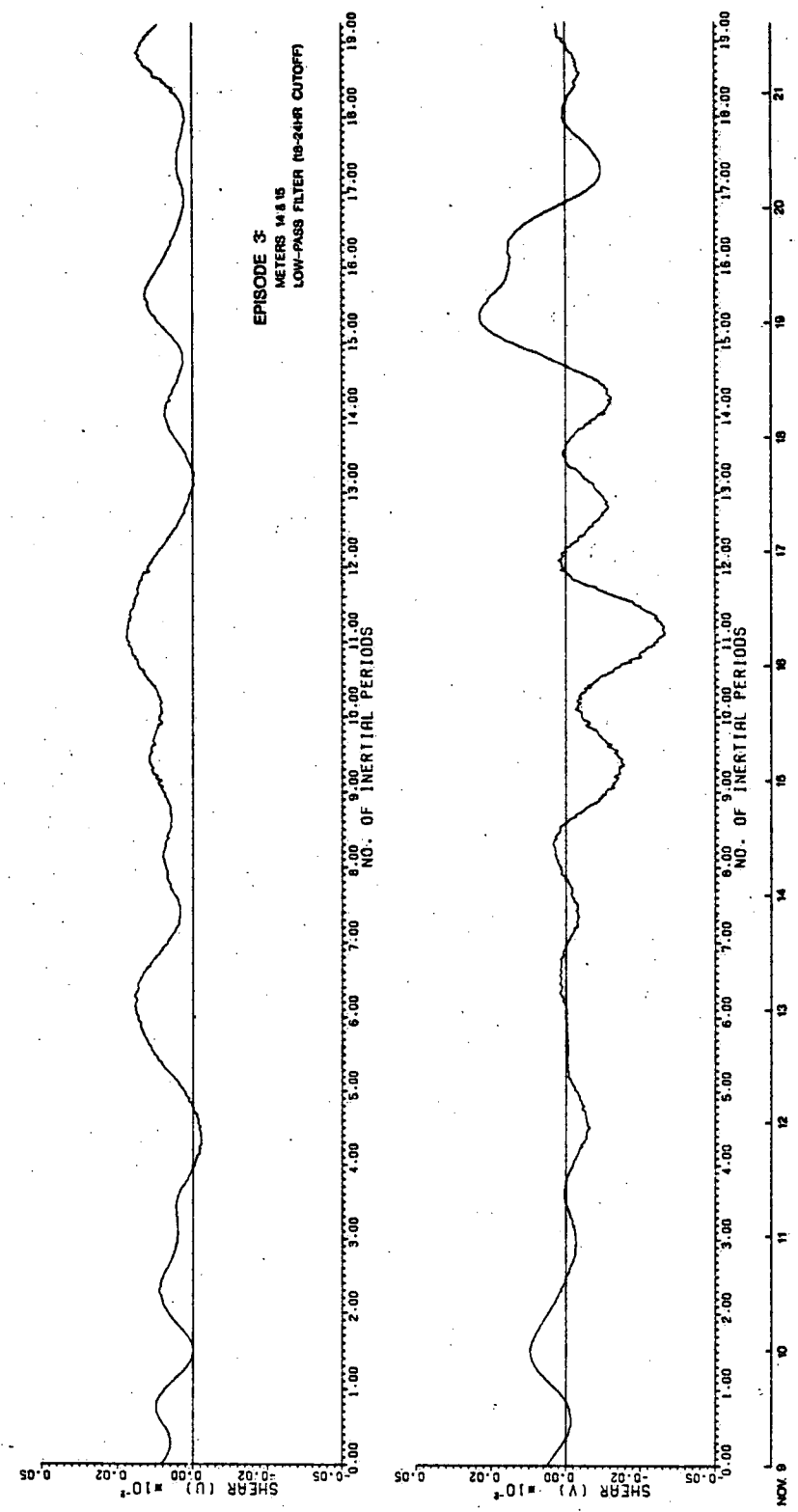
KINETIC ENERGY = 10¹⁰, NO. OF INERTIAL PERIODS

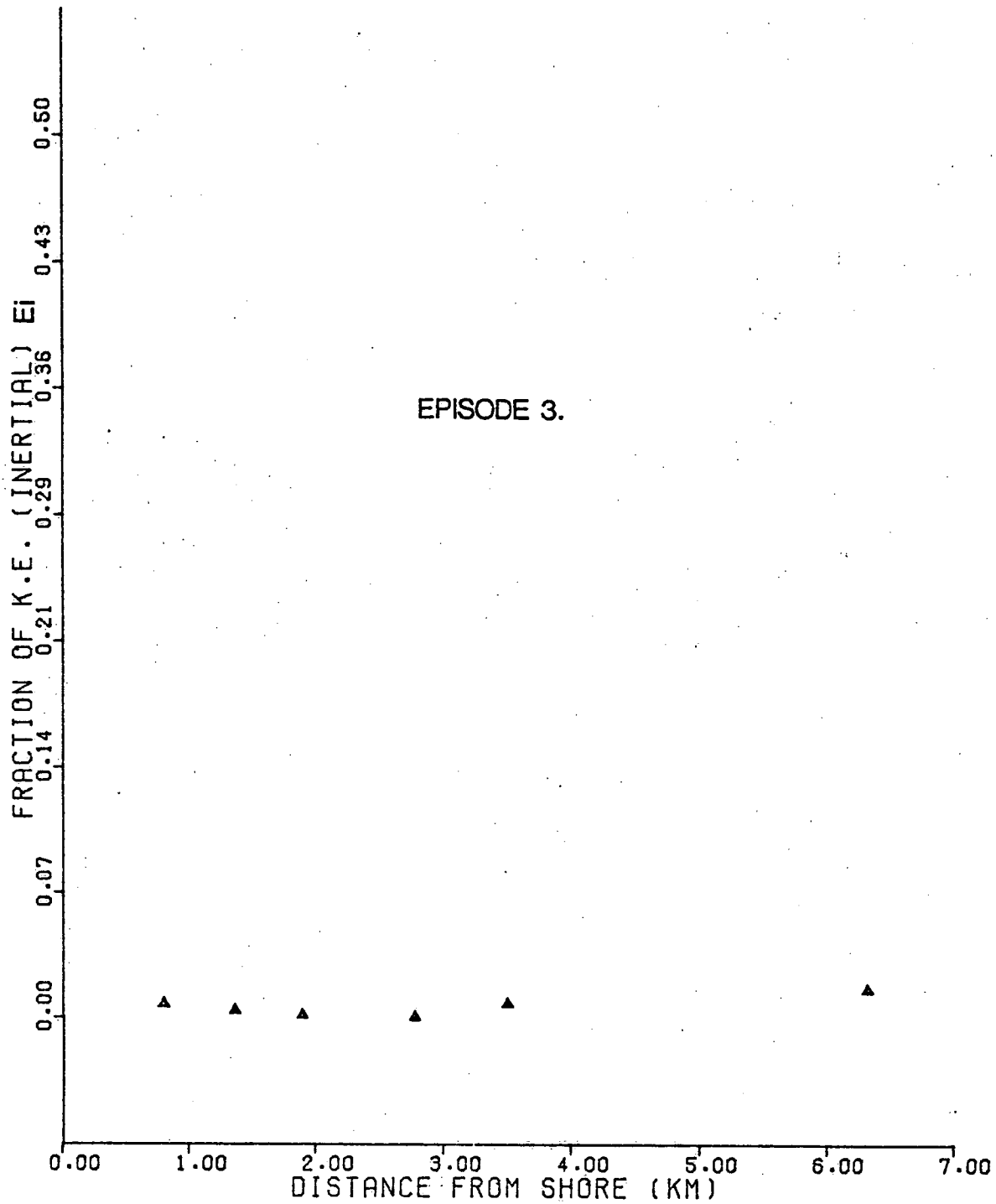
28.92 56.53 84.96 113.26 97.53 113.26 97.53



METER 9

NOV. 9 10 11 12 13 14 15 16 17 18 19 20 21





15454

ENVIRONMENT CANADA LIBRARY BURLINGTON

3 9055 1016 7644 2